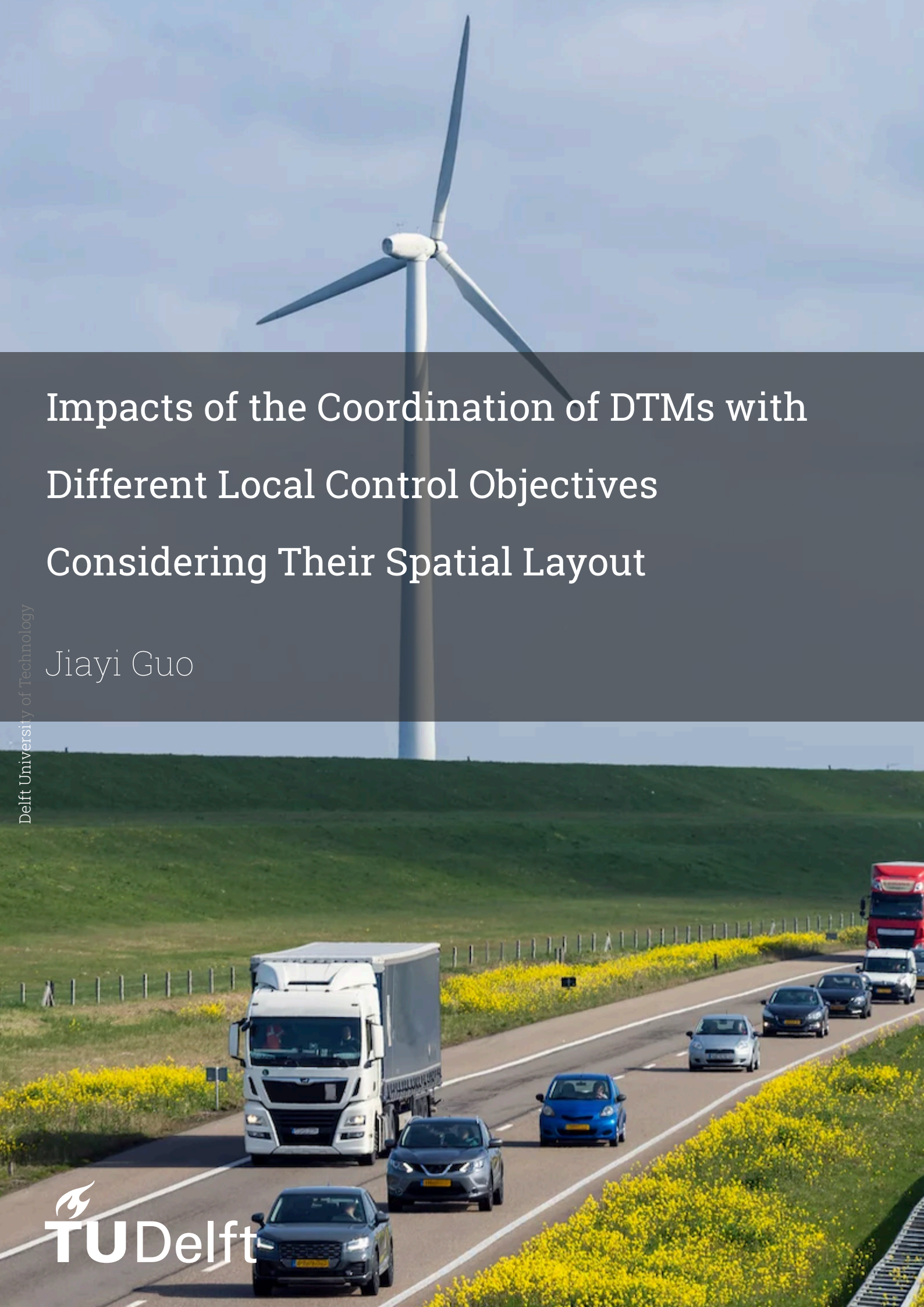

Impacts of the Coordination of DTMs with Different Local Control Objectives Considering Their Spatial Layout

Jiayi Guo

Delft University of Technology

TU Delft

Delft University of Technology

CIE5060-09 MSc Thesis

Impacts of the Coordination of DTMs with Different Local Control Objectives Considering Their Spatial Layout

---

Jiayi Guo

November 21, 2023

to obtain the degree of Master of Science in Civil Engineering at the Delft University of Technology.

Student number:	5443687	
Thesis committee:	Dr. Ir. S. Calvert	DiTT lab, Transport & Planning, chair
	Dr. Ir. H. Taale	TMDC lab, Transport & Planning, daily supervisor
	Dr. Ir. I. Martínez	hEAT lab, Transport & Planning, supervisor

TU Delft Delft University of Technology

Preface

Every time I think about the last two years, I am surprised at how much I have grown. The time I spent in Delft was the most influential in my life so far. I had survived much pressure from different courses. I had travelled to many cities in Europe. I had also finished this thesis, after working on it for almost 9 months.

I am immensely grateful for the support from this thesis committee. I am fortunate to have Dr. Henk Taale, an experienced expert in the field of road traffic management, as my daily supervisor. Through all of our meetings, I learnt not only about the theory of traffic control, but also about the real-life situation in this industry. Dr. Simeon Calvert initially inspired me on this thesis topic. Besides, he recommended the committee members for me. I was impressed and touched by the detailed comments from Dr. Irene Matínez, through which I have learnt a lot about thinking and writing as a researcher. The help from my committee members is not only in this thesis. Dr. Henk Taale gave me quite useful information on ramp metering in the Netherlands during my Bachlor thesis. With Dr. Simeon Calvert's help, I got an interesting internship opportunity at Rijkswaterstaat, which has significant influence on my further career planning. I could not be more excited when Dr. Irene Martnez offered me the PhD candidate position. This approval motivated me when I was working on my master thesis.

I would also like to express my gratitude to Dr. Andreas Hegyi, who introduced me to the world of road traffic control 3 years ago. His patient guidance during my bachelor thesis has significantly influenced my academic journey.

This two-year journey was sometimes challenging. It takes time to get used to the pace of study and living abroad. Fortunately, I have friends and colleagues, so I do not have to face them alone. I would like to thank Zhengliang, Ximing and Gert. It was a great pleasure to work with you and I wish you all the best for your future. I also want to express my gratitude to my friends in the Study Tour 2022 committee. Planning the trip with you has really enriched my life here. Thanks to Simon, Machiel and other colleagues at Rijkswaterstaat WNN. With your help, I had a very interesting internship experience and gained a lot of insight into road traffic management.

I cannot be more grateful for my family. Their unconditional support and love give me the strength and confidence to do what I want to do. It is their support that makes this journey happen, so that I can know more about the world.

Wenxuan, your support and the joy you bring to my life are truly appreciated. I am thankful for our magical encounter every day. I hope you can keep pursuing your dreams and remain true to yourself.

Jiayi Guo
Delft, November 2023

Summary

Background and research question

With the steadily increasing road traffic demand, congestion on freeways has become a major problem. Since the 1960s, Dynamic Traffic Management (DTM) on freeways has become an important way to handle issues on freeway traffic. DTM measures include ramp metering (RM), variable speed limits (VSL), dynamic route guidance (RG) and lane changing control (LCC). With the development of communication technology and automated vehicles, there are more opportunities for DTMs to be studied extensively at the coordination level and cooperation level.

In the existing literature, the coordination of RM + VSL + RG has rarely been studied. Besides, some coordination studies have limited discussion on the interaction between DTMs in non-coordinated cases. That is, the reasons for researching coordination of certain DTMs are not clearly explained. However, this kind of explanation is necessary, especially when more DTM measures are involved in coordination. To explore the interactions between DTM measures, their spatial layout is a significant factor. However, DTM interactions in different layouts are also lacking in existing DTM coordination studies. Based on these research gaps, the research question of this thesis is: **What is the impact of coordinating RM, VSL and RG on a road structure where they have potential counter-effects on each other when following local objectives?**

Simulation setting

The research considers a two-freeway structure as shown in Figure 1. There are two bottlenecks on two roads. To prevent congestion before these bottlenecks, DTM measures are installed upstream. RM uses the Demand-Capacity algorithm and the switch on-off rule applied on freeways in the Netherlands. VSL has a fixed reduced speed limit. It is activated once the speed detected from the road segments before the bottlenecks is lower than the threshold. Given that the RG is working upstream of the split point, DTM measures VSL1 and RM1 are inherently conflicting with RM2 and VSL2. When RM 2 regulates the ramp flow, the travel time of Route 2 also increases. This may cause more vehicles to stay on Route 1 and this is conflicting with the control objective of RM1 or VSL1. These two measures aim to keep the total flow before the bottleneck on Road 1 slightly lower than the capacity of the downstream road segments.

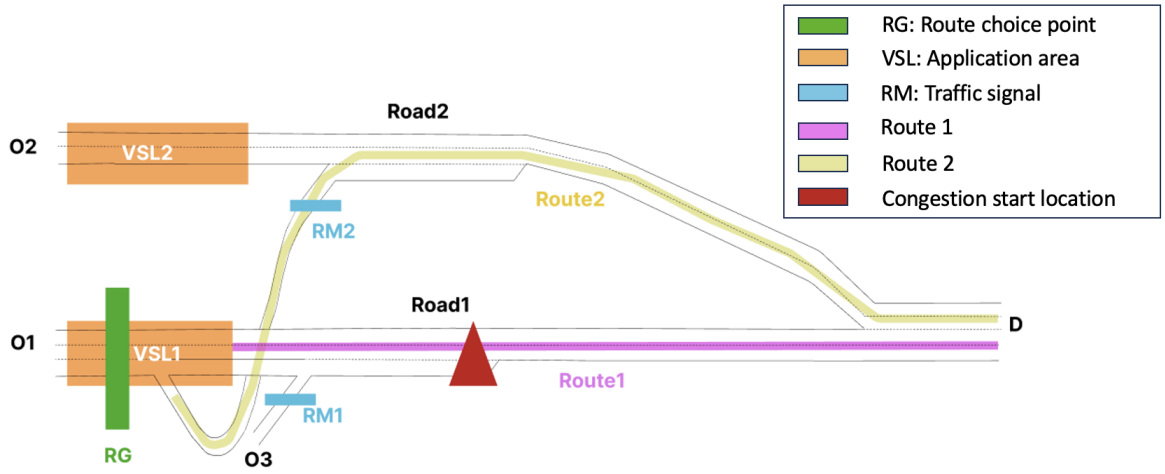

Figure 1: Conceptual road network layout

This research aims to explore the network performance on the non-coordination cases and coordinated cases. The simulation is built in SUMO, while the DTM control measures are implemented via the Traffic Control Interface (TraCI). The simulation network and the location of the DTM measures can be seen in Figure 2. The route choice behaviour of vehicles is realised using RG with variable message sign (VMS) in no-control case. 50% of vehicles are assumed to get instantaneous travel time information from the VMS board, and 80% of these vehicles will select their route according to the travel time information. The other half of vehicles keeps on Route 1 in base case. In the RG control case, a predictive RG is applied to these vehicles. Based on the predicted density and the corresponding speed in the fundamental diagram (FD), an optimal split rate before the off-ramp 1 can be calculated in predictive RG. The objective of RG is to minimise the average travel time in the segments before bottlenecks and after RM1 and 2. The travel time indicator can be both measured at level of edge in the simulation and calculated for certain routes by counting the simulation steps vehicles have experienced.

With coordination, all controller parameters (metered flows, speed limits, and split rate) work together to improve traffic in this two-bottleneck system. The coordination strategy has a model predictive control structure. The cell transmission model (CTM) is used as the prediction model for the edges EM5, EM6, EM7 and ES5, ES6 ES7. In this case, all the effects of considered DTM measures can be integrated into the expression of the inflow to the first cell on the basis of certain assumptions. Considering that there are 5 control variables, genetic algorithm (GA) is used for the optimisation process in the MPC control. The control structure is shown in Figure 3.

A commonly used objective for DTM coordination is to minimising the total travel time. However, in the predictive model, only several road segments around the bottleneck are considered. This makes the queue before the most upstream cells difficult to model. Therefore, maximising the total outflow after bottlenecks 1 and 2 is selected as the objective.

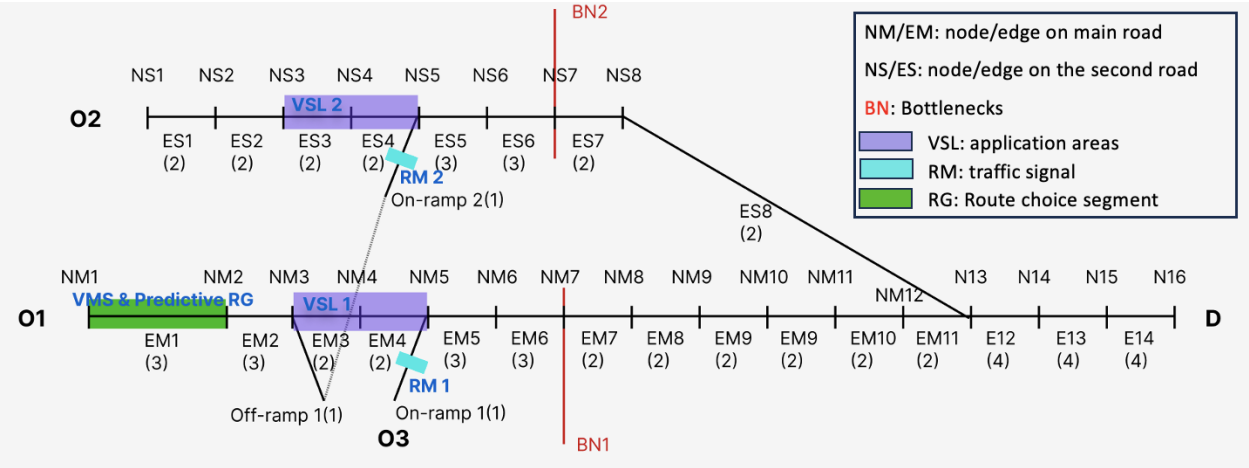

Figure 2: Simulation network with DTM locations

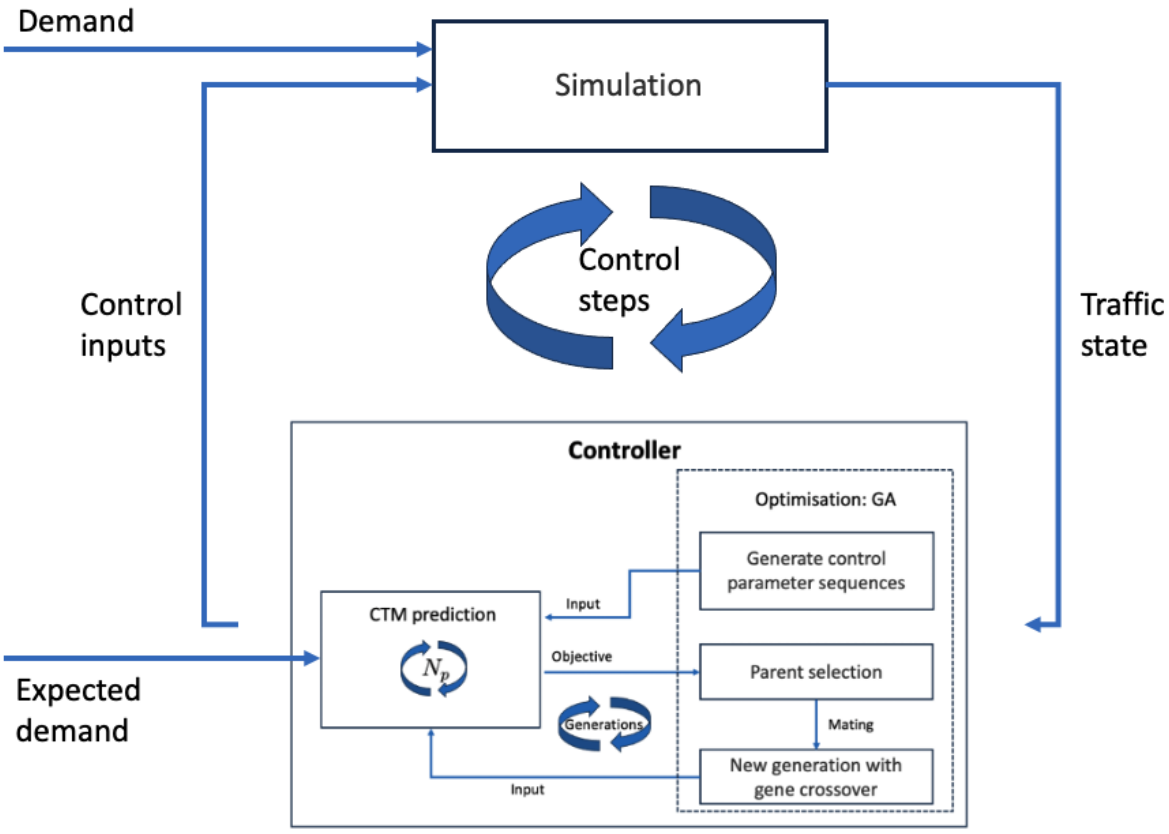

Figure 3: MPC control loop

In the simulation, the VSL is off most of the time, since it has a negative effect on maximising the outflow in the model formulation. However, there is still a desired function for VSL to realise. That is, to keep the total demand before the bottleneck close to capacity when RM cannot restrict ramp flow. This situation occurs when the queue on the ramp is too long and RM has to be switched off to release vehicles. In the non-coordinated cases, VSL is often on due to the congestion caused by the queue discharge of the ramps (as can be seen in Figure 4a). In coordinated control, a special rule is applied for VSL. That is, the speed limit should be reduced when the ramp queue needs to be discharged. This rule is used to compensate for the switching off of RM and to keep the total flow before the bottleneck stable. For simplification, this queue discharge mechanism is not captured in the predictive model. Hence, it is not considered in the GA process. By comparing Figure 4b with 4a, it can be seen that VSL acts after the sudden increase in ramp flow without coordination. Meanwhile, the speed limit is reduced simultaneously with the discharge from the ramp queue after applying the VSL rule in the coordination.

Simulation results

There are multiple sources of randomness in the simulation, including the attributes of the vehicles in the car-following model and departure times. Determining which vehicles will change their route is also a random process. Since these kinds of randomness are included in the microsimulation, each scenario is run 20 times. The mean values among the simulation runs of the average travel time per vehicle and the total delay are shown in Table 1. It could be seen that predictive RG is the most effective measure in single-control cases. The reason why RM and VSL lead to even longer average travel time is that the capacity drop phenomenon is not captured in the simulation. RM has the effect of changing the distribution of delay over different routes, while the VSL case has no significant difference from the no-control case. The combined cases did not have significant improvement compared to the best single-control case (i.e. the RG only case). This is also because the effect of predictive RG is much stronger than that of RM and VSL.

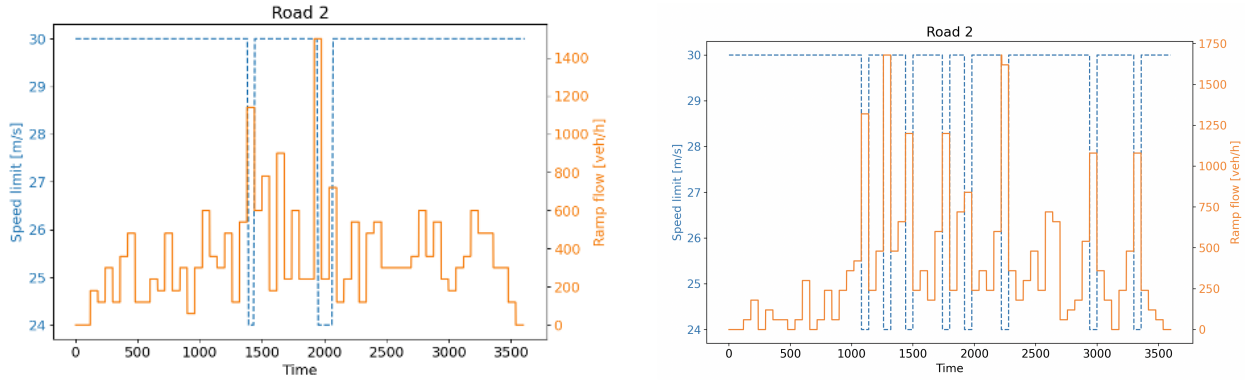

(a) RM+RG+VSL (b) Coordination

Figure 4: Speed limit and ramp flow curves before and after coordination

The first coordination case has similar performance to the RG only case. In this case,

Table 1: Simulation results

Scenarios	Network average travel time [s]	Total delay [veh*h]
Base	229.8	82.6
RM	+0.7	+1.7
VSL	+0.3	-0.7
RG	-1.5	-3.1
RM+VSL	+0.9	+0.4
RM+RG	-1.5	-2.7
VSL+RG	-1.4	-4.0
RM+VSL+RG	-1.2	-3.0
Coordination	-1.6	-2.7
Coordination (with VSL rule)	-2.1	-4.5

VSL is not active. Compared to RM+RG cases, the coordinated control did not have significant added value. There are decreases in travel time on some routes and increases on some of the others. The second coordination case is the overall best performed one. The improvement is that it further solves the congestion caused by the sudden increase in ramp flow.

Conclusion

The conclusion of the research is that there is benefit for applying DTM coordination on such a road structure with two parallel freeways. However, the improvement caused by a predictive RG is the major part of the benefit. This can be seen by comparing the RG-only case and the coordinated case. Therefore, it is more prior for this kind of road structure to improve the in-vehicle RG on this road structure than to apply coordinated control.

The contribution of this research is that it compares the effects of DTM measures in non-coordinated and coordinated cases for a certain road layout. In this way, the impact/value of the coordination is explored. It presents a coordination method for RM, VSL and RG on a two-freeway structure, which optimises the traffic at the two bottlenecks on two alternative routes simultaneously. The coordinated MPC control with a macroscopic prediction model is tested in a microscopic simulation environment. The simulation results indicate that a predictive RG is more effective compared to coordinated control. It also leads to the best travel time equity among routes.

The main limitation of this research is that the capacity drop phenomenon is not captured in the simulation. This causes the performance in RM and VSL cases to be even worse than in the base case. It is possible that the coordination method will have a greater improvement in a different simulation setting. To further test this coordination method, real-life data is required for calibration and simulation. This coordinated control should then be implemented in a simulation network built based on the real-life structure.

List of Figures

List of Tables

Nomenclature

Table 2: Abbreviations

Abbreviation	Meaning
API	Application Programming Interface
CTM	Cell Transmission Model
CV	Coefficient of Variation
DTM	Dynamic Traffic Management
FD	Fundamental Diagram
GA	Genetic Algorithm
GUI	Graphical User Interface
LC	Lane Control
LCC	Lane Changing Control
MPC	Model Predictive Control
MTFC	Mainstream Traffic Flow Control
PDF	Probability Density Function
RG	Route Guidance
RM	Ramp Metering
TraCI	Traffic Control Interface
TTD	Total Travel Delay
TTI	Travel Time Index
TTS	Total Time Spend
VMS	Variable Message Sign
VSL	Variable Speed Limit

Table 3: Notations and corresponding descriptions

Variable	Description	
α	Weight for the calculated control parameters; (1-alpha) is the weight for the control parameters of last control step	
β^{adj}	Adjustment coefficient for vehicles following VMS guidance	
$C_{l,i}$	Capacity of cell i, route l	veh/h

C_l^{ds}	Downstream capacity of segment l	veh/h
$D_{l,i}$	Demand on cell i, route l	veh/h
d_l^{ramp}	Ramp demand to segment l	veh/h
dt	time step	s
dx	Length of cells	km
i	Cell index	
I_{RM}	Overall indicator for RM to be on or off	(0,1)
I_{flow}^{off}	Indicator for RM to be off (flow)	(0,1)
I_{speed}^{off}	Indicator for RM to be off (speed)	(0,1)
I_{flow}^{on}	Indicator for RM to be on (flow)	(0,1)
I_{speed}^{on}	Indicator for RM to be on (speed)	(0,1)
I_{RM}^{queue}	Indicator for RM to be on and off (queue length)	(0,1)
l	Road index	
L_l	Length of segment l	km
N_{change}	Number of time steps for VSL to have a certain trend	
N_p	Prediction horizon for RG	
N_{th}	minimum number of steps for VSL to change to the value of the trend	
N_p^{coor}	Prediction horizon for coordinated control	
N_l^{veh}	Number of vehicles on segment l	
p^{RG}	Split rate to Route 1 (predictive RG)	%
$Penalty^{ib}$	Penalty term for imbalance between routes	
$q_{l,i-1/2}$	Flow passing through the interface between cell i and cell $i+1$ on route l	veh/h
q^{target}	Target flow	veh/h
q^{um}	Upstream main road flow	veh/h
q^{ur}	Upstream ramp flow	veh/h
$q^{control}$	metering rate	veh/h
q_l^{in}	Inflow to segment l	veh/h
q_{th}^{off}	Flow threshold for RM to be off	veh/h
q_{th}^{on}	Flow threshold for RM to be on	veh/h
q_l^{out}	Outflow from segment l	veh/h
$\bar{q}_{total}$	Total demand befor the merge	veh/h

$queue$	Queue length on the ramp	m
$Queue^{max}$	Maximum queue length	m
$Queue^{min}$	Minimum (desired) queue length	m
$\rho_{l,i}$	Density on route l, cell i	veh/km
$\rho_{l,i}^{cong}$	Critical density of cell i, road l	veh/km
$S_{l,i}$	Supply on cell i, route l	veh/h
$S^{control}$	Applied control parameter	
t	Time index	
T_c	RM cycle time	veh/h
v_{dm}	Downstream main road speed	km/h
v_l	Speed on segment l	km/h
$v_{l,i}$	Speed on route l, cell i	km/h
v_{off}^{th-vsl}	Speed threshold for VSL to be off	km/h
v_{on}^{th-vsl}	Speed threshold for VSL to be on	km/h
v_{um}	Upstream main road speed	km/h
v_{bn}	Speed before the bottleneck	km/h
v_l^{free}	Free-flow speed on segment l	km/h
v^{max}	Max speed limit	km/h
v_{th}^{off}	Speed threshold for RM to be off	km/h
v_{th}^{on}	Speed threshold for RM to be on	km/h
$v^{reduced}$	Reduced speed limit	km/h
v^{VSL}	Speed limit determined by VSL system	km/h
v_{app}^{VSL}	Applied Speed limit	km/h
v_{cal}^{VSL}	Speed limit decide by the VSL rule	km/h
$y_{solution}$	Calculated optimal control parameters	

Contents

Chapter 1

Introduction

In this chapter, the background of this research is presented in Section 1.1. With a research idea, the target topics in the literature review are listed in Section 1.2. Section 1.3 shows the structure of this thesis.

1.1 Background

Road transport is an important part of both passenger and freight transport. With increasing transportation demand, road traffic, and hence also freeway traffic, face issues on efficiency, emissions, and safety. The vehicle demand on freeway keeps growing in countries such as the United States and the Netherlands, except for the duration of the pandemic. Without a significant policy change, higher traffic demand usually leads to more travel delays on freeways (Texas A&M Transportation Institute: Mobility Division, 2021; Ministerie van Infrastructuur en Waterstaat, 2022). According to the International Energy Agency (IEA), passenger cars and trucks are the first and second largest sources of CO2 emissions in the transportation industry in the last 20 years (International Energy Agency, 2020).

There are many different ways to solve these problems in traffic on freeways. From the perspective of network-wise policy, promoting shared mobility and public transport aims to reduce the demand for private vehicles. The introduction of more electric vehicles can reduce the amount of emissions. From the perspective of traffic control, certain controllers can be applied on freeways to prevent / solve congestion. Traffic management methods that can act based on real-time traffic states are called Dynamic Traffic Management (DTM). DTM measures can solve challenges such as congestion before bottlenecks, suboptimal route choice, and the blocking of ramps (Hegyi et al., 2009).

With the development of sensor and communication technology, intelligent transportation systems (ITS) provide opportunities for DTMs to improve. With the realisation of vehicle-to-vehicle (V2V) and vehicle-to-infrastructure (V2I) communication, a more complex optimisation process can be completed in real-time control. The control instruction can also be applied to individual vehicles. The development of automated vehicles (AVs) also shows new directions for DTM research. AVs are more adjustable for DTM since their detailed

behaviour, such as acceleration behaviour or speed choice, is controlled instead of advised.

On freeways, mutiple locations may have the problems of a bottleneck queue, suboptimal route choice, and ramp blockage. Therefore, there will be multiple DTM measures on the freeways to solve the problems. With more advanced communication technology, DTM measures close to each other can be coordinated to optimise traffic for a larger road system. This raises the question whether the inclusion of a DTM measure can always further improve traffic. In other words, is the effect of coordination always beneficial enough? The answer to this question would be structure-specific. For certain road structures, DTMs may have a boosting effect on others, while they may also have a counter effect on each other in a different layout.

1.2 Reviewing topics

This research aims to simulate the impact of coordinating DTMs in a certain network structure, in which some counter effects between DTMs are expected. To form the research questions, research scope, and the research approach, a review of the existing literature is required. The topics for the literature review are listed below.

1. **DTM measures, their effect, and control strategies.** The first step of the review is to describe different DTM measures. By understanding their mechanism, the network structure where DTMs may have counter effects on each other can be designed preliminary. In addition, suitable DTM algorithm should be selected for the simulation.

2. **DTM coordination and the coordination approach.** By reviewing existing DTM coordination research, the research gap can be found. Besides, the approach/model used in the literature is also valuable in developing the approach for this research.

3. **The impact of coordination and the discussion about road structure.** The impact of coordination and the road structure where the DTMs are installed are two key points in this research. The relationship between road structure and the impact of coordination is expected to be found in some of the DTM coordination research.

4. **The network structure in coordination studies.** By comparing different network layouts, a suitable spatial scope can be determined for this research. The desired network should be able to include considered types of DTM.

1.3 Thesis structure

The rest of this thesis is arranged as follows: In Chapter 2, literature review and the identified research gaps are discussed. In Chapter 3, the problem is described in detail with a conceptual framework. The conceptual network and the selection of the simulation tool are also included. In Chapter 4, the models and algorithms included in this research are introduced, including DTM algorithms for RM, VSL and RG, as well as the coordination

algorithm. Chapter 5 describes in detail how each DTM measures and their algorithms are implemented in the simulation, together with the parameter settings. The simulation results are organised and interpreted in Chapter 6, followed by the conclusions in Chapter 7 and the discussions in Chapter 8.

Chapter 2

Literature review

This chapter presents the result of the literature review for this research. Section 2.1 discusses different types of DTM measures for freeway traffic management. Studies of DTM coordination are introduced in Section 2.2. Section 2.3 discusses network structures in the reviewed studies. The research gaps are presented in Section 2.4.

2.1 Freeway Dynamic Traffic Management

For freeways, there are mainly three types of dynamic traffic management (DTM) strategies (Amini et al., 2022): ramp management, mainstream control, and route guidance. Ramp management and mainstream control usually focus on solving (or preventing) congestion locally, while route guidance aims at a better traffic dynamic to prevent congestion. In addition to these three classes, lane control (LC) could also be a dynamic measure to improve freeway traffic, including lane changing control (LCC) and using peak-hour lane. The following paragraphs introduce the DTM mentioned above in detail with reference to the existing literature.

Route guidance (RG) can be classified as infrastructure-based RG and infrastructure-less RG (Khanjary and Hashemi, 2012). The former requires road infrastructure such as traffic detectors and Variable Message Sign(VMS). Centralised infrastructure-based RG gives route suggestions based on the calculated optimal routes (at the traffic management center) for the whole network, while in the decentralised infractructure-based RG, the calculation of optimal routes is realised locally on each vehicle. Infracture-less RG is essentially decentralised. It can also be divided into static RG and dynamic RG. The difference is whether to take real-time traffic state into consideration. The performance of dynamic infrastructure-less RG depends on the penetration rate of the required in-vehicle devices.

A network-level research about route guidance is presented by Ahn and Rakha (2013). In this case, route guidance is provided to individual vehicles through navigation tools or trip planning services. The route guidance with emission and fuel consumption concerns is discussed as eco-routing. The article simulates the traffic flow in the road network of Cleveland and Columbus, which include several interstates freeways. The results show a positive effect on the reduction of emission and fuel consumption under different scenarios generated with

different demand, congestion level, and eco-routing penetration rates. Dynamic route guidance is also a potential strategy to reduce emissions in urban road networks.

Ramp control aims to keep the mainstream flow slightly lower than the downstream capacity to prevent congestion. To achieve this, one commonly applied strategy is to restrict traffic flow from on-ramp using signals (ramp metering (RM)). There are both isolated ramp metering strategies and coordinated ramp metering strategies. Some common control algorithms include the Demand-Capacity algorithm (Masher, 1975), ALINEA (Hadj-Salem et al., 1990), FLOW (Winyoopadit, 2007). Proportional-Integral(PI) ALINEA is an extended version of ALINEA, which has been shown to have better performance than ALINEA in simulation when the bottleneck is far from the main road detectors (Kan et al., 2016).

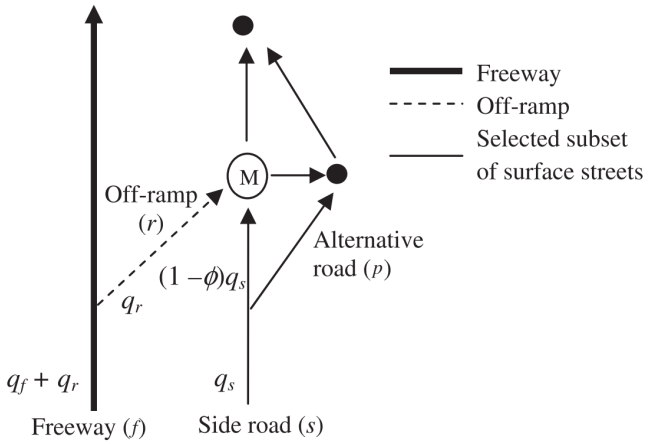

Figure 2.1: Network around off-ramp (Günther et al., 2012)

The situation on the off-ramp also matters for the main road. If there is congestion on the off-ramp, it will affect vehicles that are getting off the freeway. (Daganzo et al., 2002) discusses the temporal closure of certain off-ramps to make vehicles get off from other off-ramps. The focused off-ramps will reopen after the queues disappear. (Günther et al., 2012) presents an extended method for solving off-ramp congestion by rerouting vehicles on surface roads. As shown in Figure 2.1, the control method is to detour part of the side road flow that will merge with the off-ramp vehicles in M, so that the flow from the off-ramp can get to the surface network without any congestion. This article assumes a situation where there is no signal control at the end of off-ramp. A field experiment was carried out on an urban freeway in Santiago. Due to practical problems, the detour rate ϕ can only be 1 as it is quite difficult to detour a certain fraction of vehicles. The results show a significant reduction in delay and vehicle stops.

Mainstream traffic flow control (MTFC) is usually realised by Variable Speed Limit (VSL). VSL was first used for safety reasons or during a special period, such as when an accident occurs or when there is snow on the road surface. The two main objectives of using VSL are speed homogenisation and prevention of traffic breakdown (Lu and Shladover, 2014). VSL

with the second purpose usually has a more complicated control strategy and algorithm. Hegyi et al. (2005) introduces that VSL can work cooperatively with ramp metering to further improve freeway traffic efficiency. In this case, the VSL aims to reduce the upstream flow to prevent further propagation of congestion. An example of a control algorithm with roadside instructions is SPECIALIST (Hegyi et al., 2008). When congestion is detected, the roadside speed limit signs upstream will lower the value to prevent vehicles from driving into the jam. (Carlson et al., 2010) explains more about the purpose of the main stream flow control, which is to alleviate the effect of the capacity drop (Yuan et al., 2015). Regarding the road structure and VSL, Carlson et al. (2011) discussed a VSL strategy when there is a merging of two roads instead of a lane drop bottleneck. Martínez and Jin (2020) discussed the distance required from the start of the VSL application area to the bottleneck, as well as the relationship between the distance and the target speed limit. The speed limit instruction can also be given individually through in-vehicle devices, such as navigation tools. COSCAL (Mahajan et al., 2015) is a cooperative speed control system. Congestion is still detected by the road detectors, but the instruction of lowering speed is now given to individual vehicles.

Opening the peak-hour lane (also known as rush hour lane) is usually letting vehicles run on the hard shoulders for a certain period. In the Netherlands, peak hour lanes are commonly used. In addition to opening peak hours during morning / evening peaks, opening and closing of peak hours also depend on real-time traffic monitoring (Rijkswaterstaat, n.d.). If the traffic management center finds obstacles or accidents, peak-hour lanes might be closed.

Lane changing control (LCC) aims to reduce the disturbance caused by (mostly) mandatory lane changing. To avoid hindrance between vehicles from on-ramps and main road vehicles, Park and Smith (2012) simulates a lane change advisory system. If there is spare capacity on the leftmost lane and the gaps are within lane-changing acceptance threshold, advise will be given to main road vehicles. By advising more vehicles to change to a more left lane, there will be more space for on-ramp vehicles to merge in. The simulation shows that the system is more effective in intermediate congestion situations.

An essential problem for LCC is where should the advice/instruction be given. Gong and Du (2016) defines two zones before the bottleneck. The green zone is where vehicles can change the lane smoothly without speed decreasing, while in the yellow zone, which is closer to the bottleneck, vehicles must reduce their speed to change their lane. The lengths of the two zones can be found using optimisation. An optimal location for lane changing advice is found from scenario-based simulation. C. Zhang et al. (2019) argues that an optimal distribution of the location of lane change will be more effective than advising all vehicles to change lanes at a certain location. This conclusion is drawn from both the traffic flow theory and the simulation results.

DTM measures have also been tested in real-life applications. In the Netherlands, 11 RM sites are evaluated (Middelham & Taale, 2006). Capacity increase range from 1% to 5% and the speed increases range from 4km/h to 30km/h are observed. Mizuta et al. (2014) introduces traffic efficiency and environmental improvement achieved by ramp metering in several cities in the US. On Monash Freeway in Melbourne , coordinated ramp metering

with HERO algorithm is also proved to make further improvement (Papamichail et al., 2010). Hegyi and Hoogendoorn (2010) finds a 35 veh-hour travel time saving per resolved shock wave by SPECIALIST on A12 freeway in Netherlands. From the perspective of the flow-density relationship, Nissan and Koutsopoulosb (2011) finds no statistically significant differences with and without the advisory VSL system in Stockholm. Based on data analysis in Geistefeldt (2012), applying peak-hour lanes on two major freeways in the German federal state of Hesse increases capacity by 20-25%, and reduces the total congestion hour by 90%.

2.2 DTM coordination and performance

There have been studies about the combination of traffic measures. Most of them focus on simulating the effect of designed traffic combinations, in which measures are designed to cooperate.

One research direction is the coordination of the same kind of DTM, which includes: (1) Coordinated control with several DTM measures and (2) Combination of DTM and DTM considering the feature of ITS. A typical example is the coordination of ramp metering systems, in which the metering rate depends not only on flow on the main road but also the on demand/queue on other on-ramps. Research examples include heuristic ramp metering coordination (HERO) (Papamichail and Papageorgiou, 2008) and ANFIS Ramp Metering Cooperative (ARMC) (Greguric et al., 2015). Müller et al. (2016) simulate mixed traffic under two types of VSL control. In the simulation, traditional vehicles will (partially) follow the instruction of point-level VSL, while automated vehicles will directly receive individual speed instructions from the coordinated VSL (C-VSL). The results show that the performance is better with C-VSL alone than with C-VSL and VSL.

Another direction of research is coordination between different DTMs. Among all DTM combinations, the coordination between RM and VSL/MFTC is discussed more frequently. Hegyi et al. (2005) introduces a model predictive control that uses VSL to overcome the defect of RM. That is, RM can only prevent congestion instead of solving it. This control system shows better performance than a single RM in terms of total travel time. In Schelling et al. (2011), RM is coordinated with VSL with the SPECIALIST algorithm. Carlson et al. (2014) simulated different integrated control of RM and VSL with different control strategies. The TTS of integrated control scenarios are quite close to the scenario where only feedback RM is applied. Goatin et al. (2016) sets both the metering rate and the reduced speed limit as decision variables of an optimisation problem, in which maximising flow and minimising travel time are objectives. In this paper, two freeways are considered, while the split rates of vehicles at diverging points are set constant.

Pasquale et al. (2017) uses a multi-class Model Predictive Control that includes both route guidance and ramp metering. The control strategy shows a significant effect on emission reduction. Y. Zhang and Ioannou (2017) designs a combined lane changing control (LCC) and VSL control for different accident scenarios, macro and microscopic simulations showing further improvement by the combined control. Focusing on accident-caused lane-drop,

Guo et al. (2020) simulates the performance of coordinated VSL and LCC model predictive control. With a reduction in TTS from 20% to 40%, the coordinated control can outperform the VSL-only control. Tajdari et al. (2019) simulates an LCC + RM control system in a scenario in which half of the vehicles are conventional and the other half are automated. Although the lane changing behaviour of conventional vehicles acts as noise, in this case the controller can still smooth the density and prevent congestion. The author also simulates the case where LCC is off in low density situation. This will lead to slightly more TTS than always using LCC, but it is still 23% lower than the no-control scenario.

In several research studies, more than two types of DTM are integrated. Roncoli et al. (2016) includes RM, VSL and LCC in the dynamic density equation and designs a hierarchical MPC. In microscopic simulation, conventional vehicles and automated vehicles respond differently to LCC and MTFC. This control strategy shows an effect on preventing congestion mitigation. Wang et al. (2009) presents the coordination of all three DTM measures (RM,VSL, route guidance) on a corridor where there is a freeway, a street of lower level, and several ramps connecting them. Three control strategies are simulated. They are, respectively, isolated control; coordination of RM, VSL and signal on the street; integration of route guidance with the coordinated control. The result found that there is no significant improvement in traffic delay from isolated control to coordinated control. However, the integration of route guidance can considerably decrease the delay on the freeway (while the street has a slightly higher delay than before).

When there are more DTMs included in the coordination, the interactions between DTMs under non-coordinated cases are not discussed very explicitly. There is no explanation for why the DTMs cannot work well together when they work separately according to their own objectives.

Table 2.1 summarises the effects of coordinated DTMs. If not mentioned specially, the improvement is compared with the no-control scenario. In most of the research, the improvements after applying coordinated control are described as the percentage of TTS or Total Travel Delay(TTD) reduction, while in others, figures are used to show the improvements. Figure 2.2 shows that the combined control performs much better than only using RM, but TTS is similar to only using VSL. In Carlson et al. (2014), optimal integrated control has an improvement similar to that of using the optimal RM strategy. The possible cause might be that the road segments considered in these two studies are significantly longer than in other researches. Therefore, different mainstream and on-/off-ramp demands can lead to variation in the performance of RM and VSL.

The improvement reached by combinations including LCC is generally higher compared to coordinated control without LCC. This is reasonable, since LCC improves the merging behaviour at a microscopic level. The effect of LCC-included coordinated control is even greater when there is an accident. A counterintuitive observation from the summary is that, when more than two DTMs are combined, the improvement magnitude is actually lower than the combination of two DTMs. For example, Wang et al. (2009) and Roncoli et al. (2016) only reach a reduction of TTS / TTD of less than 10%. This could, on the one hand, be

because the control strategy design is more complex in the three-DTM coordination case. On the other hand, there may exist more implicit interactions between DTMs when more DTM is included. These interactions may also have a negative effect on total control performance.

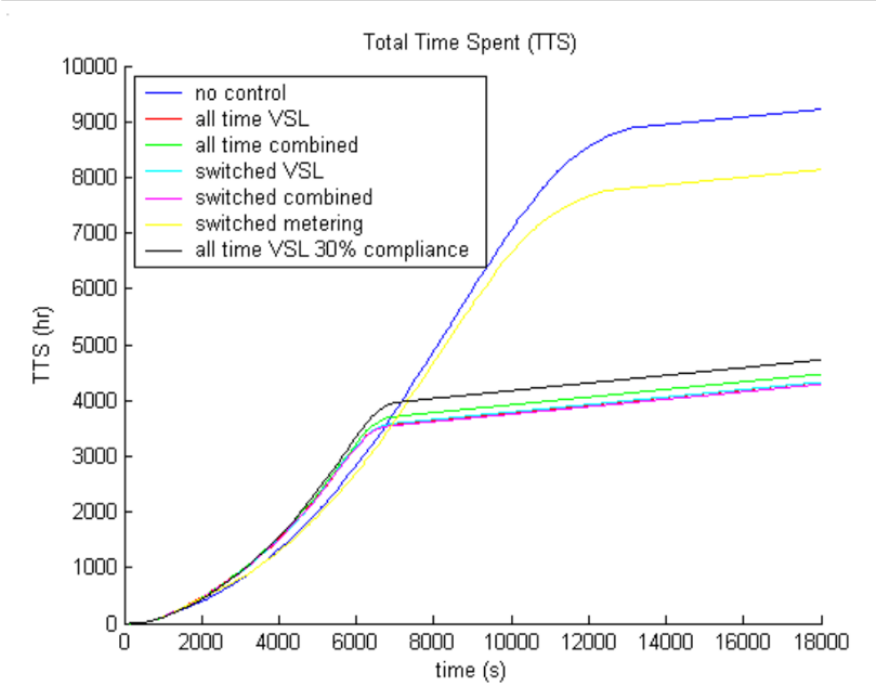

Figure 2.2: TTS curve over time under different control methods (Lu et al., 2010)

Table 2.1: DTM Coordination Effect

Paper	Impact of coordination	DTM combination	Road structure
Hegyi et al. (2005)	RM only: 5.3% TTS reduction Coordinated speed limits and ramp metering: 14.3% TTS reduction	RM+VSL	One road with an on-ramp
Lu et al. (2010)	Switched combined control performs much better than RM only, but similar to VSL only	CRM+VSL	a 6.5-mile freeway section
Lu and Shladover (2014)	Optimal integrated control has travel time reduction of 49.3%, but optimal RM can also reach 48.7%	RM+VSL	32 km long, with 21 on-ramps and 20 off-ramps
Goatin et al. (2016)	Optimal coordinated control made 12% improvement on a combined objective of TTS and total outflow	RM+VSL	Two roads with on-ramps
Pasquale et al. (2017)	Coordinated control has around 25% reduction on both TTS and emission	RG+RM	12 freeway links with 3 on-ramps
Wang et al. (2009)	Intergrated control leads to 7% delay reduction	RG+RM+VSL	One freeway and one urban road with several connections
Tajdari et al. (2019)	26% TTS reduction	RM+LCC	One segment with an on-ramp and a lane-drop following
Y. Zhang and Ioannou (2017)	VSL only scenario even leads to higher travel time, coordinated control reduces travel time by 10.6% and 18.8% respectively under low and high demand scenarios	VSL+LCC	One road corridor with temporal lane drops (accidents)
Guo et al. (2020)	23.8% TTS reduction for accident scenario, the reduction is larger when the duration of lane closure is longer	VSL+LCC	One road corridor with temporal lane drops (accidents)
Roncoli et al. (2016)	3.3% to 9.1% TTS reduction compared with no control	RM+VSL+LCC	One road with an on-ramp

2.3 Network structure

The network layouts in coordination studies are summarised in the last column in Table 2.1. In Appendix A, four examples of network structure are shown. For RM+VSL coordination, one corridor is considered (as shown in Figure A.1). Goatin et al. (2016) did simulation on a multi-road structure, but only for VSL optimisation. The RM+VSL coordination is still researched for one corridor. For coordination studies including RG, Wang et al. (2009) considers a structure with a freeway and a parallel urban road, including multiple intersection signals, RM signals, and split points (Figure A.3). Pasquale et al. (2017) has a large freeway network with three on-ramps and two split points with VMS route guidance (Figure A.4). Among the road structures in the reviewed studies, it can be seen that the structure either focuses on one corridor or considers many on-ramps and freeway links. There is no structure with a scope in the middle. For example, a two-freeway structure with only three or four ramps. This kind of structure may be more useful to explore the interactions between DTM measures, since the total number of possible DTM combination is more manageable.

2.4 Research gaps

The first research gap is that most studies focus on two types of DTMs. The two exceptions are Wang et al. (2009) and Roncoli et al. (2016). Both of these studies include RM and VSL. Wang et al. (2009) considers a freeway and a subordinate road connected to each other. In addition to RM and VSL, RG between two roads, as well as signal control on the subordinate road are also integrated in the coordinated control. Roncoli et al. (2016) coordinates RM, VSL and LCC. When the queue on the ramp is too long, the coordination increases the lateral flow towards more left lanes through LCC, as well as restricting the mainstream flow through VSL. Both studies do not have a downstream bottleneck after the ramp on the freeway. The cause of congestion is the accident on the main road in Wang et al. (2009) and the merging of vehicles at the merging point of the ramp and the main road in Roncoli et al. (2016). However, a downstream bottleneck is an important application situation for both RM and VSL. There should be research on coordination for more than two DTM types where there exist downstream bottlenecks after on-ramps.

The second gap is that coordination research often lacks discussion about the interaction between DTMs. What can be commonly seen in coordination research is that coordination performs better than the base case and single controlled cases. However, an explicit discussion of how coordination can improve the DTM interaction is usually ignored. For some of the studies, there lack scenarios for single DTM control. Therefore, it is difficult to conclude the value of coordination. For some other studies, there lack discussion about how two different DTM measures may not work well together when not coordinated. This kind of discussion is clearer in research studies using a heuristic/rule-based strategy (such as heuristic coordinated ramp metering (Papamichail and Papageorgiou, 2008)) than in research using optimisation control. Considering this research gap, an important question for DTM coordination study is: How does the interaction between DTMs change after coordination? To better answer this question, it is necessary to understand the original DTM

interaction considering the spatial layout of the DTMs.

The last gap is that the simulation model and the model used for predictive control are usually the same. There lacks the test of the coordination in a different environment. For example, a coordination algorithm built on macroscopic level can also be tested in a microscopic environment. With a different (more complex) model in the simulation, factors ignored in the assumptions of the predictive model can also affect the performance of the control. A more complex model may not be computationally efficient enough, but it can create a simulation environment closer to the real world.

Chapter 3

Problem description

This chapter describes the process and the scope of the research problem. Section 3.1 discusses the purpose of the research. The research questions are presented in Section 3.2. A detailed research process is introduced in Section 3.3. In Section 3.4, the network structure and the expected DTM interaction are discussed. In Section 3.5, the selection of the simulation model and tool is discussed.

3.1 Research purpose

Since there lacks traffic data when multiple DTMs are active, simulation-based analysis in a hypothetical network is more suitable for this research. This also provides more flexibility to test different DTM combinations. The major difference between this research and most existing research is that the requirement of coordination will be proved by simulation on this hypothetical network. That is, a situation is proposed in which different DTMs may work well with others. Then, a certain method to coordinate DTMs in this situation will be designed. After the simulation, the expected counter effect can be tested and the benefit of coordination can be analysed.

Eventually, this research is expected to give useful suggestions/rules about what should be noticed when a certain DTM combination is planned to be applied on a certain road structure. Besides, the simulation will show how much the performance can be improved once coordination is applied on the network. These suggestions may have value on both the research and the application sides. For further research, it can suggest the direction of the research. In other words, the coordination of some DTMs may be more beneficial considering the layout of the road and the traffic condition. For real-life applications, the results of this research can point out what might happen when adding a new DTM measure, and how much improvement can be reached if it is coordinated with existing measures.

3.2 Research questions

Based on the research gap, the research selects RM, VSL, and RG as the considered DTM measures. This is to keep the research within a reasonable scope. According to the litera-

ture review, there has been no coordination research on RG and LCC. This is because that LCC can only be simulated in a microscopic environment or macroscopic environment with special lateral flow model. However, to investigate RG a relatively large network needs to be considered. The purpose of this research is to explore the value of coordinating these three DTMs on a certain network structure. The coordination will be designed to solve the potential counter effect of DTMs in a non-coordinated situation. Therefore, the main research question of this research is: **What is the impact of coordinating RM, VSL and RG on a road structure where they have potential counter effects on each other when following local objectives?**

To answer the main research questions, several subquestions must be answered first. The subquestions are listed below:

1. **In what kind of road structure will RM, VSL, and RG have potential conflicting effect?** The answer of this subquestion affect the simulation network (either conceptual or real-life road network). To answer this subquestion, the network layouts in real-life and DTM coordination research studies need to be reviewed.

2. **What are appropriate control algorithms for each DTM?** After the literature review, there are many control strategy options for each kind of DTM. This subquestion should be answered with consideration on the simulation environment and the feasibility of including the measures in the coordinated control.

3. **What kind of coordination method can be used to tackle the conflict and improve network performance?** The answer to this subquestion depends on the road structure and the potential conflicting effect between DTMs.

4. **How should the simulation be set?** There are different models and environments for the simulation. The answer to this subquestion should consider the requirement of the research, with regard to the DTM algorithms and coordination method.

5. **What are suitable indicators to measure network performance?** The answer to this subquestion should include both the indicators and the corresponding way to obtain it from the selected simulation method.

3.3 Research process

As shown in Figure 3.1, the approach of this research can be divided into 4 stages. The first stage is modelling and scenario setting. The scenarios will be set by combining different DTMs with different spatial layouts. There will first be a network which can include all considered DTMs. This will be done with reference to three aspects: (1) real-life examples where DTMs with different local objectives are located close to each other; (2) inspiration from existing DTM coordination research; (3) conceptual analysis on which combinations have theoretical (counter) effects between DTMs. In addition to scenario setting, traffic flow models and simulation tools must also be reviewed and selected. Based on the network structure and selected DTM mechanisms, a coordination algorithm is also designed at this

stage.

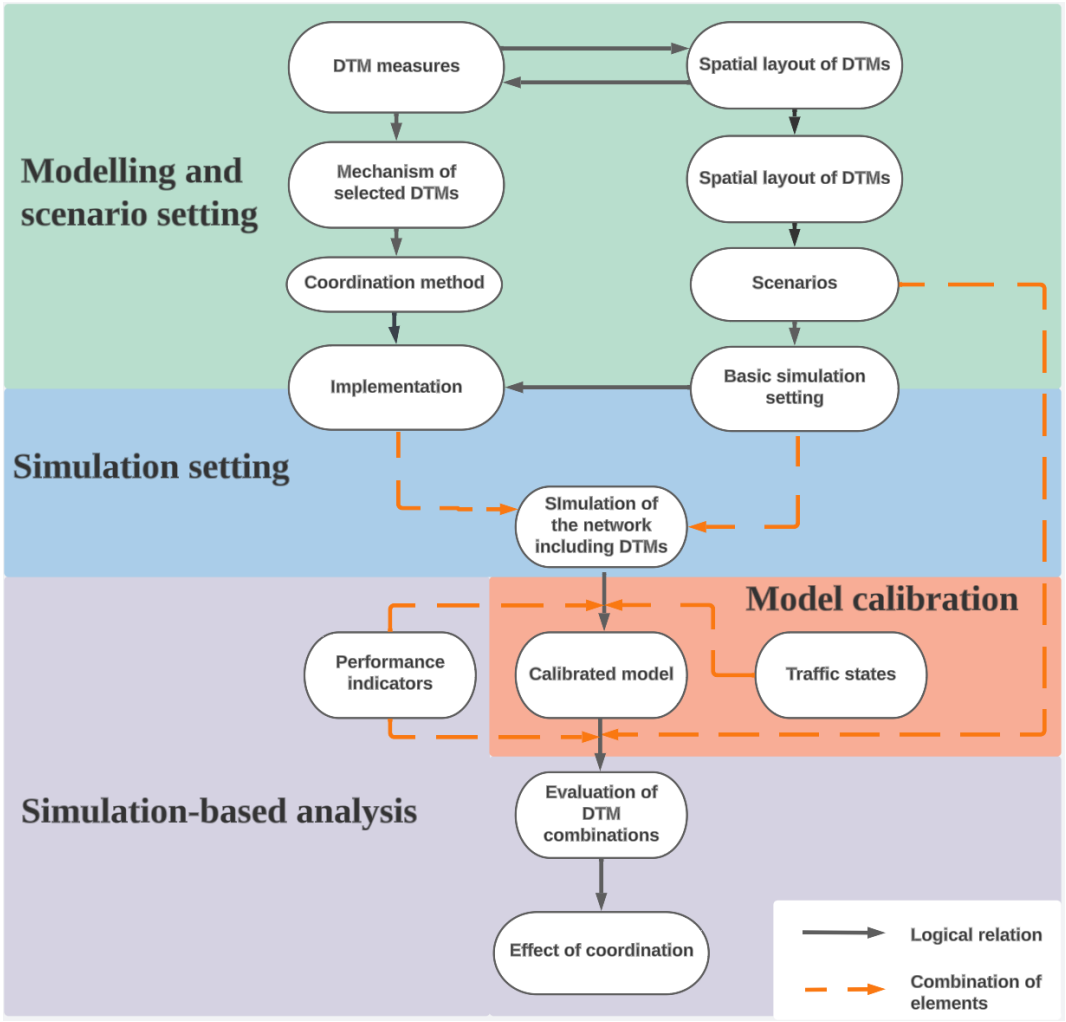

Figure 3.1: Research process

The second stage is simulation setting. At this stage, the network will be built in a simulation tool. DTM with the selected algorithms are required to be implemented in the simulation environment. The designed network should include possible counter effects between DTMs. The expected interaction will be given for these DTM measures, and a coordination strategy will be designed to solve the potential counter effect.

In stage 3, the simulation in stage two can be calibrated to ensure that the DTMs are working as expected. The correctness of the simulation as well as the effects of each DTM type will be verified. Parameters in the traffic flow model and in the DTM algorithm are also required to be calibrated. At the end of this stage, it is also required to find ways to derive and visualise performance indicators from the simulation.

The fourth stage is the simulation and analysis. The evaluation of the interactions be-

tween DTMs will be based on several performance indicators, such as the total time spent and the total amount of emission. The evaluation of different combinations of DTM will be interpreted.

3.4 Conceptual network and expected interaction

For simplification, only the freeway is considered and urban roads are not involved, therefore, intersection signal control, also as a DTM measure, will not be discussed. Research will focus on RM, VSL and RG. For these DTM measures, the network needs to have the following structures:

1. To have a route choice, there should be at least two routes for reaching the same destination;
2. On-ramps should be included since RM is one of the considered DTM measures. They should also be long enough to include ramp queue detectors;
3. There should be bottlenecks which might generate congestion. In such cases, VSL for preventing traffic breakdown can be used.

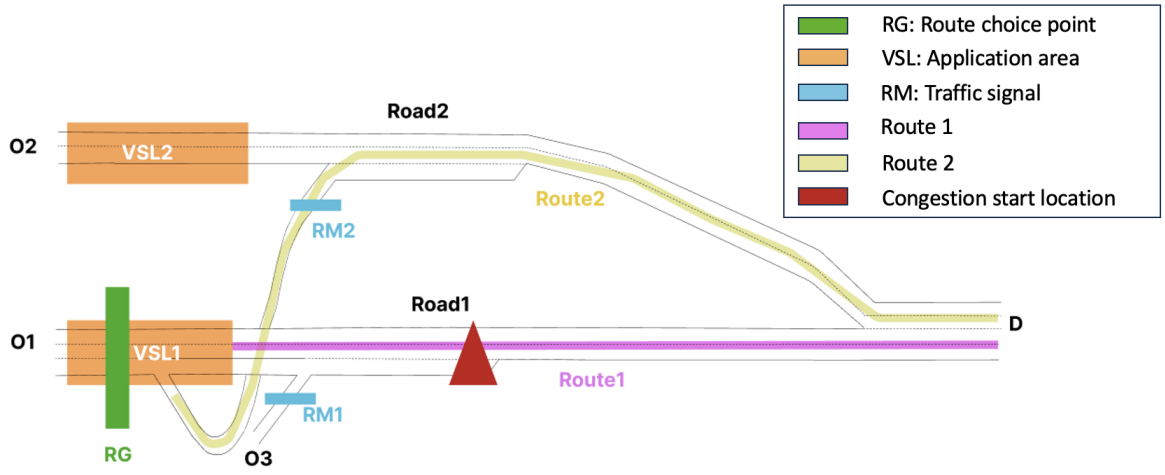

Figure 3.2: Conceptual road network layout

The conceptual network is shown in Figure 3.2. Two freeways from two main origins O1 and O2 will go to the main destination D. There is also demand travel from subordinate origins O3, which also have D as destination. A real-world reference of this kind of structure can be seen in Figure 3.3. On the northwest of Amsterdam, A9 and A22 freeways form a structure similar to the conceptual network in this research. To travel from South to North, there are two route choices. The length of Route 1 is 5.6 km, and the length of Route 2 is 7.1 km. There are two bottlenecks on the two routes.

For each on-ramp, ramp metering is available. The upstream segments of the bottlenecks

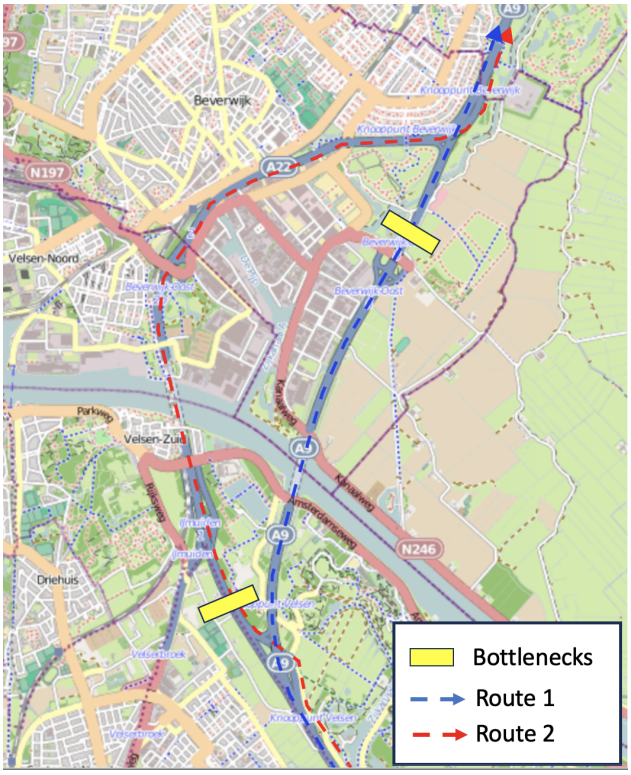

Figure 3.3: Similar road structure in real life

have VSL available. Through the connection between routes 1 and 2, vehicles can change their route from 1 to 2, making RG available upstream. In the following part of this report, the route from O1 to D via Road 1 is called Route 1 and the route from O1 to D via Road 2 is called Route 2.

As can be seen in Figure 3.2, the distance of Route 2 is longer than that of Route 1. Based on Wardrop's principle (Wardrop, 1952), there will be no vehicle using Route 2 when both routes are in the free-flow state. However, when congestion occurs first before the bottleneck on Route 1 (shown with the red triangle in Figure 3.2), the travel time will then increase on Route 1. When the travel time is longer, RG will guide vehicles to Route 2. In a RG-only scenario, it is possible that congestion occurs alternatively before bottlenecks on Route 1 and Route 2. In such a case, the traffic on both routes will be unstable and the congestion could become severe.

To prevent congestion, more DTM measures, such as RM and VSL could be used to meter either the ramp flow or mainstream flow. However, these measures will have conflicting objectives against others, since they are designed for different roads. For example, if RM2 restricts the flow into Road 2, the congestion may not occur there and the travel time will be shorter. Meanwhile, the connection part is also considered when calculating the travel time for Route 2. This means that the travel time of Route 2 could still be higher than that of Route 1, which keeps vehicles on Route 1 and worsens congestion there. From this point of view, RM 2 is inherently conflicting with RM1 and VSL1.

The purpose of this research is to explore the conflicting effects between DTMs and to build a coordination algorithm for the DTMs in the conceptual network to further improve performance.

3.5 Simulation model and tools

3.5.1 Models for simulation

To simulate the traffic in the proposed research network in Figure 3.2, both macroscopic model and microscopic model can be used. The former models the traffic state on small road segments and how the flow transmits from one segment to the next. Examples are the Cell Transmission Model (Daganzo, 1994) and METANET (Messmer & Papageorgiou, 1990). Microscopic model captures the states of individual vehicles, which normally contains a longitudinal car-following (CF) model and lateral lane changing (LC) model. Examples of CF models are the Intelligent Driver Model (Treiber et al., 2000) and Newell's model (Newell, 2002).

The trade-off for selecting these two types of models is about the computational efficiency and the level of realistic. Macroscopic simulation runs faster, while it only includes aggregated traffic states such as flow and density. Microscopic models can include more randomness in vehicle departure and interactions between individual vehicles, while the simulation time will be much longer. For this research network, most of the route changing behaviour will happen on the short segment before the off ramp on Road 1. This means that plenty of lane changes may happen on this segment. It is then better to include the lane-changing model for the simulation, which makes microscopic models preferable.

3.5.2 Simulation implementation

With the simulation model, one factor to consider is that how to realise the simulation based on the preferred model. In Table 3.1, three ways of simulation implementation are compared. The first are self-implemented macroscopic traffic flow models. The second are macroscopic simulation tools. CTMsim (Kurzhanskiy, 2023) is one of them. It has a graphical user interface (GUI) for users to define network information such as Fundamental Diagram (FD) parameters and demand. Thirdly, microsimulation tools such as Vissim and SUMO can be used. For the selected research network, it would be too time consuming for one to build a microsimulation by himself. Therefore, self-implemented microsimulation is not discussed here.

The advantage of building the simulation is that one can make required extension to the traffic flow models. However, more time is needed to build the simulation environment. The advantage of using simulation software is that multiple traffic flow models are already available. Meanwhile, the time for tuning the simulation may be longer, since the underlying models in the software are not always clearly described. For this research, the focus is not on the traffic flow models. Therefore, it is more reasonable to use an existing simulation tool

than to build a new simulation environment.

This research has mainly five requirements. Firstly, the research is about the evolution of dynamic traffic. All three tools can model dynamic traffic states. The second requirement is to model multiple routes. In self-implemented macrosimulation and microsimulation, the structure of the network can be defined flexibly, while building multiple routes is not possible in CTMsim. As for the traffic flow model, CTMsim and microsimulation tools already have traffic flow models implemented. For self-implemented macrosimulation, the time to create the simulation environment would be longer.

Among the three tools, CTMsim is not able to capture lane changing behaviour. Self-implemented macrosimulation has the possibility of including a lateral model (Tajdari et al., 2019), but it can also significantly increase the difficulty of implementation. As for microsimulation tools, different types of lane changing models are available. The last requirement is the feasibility of implementing customised control strategies. This can be done in both self-defined macro-simulation and microsimulation tools. Through comparison, micro-simulation tools are the most suitable for this research. It does not require too much of the model implementation. In addition, it gives more space to include several control strategies via the Application Programming Interface (API).

In all, microsimulation software is the most suitable way to perform simulation. It meets the five requirements of the simulation. Although it will lead to a longer simulation time, it can capture more detailed vehicle behaviour. It is also the most flexible simulation way when one needs to define customised control on the research network. Among microsimulation tools, SUMO has the advantage of being open source and having compatibility with different operating systems. Therefore, SUMO software and TraCI ("TraCI - SUMO Documentation", n.d.) interface compose the simulation tool for this research.

Table 3.1: Simulation tool comparison

Requirements	Self-implemented Macrosimulation	CTMsim	PTV Vissim /SUMO
Capture dynamic traffic states	✓	✓	✓
Model multiple routes	✓	×	✓
Traffic flow model	Need to be implemented	✓	✓
Lane changing behaviour	Additional lateral model	×	✓
Implement customised control strategy	✓	×	✓

Chapter 4

Control algorithm

The research process and the selection of simulation tools have been discussed in Chapter 3. Before the simulation, the specification of DTM controls needs to be determined. In this chapter, the algorithms and models used in this research are described. Section 4.1 presents the mechanisms of RM, VSL and RG. The coordination method is discussed in Section 4.2. Section 4.3 discusses the method for smoothing control parameters over control steps.

4.1 DTM algorithm

The selection of DTM strategies considers both the feasibility of a single DTM and the feasibility of coordination. In a microsimulation environment, traffic control can be given to individual vehicles (cooperative control) or to all vehicles at a certain location (roadside control). For RM, the control is carried out by the traffic signal on the ramp. Vehicle-level RM is also possible with connected automated vehicles (Zhao et al., 2021). However, this is not within the scope of this research, and the implementation will be too complex. This is because the individual level RM requires control on the acceleration and deceleration of vehicles.

As for VSL, both road-side instruction and in-vehicle advice can be used. SPECIALIST (Hegyi and Hoogendoorn, 2010) and COSCAL (Mahajan et al., 2015) are examples for the two types of VSL control. In this research, consider the scope and network scale, the VSL algorithm should be road-side based. This is because the control parameters of a cooperative VSL are more complex. Taking COSCAL as an example, it has different instructions for vehicles that are in different positions referring to the jam head. This also makes it difficult to include it in a coordinated control, especially when route change is also considered. In this case, there may be more overtaking behaviour, as some vehicles will get on the off-ramp and change route. This adds complexity to the implementation of trajectory-based individual control methods, such as COSCAL.

The categories of RG are introduced in Khanjary and Hashemi (2012). Different attributes of RG includes whether there is roadside infrastructure (e.g., variable message sign (VMS)), whether it is based on experience travel time, real-time travel time, or predicted travel time,

etc. As discussed in Section 3.4, a RG based on real-time travel time may cause alternative congestion on each route. Therefore, to improve the performance of the network, a centralised RG should be used, which considers the system optimal instead of user equilibrium. To make the situation more realistic, it is assumed that a proportion of vehicles will use instantaneous travel time information on the VMS board and the other vehicles will comply to the in-vehicle guidance instruction.

The research selects an RM system with ramp traffic signal, roadside VSL and a RG combination of both VMS-based RG and predictive, centralised RG. The algorithms are discussed in Section 4.1.1 to 4.1.3

4.1.1 Ramp metering algorithm

One of the goals of this research is to provide an impact evaluation on adding a new DTM measure on the road segment with existing DTM measures around it. Ramp metering is a commonly applied control on freeways in the Netherlands, with the demand-capacity (Masher, 1975) algorithm implemented. The feed-forward strategy calculates the remaining capacity for the downstream main road to determine the allowed inflow from on-ramp (metering rate). The main equation is as follows:

$$q^{control}(t+1) = q^{target} - q_{um}(t) \tag{4.1}$$

Where t represents the time interval $[t * dt, (t+1) * dt)$. In this research, the time step $dt = 1s$. The control step for RM is also 1s. However, the aggregation level for flow data for RM is 60s, which means that the minimum duration for the metering rate to change is 60s. In the following parts t will be referred to as time step. $q_{control}$ is the metering rate, q^{target} is the target flow downstream and q^{um} is the flow detected on the main road upstream. The common strategy of ramp metering is "one-car-per-green", with this mechanism, the $q^{control}$ can be realised by changing the cycle time of the ramp signal, which can be represented as:

$$T_c(t) = \frac{n * 3600}{q_{control}(t)} \tag{4.2}$$

Where T_c is the cycle time of the signal control and n is the lane number of the ramp.

RM system is not active all the time, the active time could be fixed or based on certain switch-on and off criteria. (Taale, 2023) introduces the RWS (Rijkswaterstaat) RM control algorithm together with the practical switching on and off rules. They are shown in Equation 4.3 to 4.8

$$\bar{q}_{total} = q_{um} + q_{ur} \tag{4.3}$$

$$I^{on}_{flow} = \begin{cases} 1, & \text{if} \quad \bar{q}_{total} > q^{on}_{th} \\ 0, & \text{if} \quad \bar{q}_{total} \leq q^{on}_{th} \end{cases} \tag{4.4}$$

$$I^{off}_{flow} = \begin{cases} 1, & \text{if} \quad \bar{q}_{total} < q^{off}_{th} \\ 0, & \text{if} \quad \bar{q}_{total} \geq q^{off}_{th} \end{cases} \tag{4.5}$$

In equations 4.4 to 4.5, I_{flow}^{on} and I_{flow}^{off} are the flow index for the on or off of the RM system. $\bar{q}_{total}$ is the predicted sum of q_{um} and the detected upstream ramp flow (or ramp demand) q_{ur}.

$$I_{speed}^{on}(t) = \begin{cases} 1, & \text{if} \quad v_{um}(t) < v_{th}^{on} \vee v_{dm}(t) < v_{th}^{on} \\ 0, & \text{if} \quad v_{um}(t) \geq v_{th}^{on} \wedge v_{dm}(t) \geq v_{th}^{on} \end{cases} \tag{4.6}$$

$$I_{speed}^{off}(t) = \begin{cases} 1, & \text{if} \quad v_{um}(t) > v_{th}^{off} \wedge v_{dm}(t) > v_{th}^{off} \\ 0, & \text{if} \quad v_{um}(t) \leq v_{th}^{off} \vee v_{dm}(t) \leq v_{th}^{off} \end{cases} \tag{4.7}$$

Similarly to flow on and off indexes, speed indexes are determined based on the upstream and downstream detected speed v_{um} and v_{dm} on the main road.

$$I_{RM}(t) = \begin{cases} 1, & \text{if} \quad I_{flow}^{on}(t) = 1 \vee I_{speed}^{on}(t) = 1 \\ 0, & \text{if} \quad I_{flow}^{off}(t) = 1 \wedge I_{speed}^{off}(t) = 1 \end{cases} \tag{4.8}$$

In Equation 4.8, the overall RM on and off index I_{RM} is determined based on four indexes from Equations 4.4, 4.5, 4.6, and 4.7. The rule can be summarised as: when either flow or speed shows the RM needs to be activated, it will be on; when both flow and speed show no need to meter ramp flow, it will be off.

$$I_{RM}^{queue}(t) = \begin{cases} 1, & \text{if} \quad queue(t) \leq Queue^{min} \\ 0, & \text{if} \quad queue(t) \geq Queue^{max} \\ I_{RM}^{queue}(t-1) & \text{if} \quad Queue^{min} \leq queue(t) \leq Queue^{max} \end{cases} \tag{4.9}$$

The queue on on-ramps is also required to be considered when deciding the on and off of RM system. In real life, it is dangerous if the queue spills back to upstream road. In this simulation, ramp queue that keeps increasing will contribute largely to the total delay of the network. It is also possible that the ramp queue blocks vehicles outside of the simulation network. Eq. 4.9 shows the rules applied in the simulation, the index $I_{RM}^{queue}(t)$ is 0 when the queue is higher than a certain threshold and 1 if it is lower than the minimum (desired) queue length. RM is on when $I_{RM}(t) * I_{RM}^{queue}(t) = 1$ and off in other cases. The rules relating to turning on/off RM according to the queue on ramp are different from them in Taale (2023). This is because the control algorithm in this research uses lane area detectors in the simulation, which can reflect a specific queue length. Meanwhile, in real-life applications in the Netherlands, loop detectors detect if there is a queue on the ramp via occupancy data.

4.1.2 Variable speed limit algorithm

The variable speed limit is based on a feedback control scheme, which is close to the applied VSL system in real life. When the speed is lower than the threshold before the bottleneck, the speed limit should be reduced on more upstream road segments. The control strategy can be represented as follows.

$$v^{VSL}(t) = \begin{cases} v^{reduced}, & \text{if} \quad v^{bn}(t) \leq v_{on}^{th-vsl} \\ v^{max}, & \text{if} \quad v^{bn}(t) \geq v_{off}^{th-vsl} \\ v^{VSL}(t-1), & \text{if} \quad v_{on}^{th-vsl} \leq v^{bn}(t) \leq v_{off}^{th-vsl} \end{cases} \tag{4.10}$$

Where v^{max} and $v^{reduced}$ are the maximum speed allowed on the road and the reduced speed limit when VSL is on (constant). $v^{bn}(t)$ is the speed detected before the bottleneck. v_{on}^{th-vsl}, v_{off}^{th-vsl} are thresholds for VSL to be on and off, v_{off}^{th-vsl} is supposed to be higher than v_{on}^{th-vsl} for the stability of traffic in the controlled segments. When the detected speed before the bottleneck is between these two thresholds, VSL systems keep the state of the last control step.

4.1.3 Route guidance mechanism

The research includes both road-side and in-vehicle route guidance, the road-side guidance will provide the instantaneous travel time of each route, while the in-vehicle guidance will be based on traffic state prediction.

Road-side RG

The road-side RG assumes that a certain proportion of vehicles will select their route based on the instantaneous travel time. This control aims to represent the effect of Variable Message Signs (VMS). Vehicles before the split point will receive the travel time information simultaneously and will select their routes accordingly. The road-side RG will be referred to as VMS RG for the rest of the report.

Although the road-side RG described above can help vehicles find a faster route, it has a major drawback. That is, most vehicles will select the fastest route once the travel time of that route is slightly lower than that of other alternative routes. This will soon cause an increase in travel time on the faster route, and vehicles will switch to the new faster route. This can cause oscillations on the ramp flow, and it is difficult to reach an equilibrium. Therefore, a predictive RG is introduced that aims to divide vehicles with the optimal predicted split rate. It will be called predictive RG or in-vehicle RG in the rest of the report.

In-vehicle RG

For the purpose of reducing computing time and simplification, the predictive RG will predict and optimise the traffic state for a certain segment instead of the whole network. The control step is 10s, and the prediction will be done for the next 10s (a prediction horizon of 1). It is supposed to give individual in-vehicle instructions to vehicles. As can be seen in Figure 4.1, two three-lane segments are selected before the lane drop on two routes. This is because these two segments are downstream of the split point and the merging points on each route, making the effect of RG more convenient to be included in the prediction model. These routes are represented by the index $l \in [1, 2]$.

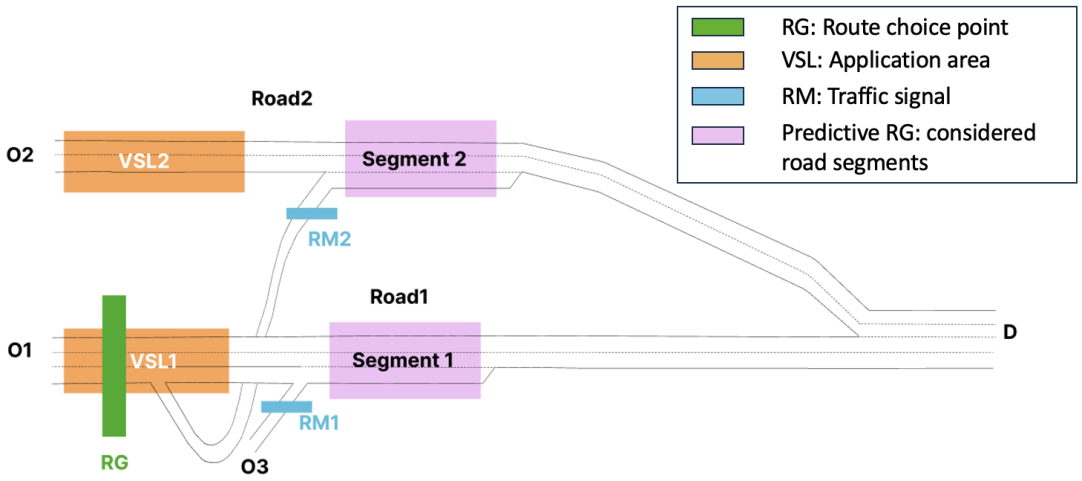

Figure 4.1: Road segments for prediction

$$J(t) = \sum_{j=t}^{j=t+N_p-1} \frac{N_1^{veh}(j) * L_1/v_1(j) + N_2^{veh}(j) * L_2/v_2(j)}{N_1^{veh}(j) + N_2^{veh}(j)} + Penalty^{ib}(t) \tag{4.11}$$

Eq. 4.11 is the objective function which aims to minimise the average travel time. Where $N_1^{veh}(j)$, $N_2^{veh}(j)$ are the number of vehicles in segment 1 and 2 at time j, $L1$, $L2$ are the length of the road segments. $v_1(j)$ and $v_2(j)$ are the average speed of each road segment. $Penalty^{ib}(t)$ is a positive penalty term that can increase the value of the objective when the travel time has a huge difference between segments 1 and 2. Since the objective is a combination of the speed on two segments, it is possible that the optimal solution leads to an imbalanced distribution of vehicles, which is not the purpose of RG. To prevent imbalanced solutions, the penalty term $Penalty^{ib}(t)$ is included. As can be seen in Eq. 4.12, the penalty is 0 when the difference between v_1 and v_2 is less than 10%, and it adds the free-flow mean travel time to the objective when the difference is greater than 10%.

$$Penalty^{ib}(t) = \begin{cases} \frac{2*(L_1+L_2)}{v_1^{free}+v_2^{free}}, & \text{if } \frac{|v_1(t)-v_2(t)|}{v_1(t)} \geq 0.1 \\ 0, & \text{if } \frac{|v_1(t)-v_2(t)|}{v_1(t)} < 0.1 \end{cases} \tag{4.12}$$

In Eq. 4.13 to Eq. 4.18, the prediction model used for the predictive RG are presented.

$$v_l(t) = V(\rho_l(t)) = v_l^{free} * exp\left(-\frac{1}{2}\left(\frac{\rho_l(t)}{\rho_l^{cong}}\right)^2\right) \tag{4.13}$$

The speed on each road segment is calculated using an exponential speed-density relationship (Eq. 4.13), where v_l^{free} is the free-flow speed of segment l and ρ_l^{cong} is the critical density of segment l. The density on segment l at time t is obtained as $N_l^{veh}(t)/L_l$. The number of vehicles is updated using Eq. 4.14. It is calculated using the inflow and outflow of the segments. dt is the time resolution of the prediction.

$$N_l^{veh}(t+1) = N_l^{veh}(t) - q_l^{out}(t) * dt + q_l^{in}(t) * dt \tag{4.14}$$

The outflow (Eq.4.15) of each segment is the minimum value of demand $v_l(t)*\rho_l(t)$ and the maximum supply (i.e., the capacity of the downstream segment) C_l^{ds}. Since it is assumed that there is no downstream bottleneck, the downstream segment will not be congested. Therefore, the maximum supply can always be reached.

$$q_l^{out}(t) = min\{v_l(t) * \rho_l(t), C_l^{ds}\} \tag{4.15}$$

As shown in Eq. 4.16 and 4.17, the inflows are directly affected by the decision variable $p^{RG}(t)$, which is the proportion of vehicles that will use route 1. The inflow to road segment 1 is thus:

$$q_1^{in}(t) = d_1^{ramp}(t) + p^{RG}(t) * d_1(t) \tag{4.16}$$

Where $d_1^{ramp}(t)$ is the demand of on-ramp 1 and $d_1(t)$ is the main road demand upstream of the off-ramp 1. $p^{RG}(t) * d_1(t)$ is the vehicles that choose to travel to road segment 1. Therefore, the rest of vehicles $(1 - p^{RG}(t)) * d_1(t)$ will travel through on-ramp 2 to segment 2. Then the overall inflow for segment 2 is:

$$q_2^{in}(t) = d_2(t) + (1 - p^{RG}(t)) * d_1(t) * \beta^{adj}(t) \tag{4.17}$$

Where $d_2(t)$ is the main road demand on road 2. A special coefficient $\beta^{adj}(t)$ for the mixed RG control. It is assumed that some vehicles are using VMS information (reactive RG) and others are following the guidance from predictive RG. If the travel time on road 2 is shorter, the flow from off-ramp 1 to route 2 will be higher than $(1 - p^{RG}(t)) * d_1(t)$. However, in this case, there is no predicted travel time available, hence the exact number of vehicles switching route using VMS cannot be predicted. The coefficient $\beta^{adj}(t)$ is for a rough estimation of the number of these vehicles. As shown in Eq. 4.18, when the speed on segment 1 is much lower than the speed on route 2, the coefficient has a value of p^{extra}, which is higher than 1. If the speed on segment 1 is not low enough, it is assumed that vehicles using VMS will keep on Route 1. In this case, $\beta^{adj}(t)$ is 1 since only vehicles using predictive RG will travel through the off-ramp.

$$\beta^{adj}(t) = \begin{cases} p^{extra}, & \text{if} \quad v_1(t) \leq 0.9 * v_2(t) \\ 1, & \text{if} \quad v_1(t) \geq 0.9 * v_2(t) \end{cases} \tag{4.18}$$

4.2 Coordinated MPC control

Coordinated control also has a model predictive structure. Compared to predictive RG control, coordinated control considers more road segments. In addition, it includes RM and VSL, as well as their evolution during the prediction horizon in the prediction model. The coordination aims to control these two parallel bottlenecks as one. That is, to keep the total flow before two bottlenecks close to the sum of bottleneck capacity.

For the purpose of reducing the computation time, the cell transmission model (CTM)

(Daganzo, 1994) is used as the prediction model. As shown in Figure 4.2, several "cells" are considered before and after the bottlenecks on two roads.

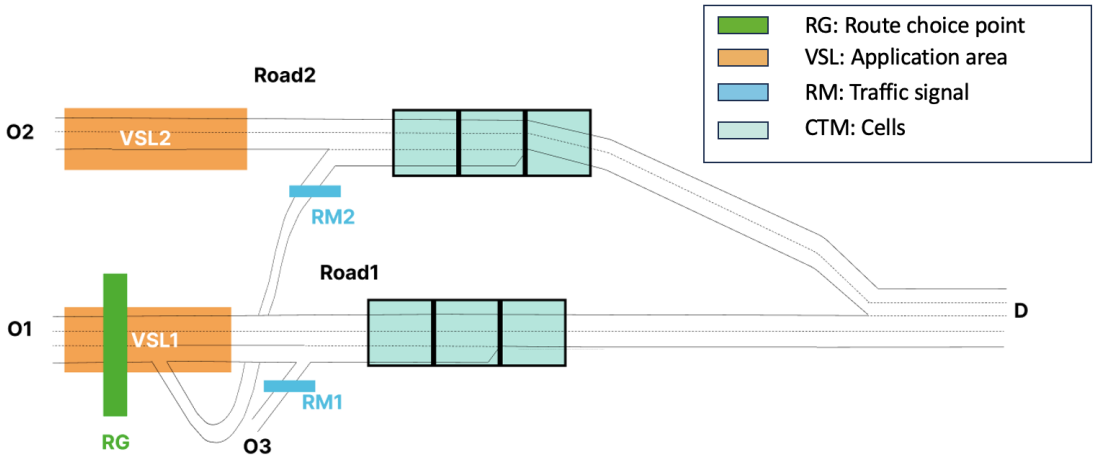

Figure 4.2: Cells for prediction model

Eq.4.19 to 4.22 show the process of CTM. Eq.4.19 is the density update equation, where $\rho_{l,i}(t+1)$, the density at time $t+1$ of cell i on road l is calculated from the density at time t, the flow difference between two boundaries of the current cell and the time and space resolution dt and dx.

$$\rho_{l,i}(t+1) = \rho_{l,i}(t) + (q_{l,i-1/2}(t) - q_{l,i+1/2}(t)) * dt/dx \tag{4.19}$$

Based on the fundamental diagram of each cell, the demand and supply of each cell can be calculated. In Eq. 4.20 and 4.21, the demand $D_{l,i}(t)$ is calculated by the flow density relationship $Q(\rho_{l,i}(t))$ in uncongested situation, and reach the capacity of the cell $C_{l,i}$ when the density is higher than the critical density $\rho_{l,i}^{cong}$. As for the supply $S_{l,i}(t)$, it can be as high as the capacity when it is not congested, and reduces according to the flow-density relationship when the critical density is exceeded.

$$D_{l,i}(t) = \begin{cases} Q(\rho_{l,i}(t)), & \text{if} \quad \rho_{l,i}(t)) < \rho_{l,i}^{cong} \\ C_{l,i}, & \text{if} \quad \rho_{l,i}(t)) >= \rho_{l,i}^{cong} \end{cases} \tag{4.20}$$

$$S_{l,i}(t) = \begin{cases} C_{l,i}, & \text{if} \quad \rho_{l,i}(t)) < \rho_{l,i}^{cong} \\ Q(\rho_{l,i}(t)), & \text{if} \quad \rho_{l,i}(t)) >= \rho_{l,i}^{cong} \end{cases} \tag{4.21}$$

As shown in Eq. 4.22, the flow that passes through each cell boundary is the minimum between the demand of the previous cell and the supply of the next cell. The calculated flow will be used in Eq. 4.19 to form the complete update cycle.

$$q_{l,i+1/2}(t) = \min(D_{l,i}(t), S_{l,i+1}(t)) \tag{4.22}$$

Since the two bottlenecks are the only locations for severe congestion to occur, the optimisation of the network performance can be simplified to optimise the performance after the bottlenecks. Therefore, the sum of outflow after the lane-drop is selected as the objective. The objective function is:

$$J(t) = \sum_{j=t}^{j=t+N_p^{coor}-1} q_1^{out}(j) + q_2^{out}(j) - Penalty^{imbalance}(j) \tag{4.23}$$

Where N_p^{coor} is the prediction horizon, $Penalty^{imbalance}(j)$ is the penalty value for traffic state imbalance. The usage of this penalty term is because that the objective is the sum of flow on both routes, which may lead do imbalanced states on different routes.

In coordinated control, every DTM measure should serve the same objective (Eq. 4.23). During the prediction process, the control parameters will change sequentially based on the initial parameters selected. This means that every control parameter should be influential in the objective. Eq.4.24 to Eq. 4.27 integrates all the control parameters in the inflow to cells on each road. The five control parameters are $q_1^{control}(t)$, $q_2^{control}(t)$, $v_1^{VSL}(t)$, $v_2^{VSL}(t)$, $p^{RG}(t)$.

The inflow on each road will be the sum of the main road inflow and the ramp inflow. For Road 1, the total demand for the main road will be divided by the split rate of the predictive RG $p^{RG}(t)$. When VSL is on, it is assumed that the inflow will reduce proportionally. Therefore, the inflow of the main road should also multiply the proportion of speed reduction $v_1^{VSL}(t)/v^{max}$. This implies a linear relationship between the upstream flow and speed. The inflow from the on-ramp will be the metered flow by RM1 $q_1^{RM}(t)$. As represented in Eq. 4.25, the metered flow is the minimum of the metering rate $q_1^{control}(t)$ and the ramp demand $d_1^{ramp}(t)$.

$$q_1^{in}(t) = d_1(t) * p^{RG}(t) * v_1^{VSL}(t)/v^{max} + q_1^{RM}(t) \tag{4.24}$$

$$q_1^{RM}(t) = min\{q_1^{control}(t), d_1^{ramp}(t)\} \tag{4.25}$$

In Eq. 4.26 and 4.27, the inflow on road 2 is calculated similarly to that on road 1. The difference is that the demand of on-ramp 2 is not constant. Instead, it depends on the RG split rate and also on the adjustment coefficient $\beta^{adj}(t)$. The rule of determining $\beta^{adj}(t)$ can be found in Eq. 4.18.

$$q_2^{in}(t) = d_2(t) * v_2^{VSL}(t)/v^{max} + q_2^{RM}(t) \tag{4.26}$$

$$q_2^{RM}(t) = min\{q_2^{control}(t), (1 - p^{RG}(t)) * d_1(t) * \beta^{adj}(t)\} \tag{4.27}$$

The rule to determine the imbalance penalty is similar to Eq. 4.12. In the MPC control, the outflow imbalance is considered.

$$Penalty^{ib}(t) = \begin{cases} P, & \text{if } \frac{|q_1^{out}(t) - q_2^{out}(t)|}{q_1^{out}(t)} \geq r^{max} \\ 0, & \text{if } \frac{|q_1^{out}(t) - q_2^{out}(t)|}{q_1^{out}(t)} < r^{max} \end{cases} \tag{4.28}$$

P is the value of penalty term, which should have a equivalent unit of veh/h. r^{max} is the difference rate threshold to decide whether the penalty should be applied.

The implementation of coordinated control is to build an overall algorithm to generate control parameters based on current states. That is, all DTMs are now controlled by one controller. For predictive RG, there is only one decision variable to optimise. In that case, the calculation could be done for all possible split rate values (discrete) and the optimal value can be easily found. However, with 5 control parameters $q_1^{control}$, $q_2^{control}$, v_1^{VSL}, v_2^{VSL}, and $p^{RG}(t)$, there are too many possible combinations. Therefore, it is necessary to find a method to optimise the DTM combination.

Genetic Algorithm (GA) is an evolutionary algorithm (Holland, 1992) that models the natural selection process to find the optimal solution. It has the ability to handle a multi-input problem and complex objective function (Yang, 2021). The process will select a population with genes that lead to higher values of the fitness function (objective function) as parents for the next generation. During the evolution of generations, elite genes (better solutions) will be kept. When the maximum generation number is reached, the best solution is the one with the highest objective value in this generation.

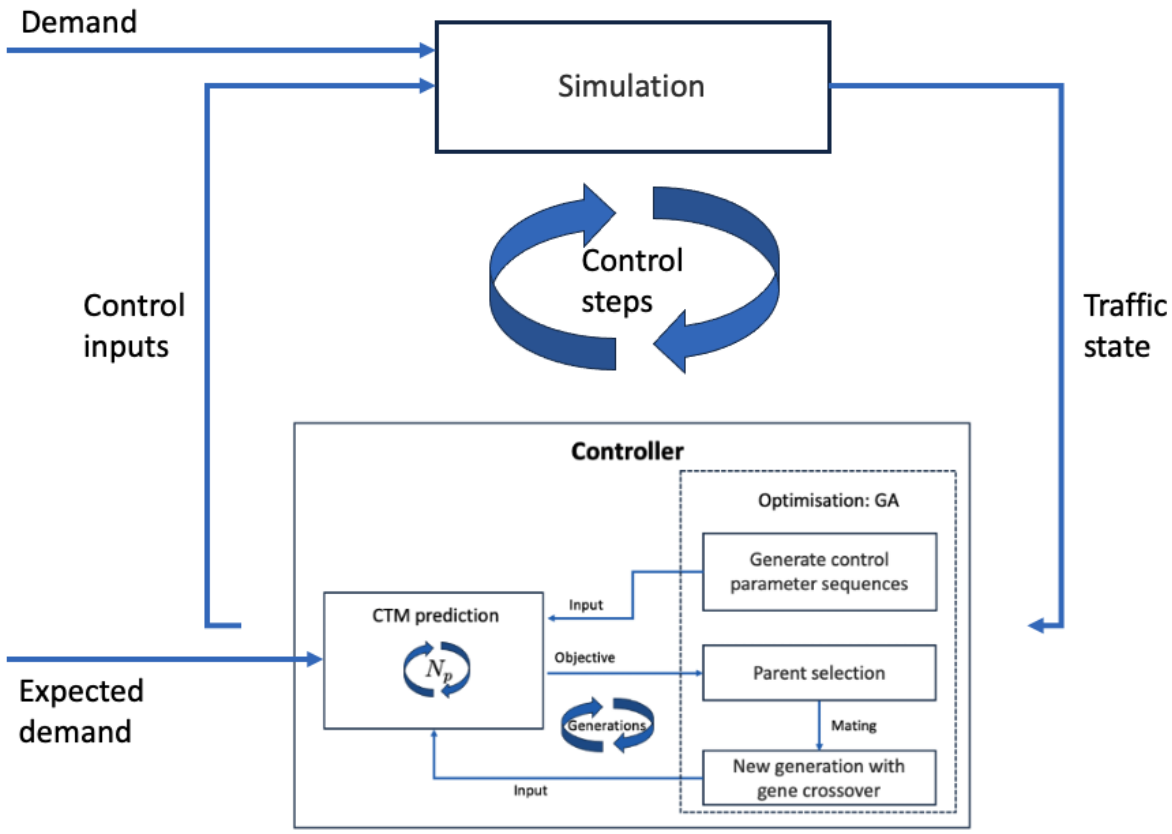

Figure 4.3: MPC control loop

Figure 4.3 shows the loop of coordinated MPC control. The outer loop shows the traffic control for each control step. The demand flux in the simulation, which causes a change in certain traffic states. In this case, the main state considered is the density of cells. The MPC controller will generate the optimal control input based on the current states and input it to the simulation for the next control step. Within the controller, the GA process will first generate the initial population and input it into the CTM prediction. CTM will calculate the objective values for the prediction horizon N_p based on the current state, the sequence of control parameters, and the expected demand. For simplification, the expected demand for the prediction horizon will be the same as the demand in the current step. This may lead to some error on time steps when the demand profile changes. Based on the objective values, the best-performed control input sequences will be selected as the parents for the next generation. After the mating process, the control parameters are crossed over. Control input sequences will be input again into the prediction model. The evolution loop continues until the target generation is reached. In this research, the control step for the coordinated control is 60s, while the prediction step is 10s for the prediction model. The prediction horizon for coordinated control is 2 steps, which means that there will be a prediction for the next 120s. The two steps are optimised together, taking the average value of the objective function in 12 prediction steps as the overall objective function value.

4.3 Smoothing of the control parameters

In predictive RG and the coordinated control strategy, optimisation of control parameters is involved. Although the optimal solution can theoretically lead to the best network performance, the solutions may fluctuate over control steps. This could lead to traffic instability. To make the control parameters change more mildly, single exponential smoothing is applied for predictive RG and coordinated control. The mathematical expression is as follows:

$$S^{control}(t) = \alpha * y^{solution}(t) + (1 - \alpha) * S^{control}(t - 1) \tag{4.29}$$

Where $S^{control}(t)$ is the value of the control parameter for the control step t, $y^{solution}(t)$ is the optimal control parameter for this step. α is a coefficient between 0 and 1. It represents the weight for the current optimal solution and the actual control parameter in the last step.

Since VSL only has on and off states, it cannot be smoothed by Eq. 4.29. However, it is necessary to find another way to smooth VSL parameter since the temporal on and off of VSL may cause extra delay. Algorithm 1 is used to determine the applied VSL parameter based on the theoretical one calculated by Eq. 4.10. A cumulative number N_{change} is introduced. When the calculated speed limit is not the same as the last calculated speed limit, the number will be reset to 0. Otherwise, the number will accumulate. When the number reaches a certain value N_{th}, it is considered that there is indeed a trend of change, then the speed limit will change to the current calculated value. If N_{change} does not reach the threshold, the applied control parameter will keep the applied parameter in the last step. This smoothing method prevents sudden on and off of VSL. The minimum time of each speed limit state is N_{th}. This is set to 2 in the simulation, which means it takes at least three control steps (30s) for VSL to switch on/off.

Algorithm 1 Smoothing of VSL control parameter

Input: Applied VSL control parameter for the last step $v_{app}^{VSL}(t-1)$, calculated VSL control parameter for the last and this step $v_{cal}^{VSL}(t-1)$, $v_{cal}^{VSL}(t)$

Output: Applied VSL control parameter for this time step $v_{app}^{VSL}(t)$

if $v_{cal}^{VSL}(t-1) \neq v_{cal}^{VSL}(t)$ **then**
    $N_{change} \leftarrow 0$
else
    $N_{change} \leftarrow N_{change} + 1$
end if

if $N_{change} > N_{th}$ **then**
    $v_{app}^{VSL}(t) \leftarrow v_{cal}^{VSL}(t)$
else
    $v_{app}^{VSL}(t) \leftarrow v_{app}^{VSL}(t-1)$
end if

Chapter 5

Simulation setting

The simulation is set in SUMO with the TraCI interface. As can be seen in Figure 5.1, there are mainly four components. For the pre-simulation input, research network is built with specified edge parameters and junction types. Vehicle demand and routes (or OD) are required to generate vehicles in the simulation. For the car following (CF) and lane changing (LC) models, vehicle attributes are required to be set. For this research, some detectors are also required to be configured for traffic control.

During the simulation, several classes in TraCI are used to record traffic data and control vehicles locally or individually. traci.edge and traci.inductionloop mainly collect traffic data, both for the calculation of the performance indicator and for the input into the traffic control. traci.vehicle can be used for both vehicle data retrieval and individual vehicle control.

The green and blue dashed arrows between the traffic control measures to TraCI classes represent where a certain traffic control gets data (blue) and which class it will affect directly (green). For instance, VMS RG gets travel time data from the edge level and affects route choice behaviour of vehicles.

The simulation proceeds with (or without) the effect of DTM measures. After the simulation, the collected data will be processed in the data processing module. Visualisations could be made for the purpose of illustrating network performance or verifying the function of DTM measures.

In Section 5.1, the network structure and detector locations in the simulation environment are introduced. In Section 5.2, the implementation of DTM measures in simulation is discussed. Section 5.3 describes the parameter setting for both DTM controls and vehicles in the simulation. The assumptions in the simulation process are summarised in Section 5.4. In Section 5.5, the simulation scenarios are explained in detail. In Section 5.6, the calculation method and the method for collecting indicator values in the simulation are discussed.

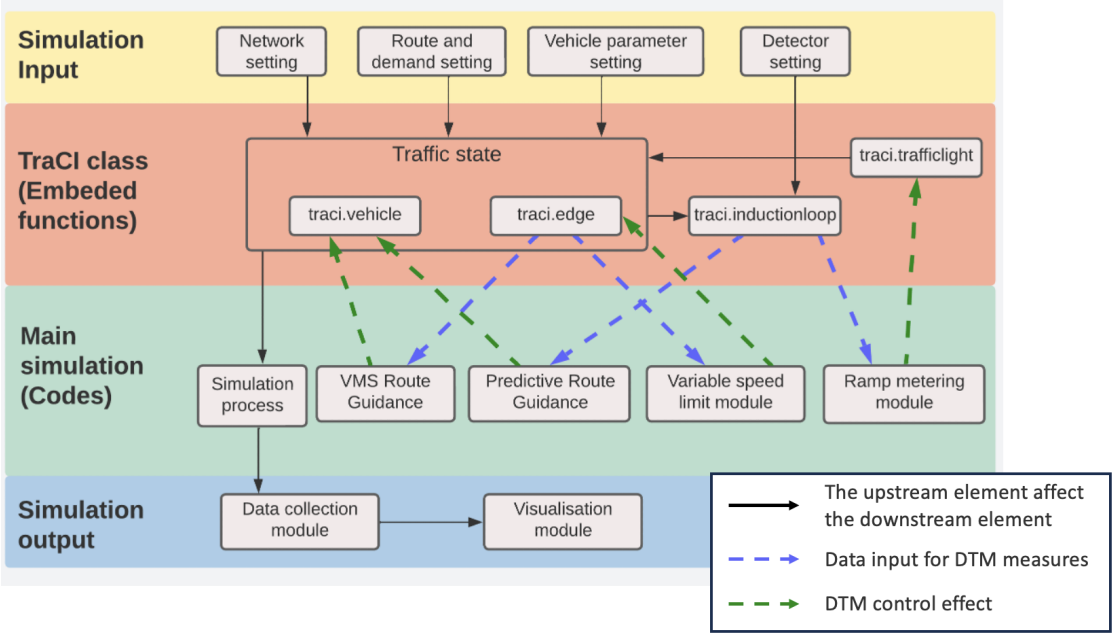

Figure 5.1: Simulation components

5.1 Simulation network

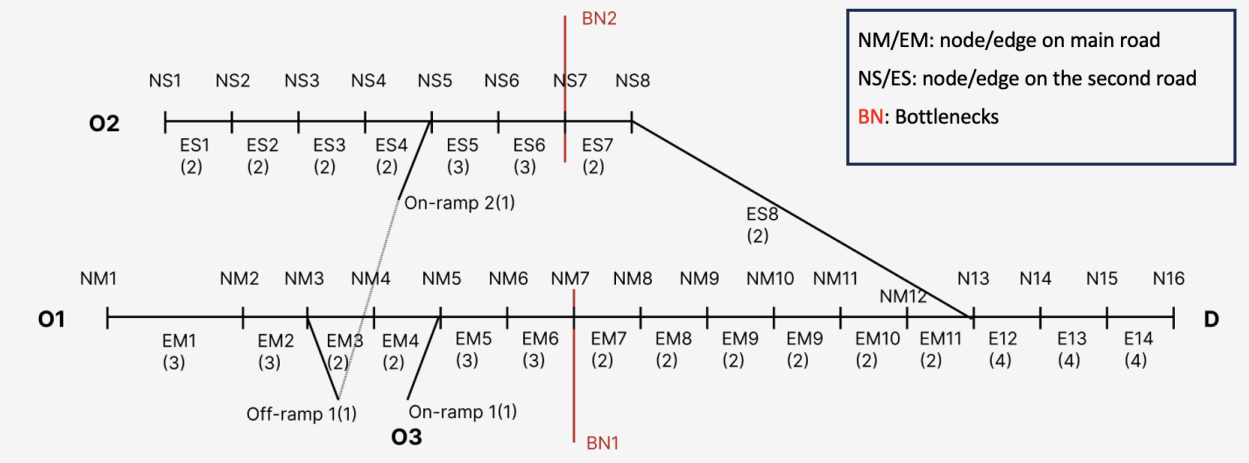

Figure 5.2: Simulation network

5.1.1 Network structure

The road network is shown in Figure 5.2. In the network, N represents the nodes and E represents the edges. The number after the edge id indicates the number of lanes of this edge. Most edges have a length of around 300m, except for EM1(1000m) and ES8(1500m). In the current simulation, there are three demand parameters. They are, respectively, O1-D,

O2-D, and O3-D. There are two bottlenecks in the structure due to the lane-drop. They are marked red on the network.

RM is available for all on-ramps in the network, namely RM1, RM2 for on-ramp 1 and 2. Off-ramp 1 is connected to On-ramp 2, which makes dynamic route changing and RG available. For each of the bottlenecks, VSL is available upstream. VSL before BN1 are called VSL1 on Road 1 and VSL2 on Road 2.

Data collection is done in two ways. The first way is to get the states directly from the edges. The function of getting vehicle IDs on a certain edge can be used to derive density values, and the function of getting mean speed of an edge can be used directly as the measured speed value. For example, the speed before the bottleneck b^{bn} in Eq. 4.10.

5.1.2 Detector locations

The flow that passes through a certain location cannot be represented by the values retrieved from edges or junctions. Therefore, induction loops are installed in the simulation network to detect the flow values required in the simulation. As shown in Figure 5.3, there are in total 12 loop detectors in the network. Det 1, Det 7, Det 6 and Det 10 measure the inflow (demand) and the outflow of the main research area. Det 8, Det 3 and Det 9 are installed for RM 2. Det 2, Det 4 and Det 5 are installed for RM1. The description of the function of each detector and its corresponding variable is shown in Table 5.1.

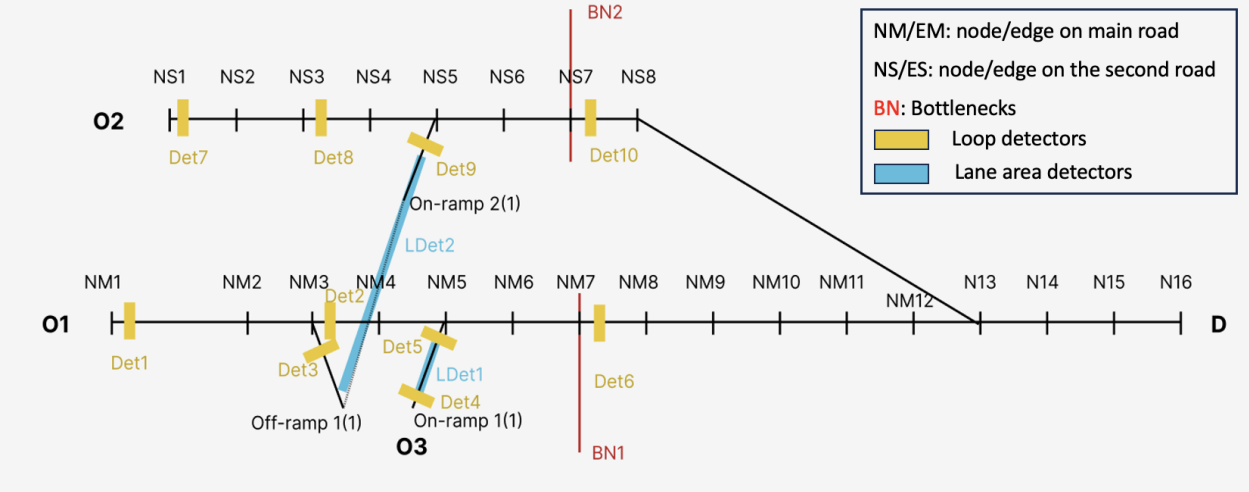

Figure 5.3: Detectors on the network

Among all these detectors, LDet1 and LDet2 are lane area detectors. They have the function of measuring the length of jam in vehicle number or in meters, as well as the average vehicle speed of the covered area. However, it only considers stand-still vehicles, which makes the detected queue shorter than the distance between the queue tail and the queue head (stop line before the signal). Therefore, an indirect way is used to determine whether the queue is longer than the maximum queue length threshold.

Table 5.1: Detector function description

Detector	Function	Related variables
Det1	Total demand on road 1	d_1
Det2	Upstream main road flow for RM1	q_1^{um}
Det3	On-ramp demand for on-ramp 2	q_2^{ur}
Det4	On-ramp demand for on-ramp 1	q_1^{ur}, d_1^{ramp}
Det5	Flow merge into main road 1 from on-ramp 1	q_1^{RM}
Det6	Outflow after bottleneck 1	q_1^{out}
Det7	Total demand on road 2	d_2
Det8	Upstream main road flow for RM2	q_2^{um}
Det9	Flow merge into main road 2 from on-ramp 2	q_2^{RM}
Det10	Outflow after bottleneck 2	q_2^{out}
LDet1	Queue length on on-ramp 1	$queue_1$
LDet2	Queue length on on-ramp 2	$queue_2$

The start and end positions of the lane area detectors are set at points that are at the desired queue length $Queue^{min}$ and the maximum queue length $Queue^{max}$ stated in Eq. 4.9. When the average speed of these areas is close to the maximum speed of the ramp, the queue must be shorter than $Queue^{min}$. When the average speed is near standstill, the queue is now longer than $Queue^{max}$. In this way, the queue length estimation is more accurate than the embedded queue length function.

The detector detection interval is set to 60 simulation steps (1 minute). Therefore, the detected vehicle numbers that passed through the detector shall be multiplied by 60 to make the unit veh/h. This will cause an inevitable numerical error. For example, a demand of 4000 veh/h will be detected as 4020 or 3960, or even higher or lower values.

In Table 5.1, no speed-related variable is mentioned, although they can also be derived from loop detectors. This is because all the detected speed values are derived from the edges or the lanes. In the simulation, the vehicles have their preferred lanes. This causes that there is no vehicle passing through a certain lane during the past interval. In this case, the average speed cannot be calculated by averaging the detected speed of all detectors, since one of them might be -1 (no vehicle detected for the past interval). For convenience, the mean speed values of edges or lanes are used as speed data, which assumes that the speed is the same for every location of an edge/lane.

5.2 DTM implementation and verification

DTMs mentioned in Chapter 4 are implemented in the simulation through TraCI. More assumptions are made due to the difference between the control in simulation and in real life. They are discussed in the following sections 5.2.1 to 5.2.4. The collected data and visualisations are used to verify the function of different DTM measures.

5.2.1 RM implementation

Two RM systems are implemented by adding two signal control points on on-ramp 1 and on-ramp 2. The location of two signals is set around 130m from the merging point. The default maximum acceleration of vehicles in SUMO simulation is $2.6m/s^2$. That means, a speed of 26m/s can be reached when a vehicle travels to the main road after stopping before the RM stop line ($130[m] = 0.5 * 2.6[m/s^2] * 100[s^2]$).

The RM systems use the one-car-per-green strategy. This means that when the first vehicle waiting in the queue passes the signal, the signal should immediately turn yellow and then red. To realise this, a detector can be added 2 meters after the stop line. Whenever the detector detects a vehicle while the signal is green, it should change to yellow. However, vehicles can already be observed to "follow" the one-car-per-green rule under a green time of 2s.

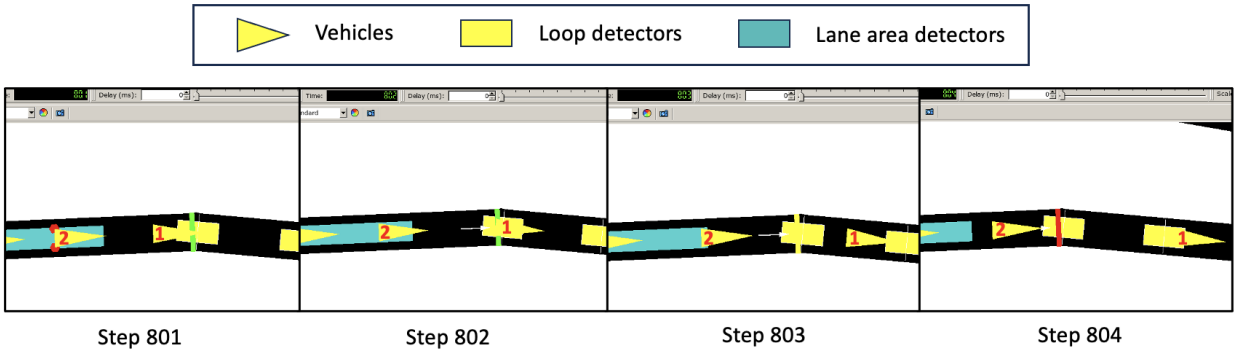

Figure 5.4: Observed "one-car-per-green" in the simulation

As shown in Figure 5.4, two vehicles 1 and 2 were waiting in front of the stop line at step 800. When the signal changes to green at step 801. Vehicle 1 moves immediately while vehicle 2 is still waiting. Vehicle 2 then starts in step 802, but one second is not enough for it to pass the stop line. Therefore, it is stopped again by yellow and red light. The observed behaviour shows that it is not possible for the second vehicle to also pass the signal within the green time of 2 seconds. This may be related to the simulation step length of 1s and vehicle attribute, such as the minimum gap between the vehicle in front. Therefore, in this simulation setting, it is not necessary to implement the one-car-per-green rule specifically.

There are two traffic signal programmes for each signal. The first programme is always green, which is used to turn off ramp metering. The other one contains three phases, green, yellow and red. The initial phase duration of this programme is set to 2s, 1s, and 2s. On the basis of one-car-per-green, this cycle time can allow for a maximum metered flow of 720 veh/h. When the metering rate is lower, the red time will be set longer to form the desired cycle time. The minimum flow allowed is set to 300 veh/h. Therefore, the range of red time is between 2 and 9s.

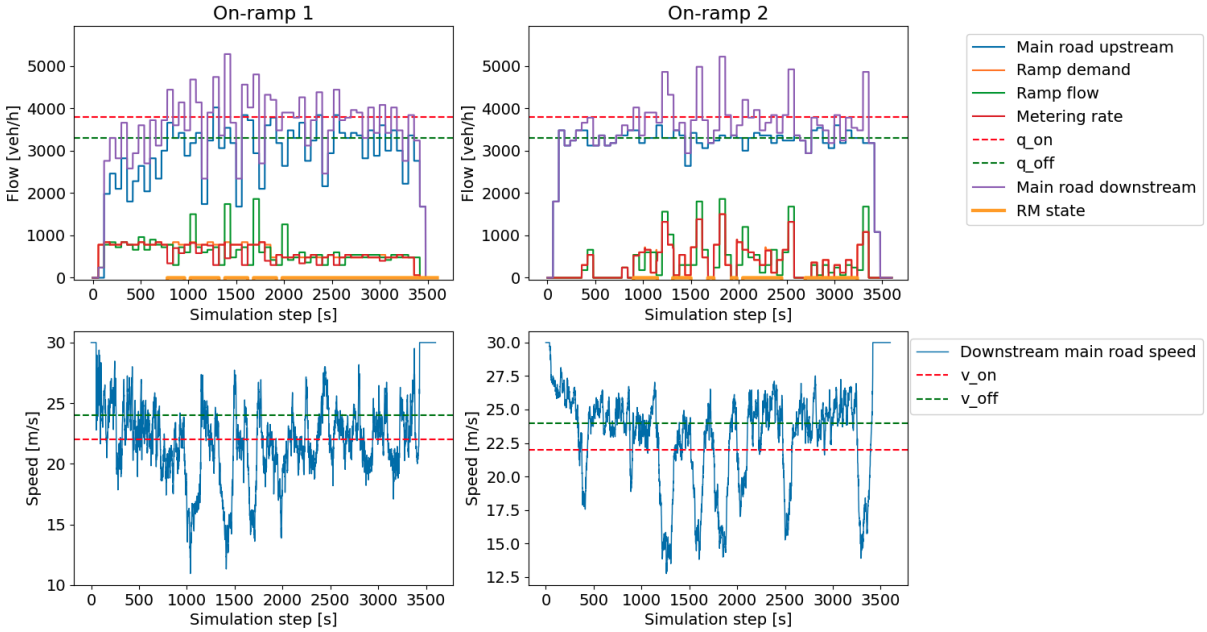

Figure 5.5: Flow and speed curve around RM 1 and 2 (q_on, q_off are flow thresholds for RM to be on and off, v_on, v_off are speed thresholds for RM to be on or off)

Figure 5.5 shows the flow and speed curves around on-ramp 1 and 2. In the flow plots, the upstream demand of the main road, the demand of the ramp, the metering rate, the actual flow of the merge from the on-ramp and the downstream flow of the main road are illustrated. The existence of the orange line on the x-axis means that RM is active. It could be seen that the downstream flow is maintained at around 4000veh/h for most of the time. However, sometimes the ramp flow increases suddenly and gets higher than the metering rate. This is because the queue length exceeds the maximum threshold, and RM is turned off (interrupted points on the horizontal orange line). In this case, the metering rate will be recorded as the on-ramp demand, while the RM is actually off and there is no metering effect.

The period when RM is off allows the queue to clear, but it also creates a sudden increase in both ramp flow and downstream flow. It may cause severe congestion before the bottleneck for a short period. An alternative way to clear the queue is to use the maximum metered flow (720 veh/h). However, in the simulation, the ramp demand will be a constant higher

than the maximum metered flow for on-ramp 1. That is, the maximum metering rate cannot reduce the queue length. Therefore, temporary turning-off of RM is necessary to avoid high delay for on-ramp vehicles, and even queue spill back outside of the simulation boundary.

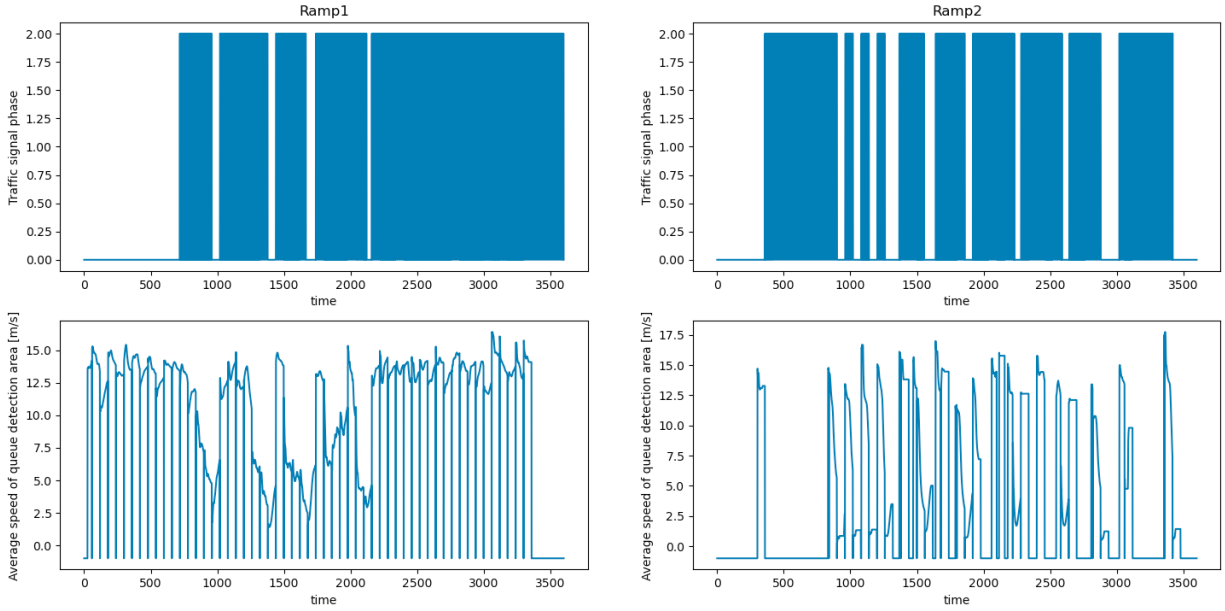

Figure 5.6: RM turning off and queue length

Turning off of RM to clear the queue can be observed in Figure 5.5, but it is not clear that RM is turned off when the queue reaches the maximum queue length value. Figure 5.6 shows the signal phase curves and the speed curves detected by the lane-area detectors. In the phase figure, 0, 1, 2 represent, respectively, green, yellow, and red. At the beginning of the simulation, RM on both roads is off and the signal remains green. When RM is on, the part filled with blue curves represents the repeating RM signal control cycles. The white gaps within the blue parts represent the period when RM is off because of the queue on the ramp. It could be seen that each period when RM is off has its corresponding ramp speed hollow. The hollows with a speed lower than 5m/s means that the queue has reached the tail of the lane-area detector (i.e. the position of maximum queue length). There are also some errors in lane area speed detection. That is, sometimes the speed is -1 even when there are vehicles in the detecting area. The solution to this problem is to only consider positive speed values. When -1 is detected, the RM state should keep the same as in the last control step.

Figure 5.7 shows the detailed signal phase curves, which is a zoomed in version of Figure 5.6. It can be seen that the red time (time when phase is 2) varies, while the green time and yellow time keep constant (2s and 1s respectively). This means that the cycle times change depending on the required metering rate.

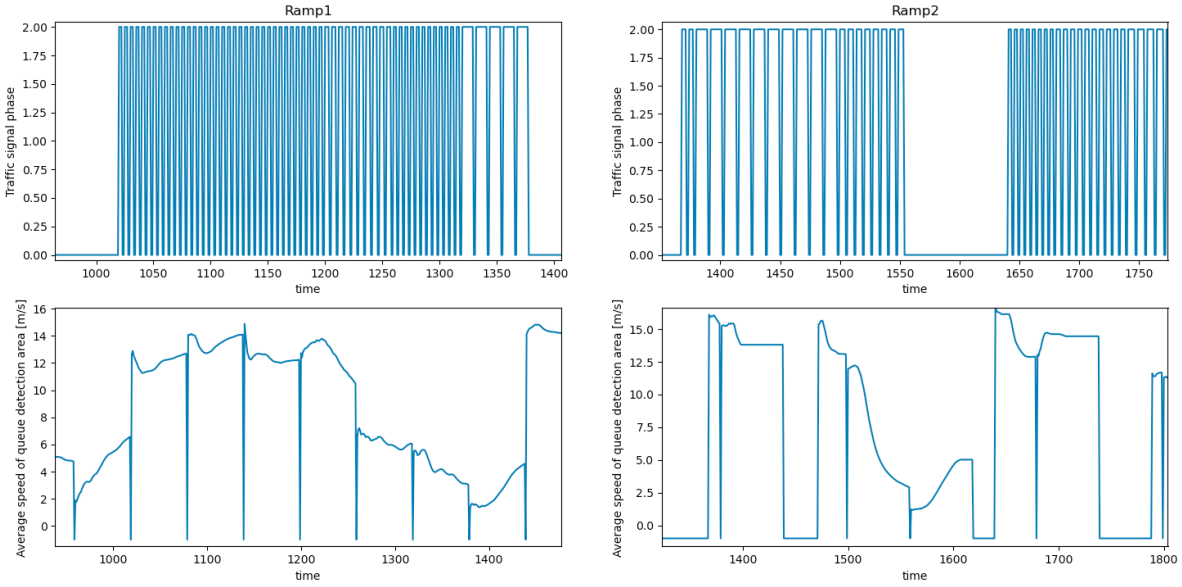

Figure 5.7: Variable cycle time

5.2.2 VSL implementation

The implementation of VSL is done by changing the speed limit of the upstream edges. In this way, the vehicle speed change behaviour will be closer to real life compared to setting speed reduction for individual vehicles. That is, vehicles will first notice the speed limit change and then react. In SUMO simulation, there exists a speed factor distribution for vehicles, which makes it possible for some vehicles to exceed the required speed limit of the edge (SUMO User Documentation, n.d.).

The VSL application area and the corresponding speed detection points are shown in Figure 5.8. The purple part on each road represents the edges where VSL is implemented. The speed detection is done on Edge EM5 and ES5. This is because most of the vehicles in the simulation finish their lane change before EM6(ES6) to react to the lane-drop on EM7(ES7). In the simulation, the congestion on both roads cannot propagate too far (except sometimes on Route 2) since the route choice behaviour of vehicles. If the VSL application area is farther from the bottleneck, the improvement will be limited, as congestion will not propagate that far even when VSL is not applied. Therefore, the VSL application area is set at the edges EM3 and EM4 on Road 1 and ES3 and ES4 on Road 2. The two application areas are directly next to the speed detection areas.

The VSL function is tested and the result is visualised (as shown in Figure 5.9). In the speed plots, the red and green dashed lines represent respectively v_{on}^{th-vsl} and v_{off}^{th-vsl}. The speed plot shows that when the speed is lower than v_{on}^{th-vsl}, VSL will be on and the speed limit will be reduced. The reduced speed limit remains until the speed recovers to a value

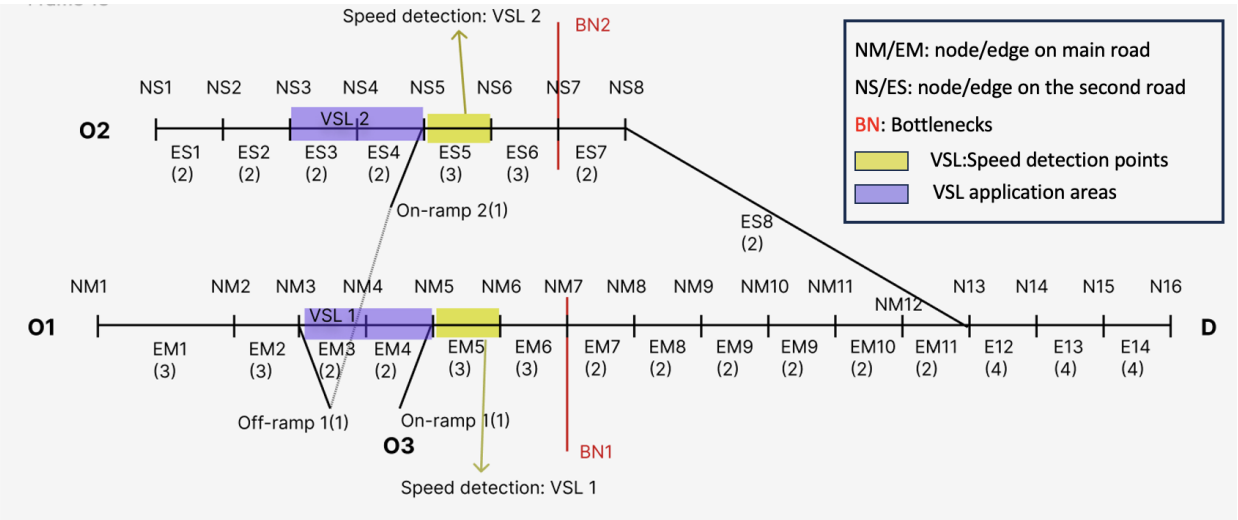

Figure 5.8: VSL application area

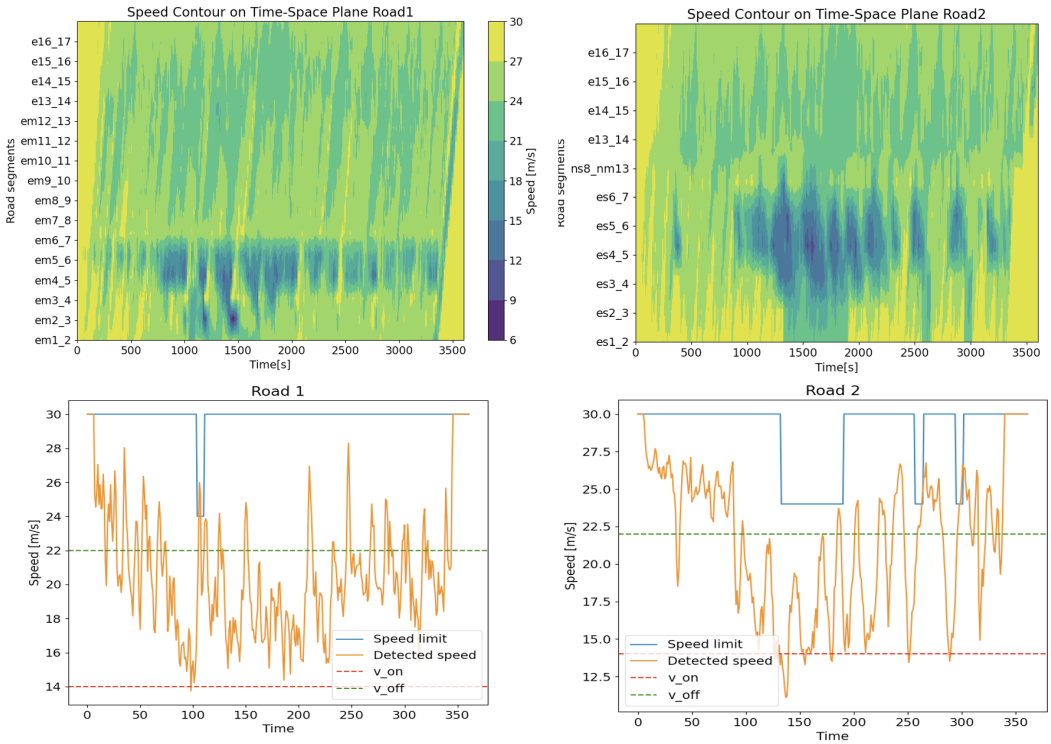

Figure 5.9: VSL control effect verification

higher than v_{off}^{th-vsl}. After ensuring that the VSL is on and off according to the predetermined rule, two speed contours are made to verify whether the VSL system has an effect on the vehicles in the simulation. The speed limit reduction period and segments can also be clearly seen in the contours, as the darker area upstream of the congestion.

5.2.3 RG implementation

In the simulation, vehicles that use VMS RG and predictive RG are randomly drawn with respect to the proportion of different RG usage $Proportion^{VMS}$ and $Proportion^{Pred}$. It is assumed that the only segment that allows the change of route is on edge EM1. The reason why this edge is made longer than others is to have more route-changing behaviour. A longer road segment means that vehicles will travel longer on the segment. During this duration, their route selection may change (sometimes even twice). Their route-changing behaviour will then be closer to real life, where some hindrance may happen before an off ramp. For VMS RG, the instantaneous travel time of each route is collected by summing the travel times of the edges. When the travel time on Route 1 is longer, vehicles following the VMS RG will change immediately to Route 2. The rest of the vehicles will stay on Route 1. As shown in Figure 5.10, the ramp is only used when the travel time on Route 2 is longer than that on Route 1. The drawback of the reactive RG is also obvious in the figure. That is, when many vehicles suddenly switch to Route 2, the travel time on Route 2 will increase rapidly and the ramp demand quickly diminishes. Therefore, congestion switches back and forth between the two routes.

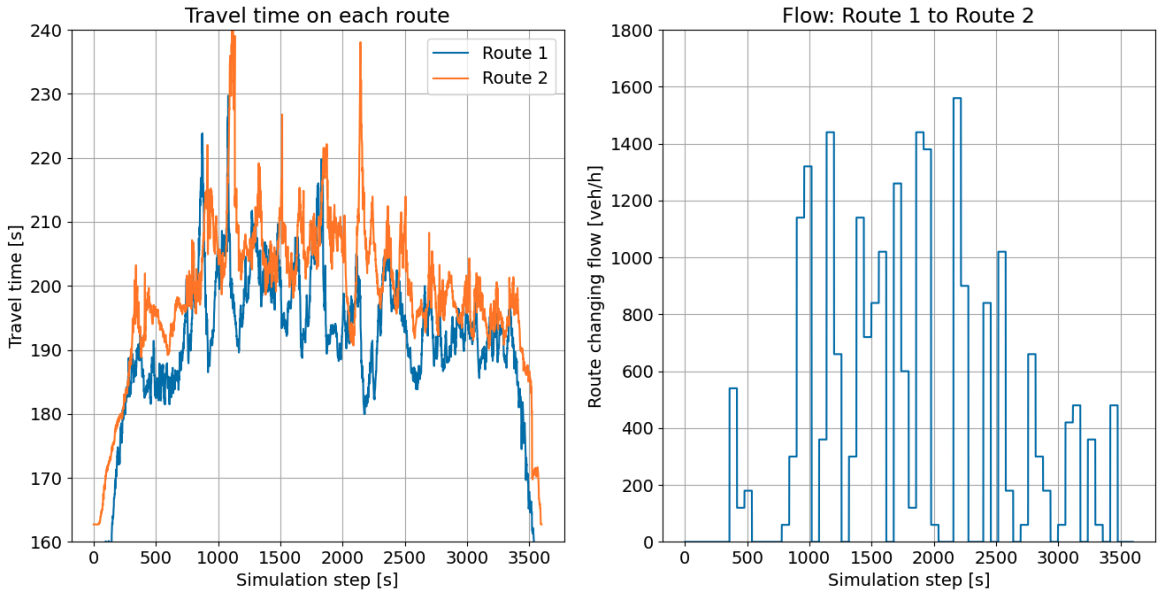

Figure 5.10: Route travel time and flow on off-ramp 1: VMS RG control

For vehicles using predictive RG (selected based on $Proportion^{Pred}$), they will follow the

guidance instruction when selecting routes. The prediction will find an optimal split rate $p^{RG}(t)$ for vehicles on the edge EM1. Vehicles will be randomly drawn to redirect to Route 2, even this means a longer travel time based on the current state. As introduced in Eq. 4.11, the objective of predictive RG is to reach the lowest total travel time. To find the optimal value for each control step, the split rate p^{RG} is discretised. Since there is only one decision variable and the solution space is not large , the optimisation process does not need a solver. All the values of the objective function are calculated for each discrete split rate, and the optimal one can be selected as the control input for the next control step.

Figure 5.11 shows the off-ramp flow and the travel time on each route in the scenario when both ways of RG are implemented. It is assumed that 50% of vehicles will use VMS RG and 50% of vehicles will use predictive RG. Among each group, there is a chance of 20% when vehicles do not follow the instructions of both RG (compliance rate of 80%). Compared to Figure 5.10, the ramp vehicle flow has a more even distribution rather than sudden increases and decreases. This is because the predictive RG considers a system optimal result instead of the shortest travel time for individuals. When the travel time is longer on Route 1, the increase in ramp flow can be seen. These are when vehicles that use VMS RG also change to Route 2.

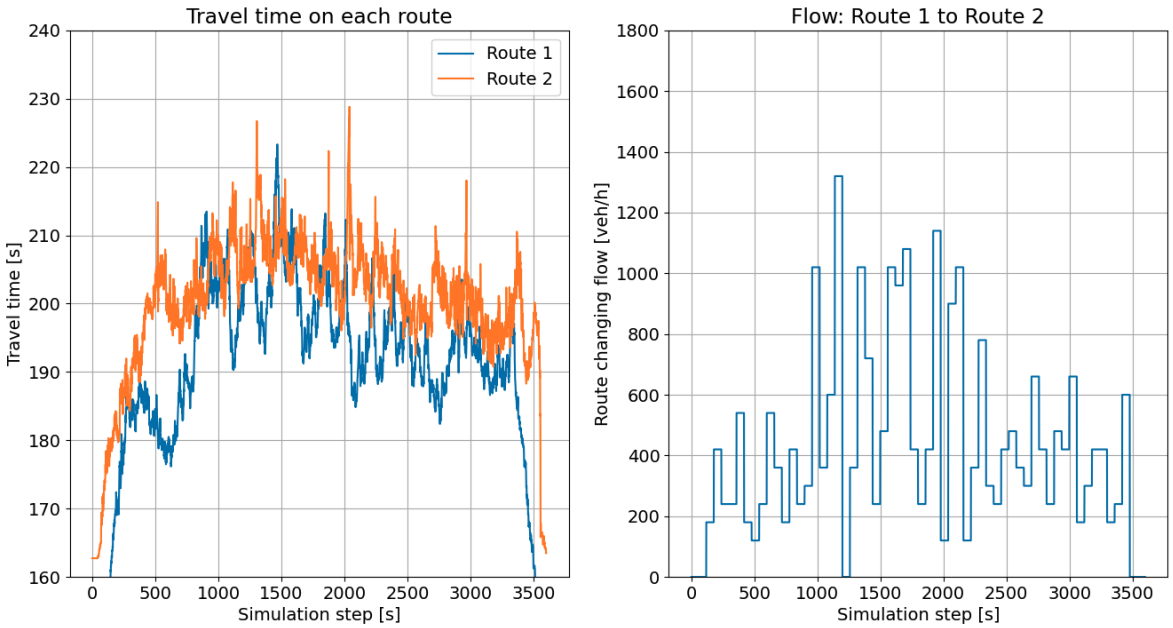

Figure 5.11: Route travel time and flow on off-ramp 1: VMS+predictive RG control

To test the behaviour of the predictive model, the objective value for the selected optimal split rate and the actual detected travel time for the considered segments are recorded. The two travel time curves can be seen in Figure 5.12. It can be seen that the value and trend of the predicted objective value is quite close to what is actually achieved in the simulation. There are some peaks when the predicted value is much higher than the actual one. This could be due to the limitation of the assumed exponential speed-density relationship and

relatively short considered segments. The vehicle behaviour in the simulation is more complex and heterogeneous.

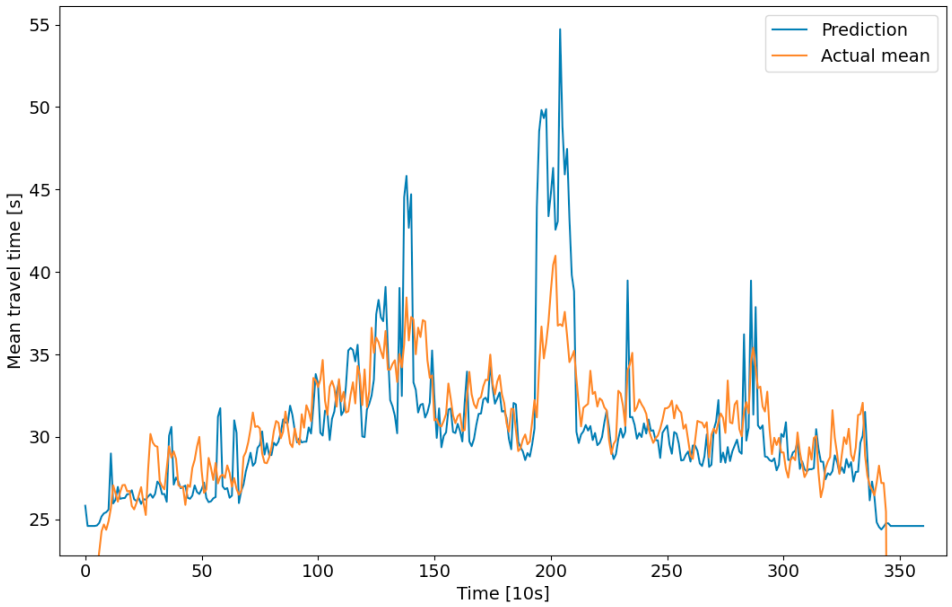

Figure 5.12: Total travel time: Detected and theoretical objective value

5.2.4 Coordinated control implementation

To apply GA in coordinated MPC, PyGAD is used as a GA toolbox. PyGAD (PyGAD 3.2.0 documentation, n.d.) is a Python library for building the genetic algorithm. It allows users to create an instance with prepared parameters and fitness function. The process of GA can be run with user-defined setting for the number of generations, crossover, and mutation parameters.

In the MPC control, control parameters are discretised. The range of values of the RM rate is 300 to 720 veh/h, with step of 10. The value of VSL can be 24 or 30 m / s. The split rate p^{RG} changes between 0.5 and 1 with a step of 0.05. The lower bound of 0.5 is set to prevent the demand from exceeding the capacity of ramp 2 (around 2000veh/h), hence preventing queuing before the off-ramp. With the spaces for each DTM parameter, there are 840 possible combinations for one control step. Therefore, only some of the combinations will be randomly drawn as the initial population. The size of the initial population is set to 300. The solutions will be ranked and 20 solutions with the highest objective values will be selected as parents for the next generation.

In the tests of the genetic algorithm, it is found that including gene mutation significantly increases running time. For one control step, the running time without mutation is 3.5s and

the running time is 8.5s when there is a mutation probability of 10%. With a sample size of 300, the initial population can cover most of the possible values of the DTM parameters. Therefore, the mutation is not included in the optimisation process. The gene crossover type is set to "uniform", in which each gene has the equal possibility to be inherited from one of the parents (Syswerda, 1989).

Figure 5.13 shows two examples of the GA convergence process. It could be seen that the optimal (or local optimal) solution appears after 10 generations. For this reason, the number of generation is set to 20.

As can be seen in Figure 5.13, the improvement in total outflow is around 300veh/h. Considering rejecting solutions that create imbalanced situations between routes, a value of 1000 is selected for P (for Eq. 4.28). Figure 5.14 shows the flow difference rate (calculated as $\frac{q_1^{out}(t)-q_2^{out}(t)}{q_1^{out}(t)}$) curve over time. Four curves show, respectively, the cases where there is no penalty, when the maximum difference rate $r^{max} = 0.3$, when $r^{max} = 0.2$, and when $r^{max} = 0.1$. It can be seen that applying the penalty does not have a significant effect on the outflow difference. The no-penalty case even has less difference than the cases with a maximum difference of 20% and 10%. This shows that the imbalance problem is not severe in the base case, which means that a more balanced solution is usually also a solution leading to high total outflow. Therefore, the imbalance penalty is removed from the objective function in the simulations for coordinated control.

Although the parameters of DTMs are controlled by the coordinated controller, there is one special case when the DTM is adjusted by another rule. Since the first cell is in the middle of the simulation network, it is not possible to retrieve an accurate value of the queueing vehicles upstream of the first cell. However, if the ramp metering is always on, the queue will grow on the ramp and gradually spill out of the simulation. To prevent this, the rule for turning off RM (Eq. 4.9) is kept, which works separately from the coordinated control.

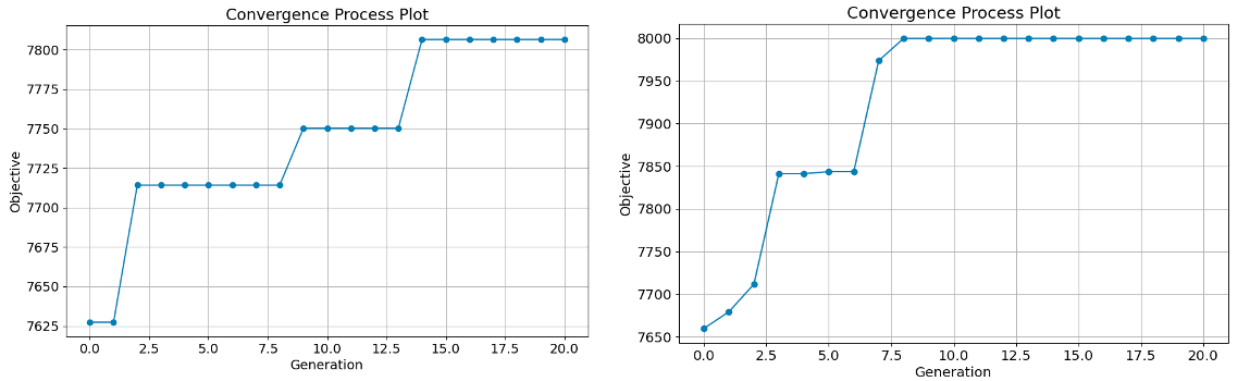

Figure 5.13: Convergence process plots of genetic algorithm

In the simulation, the MPC coordinated control keeps the speed limit at 30m/s the whole time. This means that the coordination is now only for RM and RG. This phenomenon is

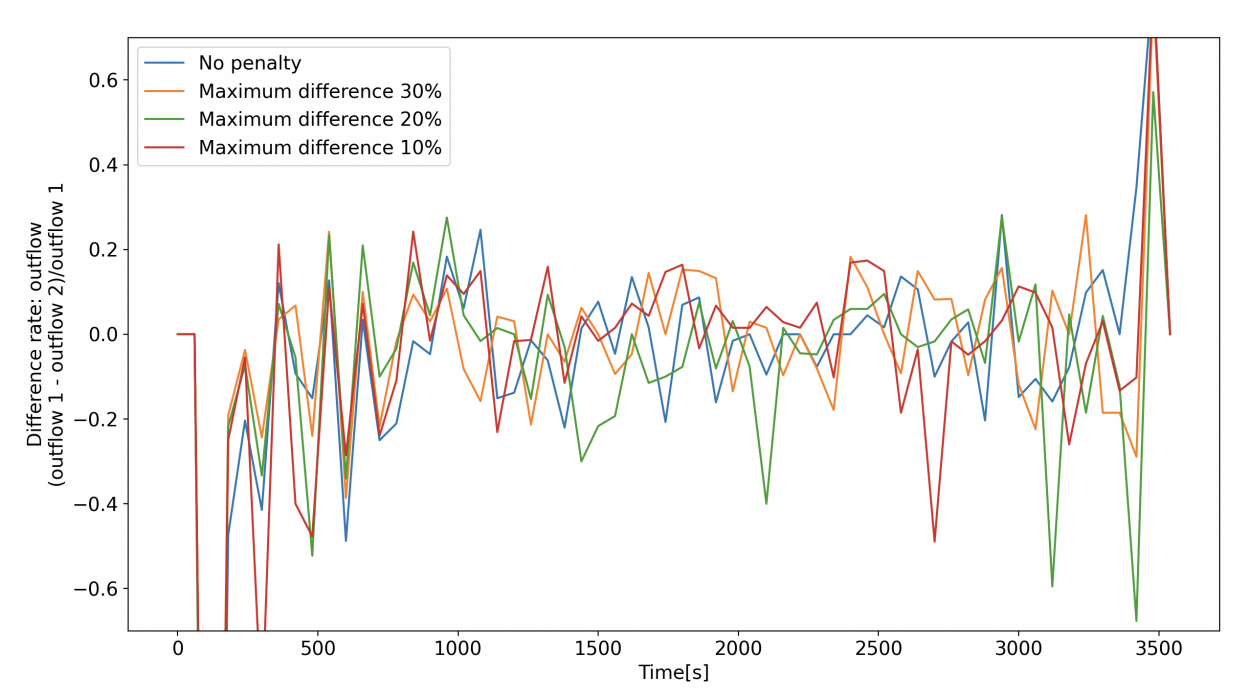

Figure 5.14: Outflow difference rate under different imbalance penalty

reasonable since the reduction of speed limit leads lower inflow in the formulation. However, this does not mean that there is no need for main road flow control in the simulation. As mentioned in the paragraph above, the queue discharge is still required, which causes a sudden flow increase. If the VSL is active simultaneously with the queue discharge, it can compensate for the impact of switching off RM.

To realise this function, an extra rule for VSL is added to the coordinated control. That is, the VSL is only active once the RM is off for queue discharge. The rule to decide whether RM should be off is still Eq. 4.9. In this way, VSL is included in the coordinated control, while fixed to off in the MPC loop.

5.3 Parameter setting and tuning

The parameter setting will be divided into two parts, namely, the simulation environment setting and the DTM parameter setting. The first sets general attributes for roads, lanes, and vehicles. The other is about tuning the implemented DTM measures.

5.3.1 Network parameters

The network parameters are shown in Table 5.2. Since the DTMs considered in this research do not need an accuracy less than 1s, 1s is selected as the simulation step length to save simulation running time. For the main road the speed limit is set at 30m/s and for the ramp

it is set at 15m/s. There are two optional lane change models "SL2015" and "LC2013". "SL2015" provides a more realistic result when the congestion occurs before a bottleneck. The parameter *lcSpeedGainLookahead* is set to 0. This is to prevent vehicles from changing lanes too soon for downstream bottlenecks.

Table 5.2: Network parameters

Network & Vehicles			
Parameter	Value	Unit	Description
Step length	1	s	Simulation step length
Speed limit	30, 15	m/s	Speed limit for main road and on-ramps
Acceleration	2.6	m/s^2	Maximum acceleration of vehicles
Decelration	5	m/s^2	Maximum deceleration of vehicles
Lane change model	"SL2015"	-	Lane change model
lcSpeedGainLookahead	0	s	Lookahead time in seconds for anticipating slow down

For the initial demand setting, there are some recommendations from previous research. Kan et al. (2016) mentioned 3 principles for designing the demand for simulation of cases, including RM and downstream bottlenecks. First, the mainstream demand should be lower than the capacity of any downstream bottlenecks, giving RM space to affect the traffic. As for the sum of mainstream demand and on-ramp demand, it should be lower than the capacity of the merging area, while higher than the capacity of the downstream bottleneck. This ensures that the combined demand could trigger congestion in front of the downstream bottleneck.

The demand profile for the simulation is shown in Figure 5.15. All the demand is reduced to 0 at time step 3300 to ensure that all the vehicles have passed the network. To create congestion on road 1, the sum of demand O1D and O3D should be greater than the capacity of the two-lane segment. In the demand profile, the demand O1D is 2500 veh/h for the first 10 minutes. After that, it increases to 3800, which makes the total demand higher than the downstream capacity. Then the main road demand and the ramp demand decrease, respectively, at steps 2400 and 1800. Then the total demand is slightly higher than the capacity of the downstream road. The demand O2D is fixed over time. The value of it should be high enough, so that when vehicles change from Route 1 to Route 2, the congestion before the bottleneck on Route 2 will be triggered.

5.3.2 Fundamental diagram estimation

Before setting the parameters for DTMs, some macroscopic attributes of the network are needed. For example, the target flow of RM is set based on the capacity of the downstream road. The speed-density relationship is also required for the prediction models. For this

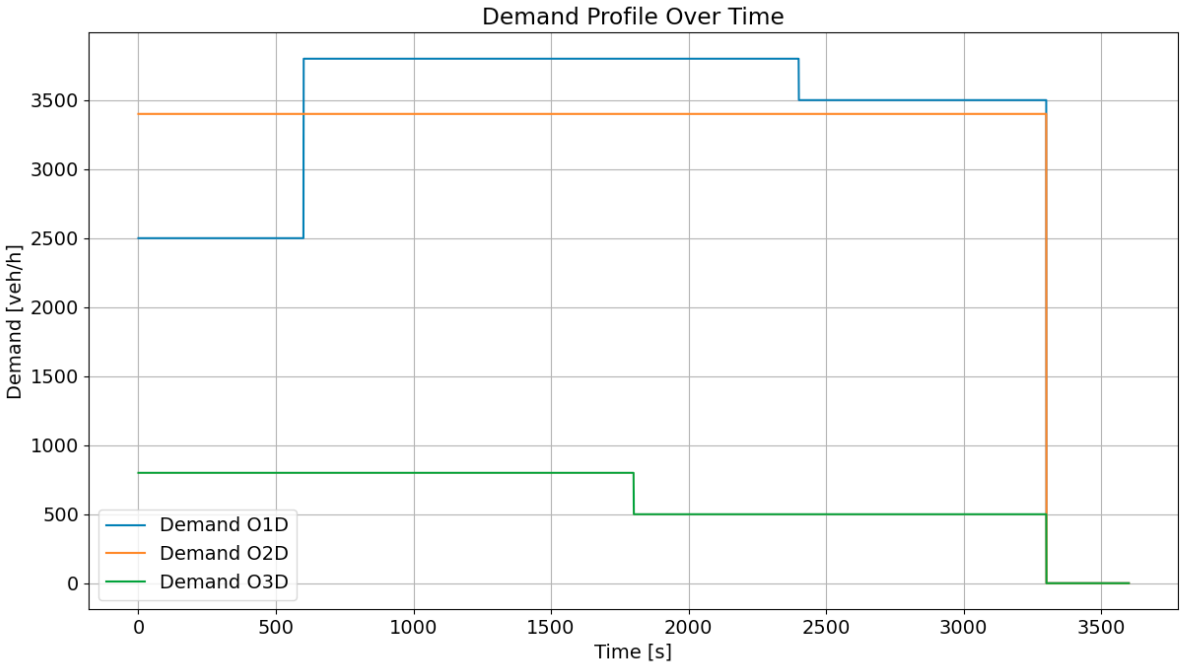

Figure 5.15: Demand profile for simulation

purpose, the Fundamental Diagrams (FD) are estimated for edges EM5, EM6, ES5 and ES6. To include more traffic states, a demand profile with multiple demand changes is made specifically for the FD estimation (Figure B.1). In the simulation, VMS is made available for 50% of the demand O1D.

Figure 5.16 shows an example of an estimation. It could be seen that on Road 2 (right) there are more congested states. This is because vehicles will be redirected to Route 2 when travel time increases on Route 1. In Table 5.3, it can be seen that the critical density is around 80-90 veh/km and the free flow speed is around 105km/h (speed limit is 108km/h). The reason why EM5 has a lower free flow speed is that it is an edge with a curve. The values of critical density and free flow speed for the predictive model in predictive RG and coordination will be determined based on calibration.

Since there is no one-lane road on the main road, the congested states on two-lane segments can hardly appear. Therefore, the capacity estimation for the two-lane segments will be performed based on Eq. 4.13. From the results in Table 5.3, the critical density of the two-lane segments will be around 60veh/km with a free flow speed of 105km/h. The resulting capacity is then 3800veh/h. With the roughly estimated capacity, the demand profile can be created for the simulation.

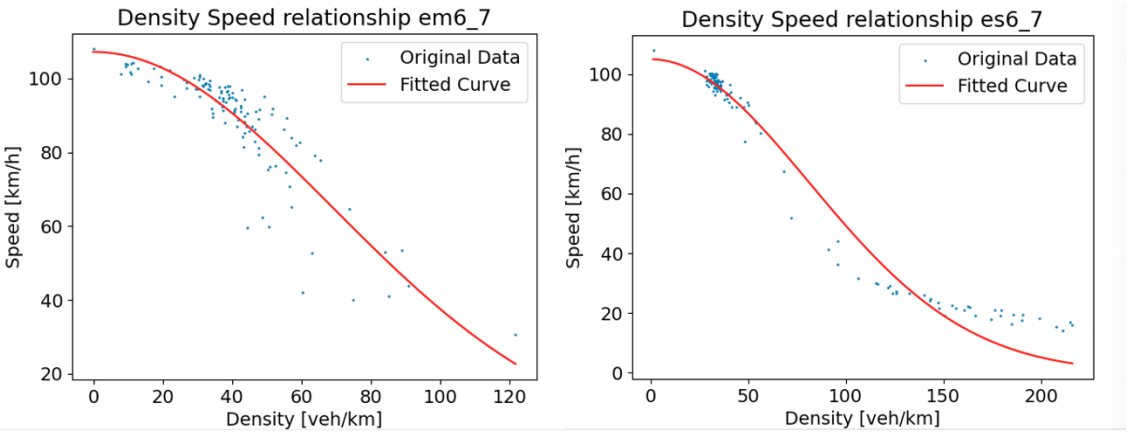

Figure 5.16: Fundamental diagram estimation example

Table 5.3: Fundamental diagram estimation results

Estimation	Results	ES5	ES6	EM5	EM6
1	ρ_l^{cong}	89.7	82.3	90.0	85.4
	v_l^{free}	104.9	105.0	92.6	100.3
	RMSE	6.0	5.6	6.3	9.6
2	ρ_l^{cong}	90.0	90.0	88.1	88.2
	v_l^{free}	106.1	102.8	95.7	100.4
	RMSE	7.7	6.6	4.8	8.3
3	ρ_l^{cong}	90.0	90.0	89.7	89.4
	v_l^{free}	105.8	104.5	91.5	101.0
	RMSE	10.1	7.1	7.0	8.0
4	ρ_l^{cong}	90.0	87.1	77.9	79.6
	v_l^{free}	105.4	102.0	93.6	101.7
	RMSE	7.4	7.2	8.1	8.2
5	ρ_l^{cong}	87.3	81.3	83.8	69.0
	v_l^{free}	106.1	104.9	97.9	107.2
	RMSE	6.2	5.6	4.2	7.0

5.3.3 DTM parameters setting

With the estimated capacity and critical densities, the parameters for DTMs can be set. Table 5.4 shows all the parameters for RM. The update time step for RM is 1s, while the detected flow changes every 60s due to the interval of detectors. Therefore, the metering rate only changes every 60s. The reason why the control step should be 1s is that the detected queue changes every second. Once the queue has reached the maximum queue length, RM

should be off to release vehicles in the queue. The target flow is set to 4000 veh/h, which is close to the downstream capacity. q_{on}^{th} and q_{off}^{th} are set with respect to the defined demand profile. The speed thresholds are set based on the observation of the simulation. Normally the speed will be higher than 24m/s when there is no congestion or disruption. The maximum queue length $Queue^{max}$ is set to 200m. In the tuning process, a too short maximum queue length will make it difficult for RM to realise the desired metering rate. However, a queue too long holds too many vehicles. The discharging of the queue takes longer time in this case, which can cause severe congestion before the bottleneck.

Table 5.4: Ramp metering parameters

RM			
Parameter	Value	Unit	Description
$t_{control}$	1	s	Time step length for control
q^{target}	4000	veh/h	Target downstream flow
q_{on}^{th}	3500	veh/h	Flow threshold for turning RM on
q_{off}^{th}	3300	veh/h	Flow threshold for turning RM off
v_{on}^{th}	22	m/s	Speed threshold for turning RM on
v_{off}^{th}	24	m/s	Speed threshold for turning RM off
$Queue^{min}$	50	m	Desired queue length on on-ramp
$Queue^{max}$	200	m	Maximum queue length on on-ramp

Table 5.5 lists all the parameters used in the VSL control. The control step is set to 10 seconds. When the criteria for VSL to be on are met, the speed limit will be reduced to 24m/s. Some tuning is done to determine an appropriate v_{on}^{th-vsl} and v_{off}^{th-vsl}. For each parameter setting, 20 simulation runs are performed. In Table 5.6, three parameter settings of v_{on}^{th-vsl} and v_{off}^{th-vsl} are tested. It can be seen that the mean value of the travel time is the shortest when the values of v_{on}^{th-vsl} and v_{off}^{th-vsl} are set to 12m/s and 15m/s. This means that a longer duration of VSL (when v_{off}^{th-vsl} is higher) will cause additional travel time. Therefore, 12m/s and 15m/s are selected as the threshold values.

Table 5.7 shows the parameters used for both VMS RG and predictive RG. It is assumed that half of the vehicles will use VMS RG and the rest will use predictive RG. This assumes that every driver receives travel time information form either of the RG in the scenarios when predictive RG is included. The compliance rate for both RG strategies is 0.8. Vehicles that do not follow the guidance will keep on Route 1. The free flow speeds are based on the estimated results in Section 5.3.2, while the critical density values ρ_1^{cong} and ρ_2^{cong} are tuned and set to 70 veh/h. During the tuning, when the critical densities are set to 90 veh/h, the estimated total travel time is much lower than the detected data. However, with a critical density of 70, the objective fits well with the actual travel time (as shown in Figure 5.12).

Table 5.5: Variable speed limit parameters

VSL			
Parameter	Value	Unit	Description
$t_{control}$	10	s	Time step length for control
$v^{reduced}$	24	m/s	Target reduced speed limit
v^{max}	30	m/s	Original speed limit
v_{on}^{th-vsl}	12	m/s	Threshold to turn on VSL
v_{off}^{th-vsl}	15	m/s	Thereshold to turn off VSL

Table 5.6: Tuning of v_{on}^{th-vsl} and v_{off}^{th-vsl}

VSL parameter tuning			
v_{on}^{th-vsl} [m/s]	v_{off}^{th-vsl} [m/s]	Mean value of average travel time [s]	Standard deviation
12	15	230.1	1.8
15	18	231.2	1.4
12	18	231.4	1.7

This could be because vehicles change lanes slightly before bottlenecks on EM5 (ES5) and edge EM6(ES6). This behaviour makes the segments considered in predictive RG have a capacity between two-lane and three-lane segments.

A p^{extra} value of 2.5 means that when the first criterion in Eq 4.18 is met, it is considered that the total flow changing to Route 2 is 2.5 times the vehicles guided to Route 2 by predictive RG. This number aims to prevent predictive RG from guiding too many vehicles to Route 2 when the travel time is longer on Route 1. However, this number can sometimes exaggerate the length of travel time. This is the reason why the predicted objective value seems to have dramatic peaks in Figure 5.12.

The predictive RG has a 1 step horizon. Since the control step is the same as the step in prediction, this means the algorithm optimises the split rate for the next control step. The penalty value for the imbalance is set to 30, while the total travel time is around 30. This aims to make the RG control consider the balance between routes.

Table 5.8 shows the parameters for the coordinated control. The control step is 60s, which aims to save computation time for optimisation and prevent too frequent changes in the metering rate of RM. For the cell transmission model, the cell length and the time step are, respectively, 0.3km and 10s. This meets the requirement for lower numerical errors for CTM: $dx = dt * v_{max}$ (Knoop et al., 2020). The determined dx and dt should prevent vehicles from travelling through more than one cell in one time step. The prediction horizon is 2

Table 5.7: Route guidance parameters

RG			
Parameter	Value	Unit	Description
$t_{control}$	10	s	Time step length for control
$Proportion^{VMS}$	0.5	-	Proportion of vehicles using VMS guidance
$Proportion^{Pred}$	0.5	-	Proportion of vehicles using predictive guidance
Compliance rate	0.8	-	Proportion of vehicles following each guidance
v_1^{free}	105	km/h	Freeflow speed of road segment 1
v_2^{free}	105	km/h	Freeflow speed of road 2
ρ_1^{cong}	70	veh/km	Congestion density of road segment 1
ρ_2^{cong}	70	veh/km	Congestion density of road segment 2
dt	10	s	time step for Predictive RG
C_1^{ds}	4000	veh/h	Capacity of the segement downstream of road segment1
C_2^{ds}	4000	veh/h	Capacity of the segement downstream of road segment2
p^{extra}	2.5	-	Value for the adjustment coefficient β^{adj}
$Penalty^{ib}$	30	-	Penalty value for imbalance
N_p	1	-	Predictive horizon for RG

control steps, this means 12 CTM updates in the prediction model.

The critical density values and the capacities are assumed to be in line with the FD estimation in Section 5.3.2. Taking into account the objective of coordinated control (4.23), the control parameters should aim to reach the maximum theoretical outflow of 8000 veh/h.

Figure 5.17 shows the comparison between the predicted objective and the total flow detected in one of the coordinated control simulations. The closeness of two curves proves the plausibility of the setting of the coordination control parameter. A mismatch on time can also be observed. This happens because the selected control inputs of a control step will be applied on the next step. The simulation result shows more fluctuation than the predicted value, which is reasonable, since the optimisation aims to reach the maximum possible outflow of 8000veh/h.

5.3.4 Absence of capacity drop in the simulation

RM and VSL both aim to reduce and regulate total flow before the bottleneck. The former regulates the ramp flow, and the latter controls the main road flow. The purpose of these two DTM measures is to prevent capacity drop (Yuan et al., 2015). Therefore, the benefit should be higher than the additional travel time caused by the DTM measure on the ramp or on the main road (Carlson et al., 2010; Papageorgiou and Kotsialos, 2002).

Table 5.8: Coordinated control parameters

Coordinated MPC			
Parameter	Value	Unit	Description
$t_{control}$	60	s	Time step length for control
$\rho_{1,i}^{cong}$	90, 90, 65	veh/km	Congested capacity of cells on road 1
$\rho_{2,i}^{cong}$	90, 90, 65	veh/km	Congested capacity of cells on road 2
$C_{1,i}$	6000, 6000, 4000	veh/h	Capacity of cells on road 1
$C_{2,i}$	6000, 6000, 4000	veh/h	Capacity of cells on road 2
dx	0.3	km	Cell length
dt	10	s	Update time step for CTM
N_p^{coor}	2	-	Predictive horizon for coordinated control

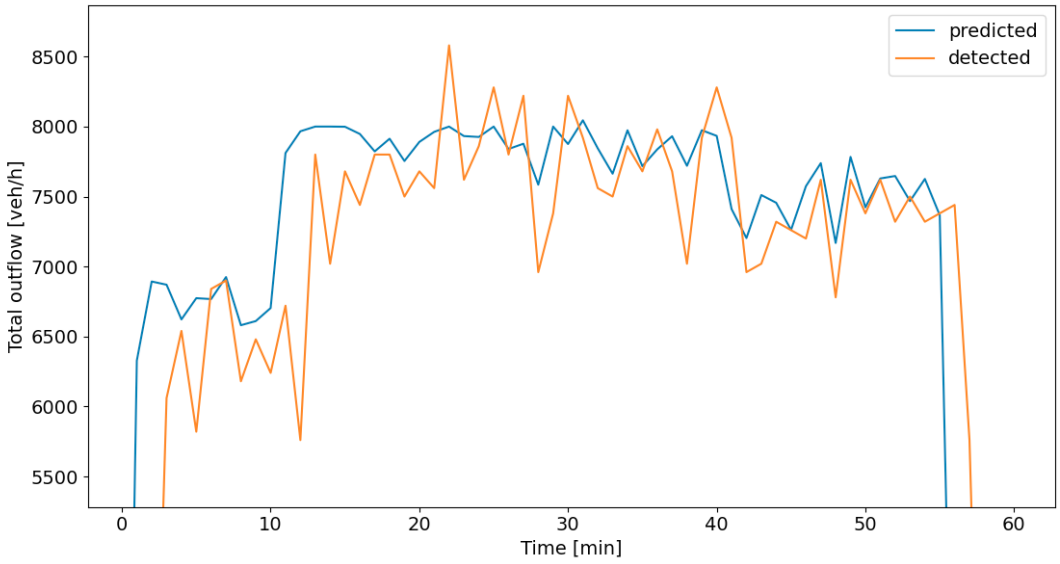

Figure 5.17: Coordinated control: predicted outflow and detected outflow

However, the phenomenon of capacity drop cannot be captured in the SUMO simulation with the simulation settings mentioned earlier in this chapter. To test the existence of capacity drop, slanted cumulative curve (Cassidy and Windover, 1995) is drawn. As shown in Eq. 5.1, the vehicle number $N_s(t)$ in the slanted cumulative curve is the result of subtracting the vehicle number $N(t)$ from the reference vehicle number calculated by the reference flow q_0 and time step dt. The purpose of using slanted cumulative curve is to show the detailed change in flow (slope of the cumulative curve).

$$N_s(t) = q_0 * t * dt - N(t) \tag{5.1}$$

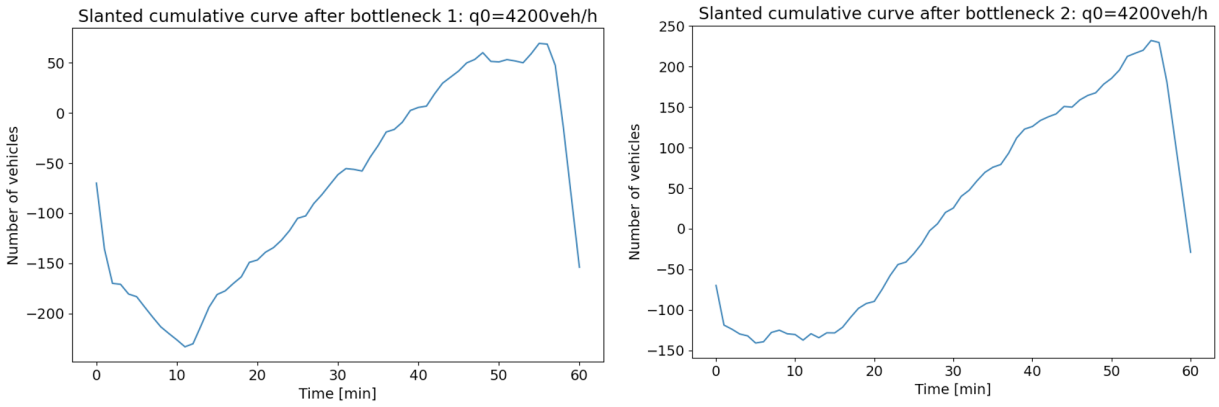

Figure 5.18: Cumulative curves after bottlenecks on each road

Figure 5.18 shows the slanted cumulative curves after bottlenecks on both routes. The result is from the base case and the reference flow set to 4200veh/h. It can be seen that there is no capacity drop after the congestion happens (after 10 minutes according to the given demand profile in Figure 5.15). The small fluctuation in the cumulative curve is caused by the change in inflow.

A parameter tuning process can be found in Appendix C. However, tuning selected lane changing and car following parameters still fails to create capacity drop in the simulation. This could be because of the selected simulation step length and the car following model. Duanmu (2023) observed capacity drop using SUMO with extended IDM model (EIDM) at a bottleneck due to lane drop. The model is suitable for simulation with time steps between 0.05s to 0.5s ("Extended Intelligent Driver Model - SUMO Documentation", n.d.).

5.4 Summary of assumptions

In the modelling and simulation, assumptions are made for simulation and DTM implementation. In the simulation setting, the following assumptions are made:

1. There are three origins and one destinations in the research network. This simplifies the demand composition on freeways. The most significant effect of this assumption is that there is no vehicle on ramp 2 until the travel time is longer on Road 1.

2. The parameter for lane change cooperation is set to the default value 1, which means complete cooperation to lane changing behaviour. This is because the route change segment in the simulation is short and there will be a lot of demand for lane changes due to the RG. When a lower cooperation parameter is applied, there will be more

congestion on the route change segment. However, this congestion is not the main concern of the research.

For DTM measures, the capacity improvement of RM and VSL is included in the applied road segments. Improvements in capacity are observed in field tests in the Netherlands (Taale, 2022). The increase in capacity is on average 2% for both RM and VSL. This is implemented in the simulation by changing the minimum headway for vehicles in the application areas.

There are more assumptions in the predictive RG algorithm and the MPC control algorithm, as predictive models are included. The assumptions are as follows:

1. Exponential Fundamental Diagram is used in both of the predictive models. This means that the capacity drop is not included in the prediction. As can be seen in Table 5.3, the RMSE values show the goodness of fit of the FD.

2. There is no demand prediction. That is, demands $d_1(t)$, $d_2(t)$ and $d_1^{ramp}(t)$ will be considered as constants within the prediction horizon. This is reasonable for the simulation, since the demand does not change frequently.

3. The predictive RG should also consider the possible vehicle flow following the VMS RG. This is simplified as a coefficient β^{adj} in the calculation of ramp flow (Eq. 4.27). A better way to apply this can be to include the VMS control signal in the predictive model. However, the existence of VMS is more a base case for vehicle route change behaviour rather than a DTM measure to be coordinated.

4. The effect of VSL is assumed to be linear. That is, the flow will change proportionally when the speed limit is reduced. This is to simplify the predictive MPC model. However, this also implies a linear relationship between upstream speed and flow. This is then also conflicting with the assumed exponential speed-density relationship. The assumed speed-flow relationship on the uncongested branch should be the curve shown in Figure 5.19.

5. The travel time before the first cell is neglected. The change in DTM parameters will directly affect the inflow through the boundary of the first cell.

6. The compliance rate is 80% for VMS RG, predictive RG and coordinated control. In an investigation into the coordination of RM and RG (Pasquale et al., 2017), complete compliance is assumed. Since the simulation is macroscopic in that research, the compliance rate will only have an effect on the macroscopic flow number. However, in this research, microsimulation includes more individual vehicle behaviour, and the effect of the compliance rate can also affect the lane change and route change behaviour of each vehicle. To include more randomness and test the robustness of the DTM measures, 80% is selected for all RG measures. Use the same compliance rate in the predictive RG and coordinated control cases makes them more comparable.

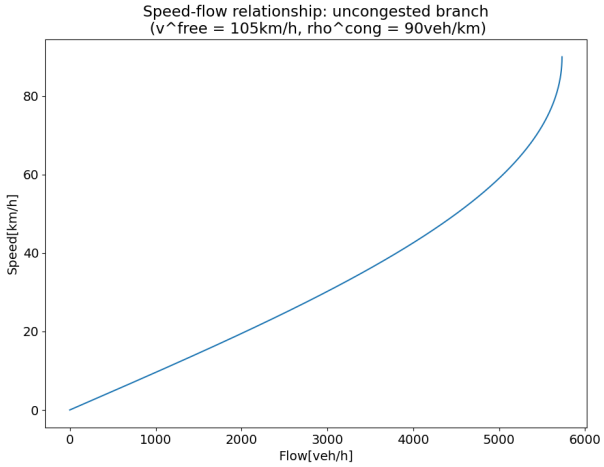

Figure 5.19: Speed flow curve on uncongested branch with selected exponential speed-density relationship

5.5 Simulation scenario setting

The simulation will test all possible combinations of DTMs to explore the interaction between DTMs. However, how the base case should be set is a crucial issue. If there is no DTM or travel time information, the demand profile will create very severe congestion on road 1. This situation is not realistic, since the vehicle in real life can observe congestion and reroute. Therefore, there should be route choice behaviour included.

The simulation is first run without any DTM measure. This aims to observe the default route change behaviour in the SUMO simulation and determine whether it is suitable to be selected as the base case. Figure 5.20a shows the speed contour on Road 1 with the default route change behaviour. It can be seen that there is route change behaviour existing. However, vehicles seem to be very stubborn to change to Route 2, even if the queue for the off-ramp spills upstream. When the queue before the off-ramp starts, the travel time of Route 2 should already be longer than that of Route 1. Therefore, the default route changing is not realistic.

Since the embedded model for route change behaviour in SUMO cannot be conveniently modified, the route change behaviour is defined as when only VMS RG is working. That is, a certain proportion of vehicles will notice the real-time travel time information and make their route selection. In Figure 5.20b, it can be seen that vehicles no longer queue before the off-ramp. Instead, vehicles using VMS RG switch between Route 1 and Route 2 alternatively. Therefore, multiple small congestion areas can be found in Figure 5.20b.

Figure 5.21 shows the locations of different DTMs on the simulation map. The travel time information is the instantaneous travel time of Route 1 and 2 obtained using the traci.edge.getTraveltime function. All vehicles are assumed to make their route choice on Edge EM1, when a vehicle is still on this edge, it is possible for it to change the route multi-

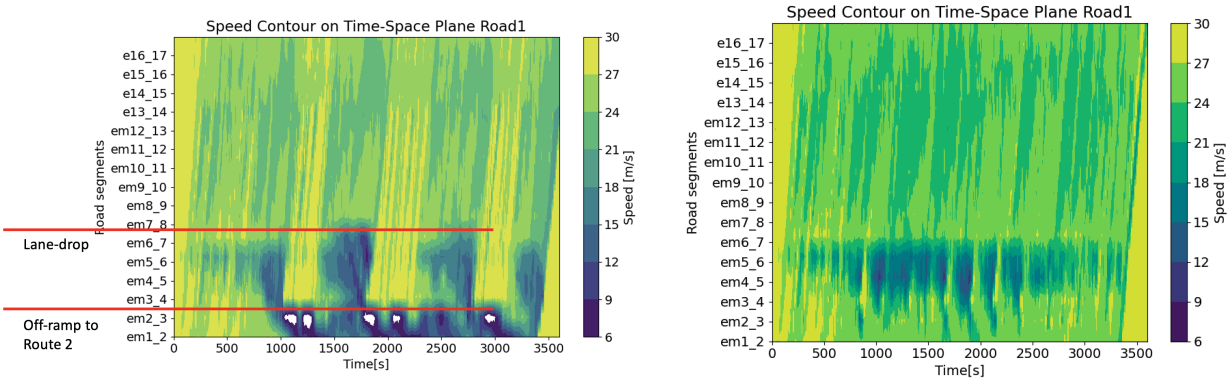

(a) Default (b) With VMS RG

Figure 5.20: Route change behaviour

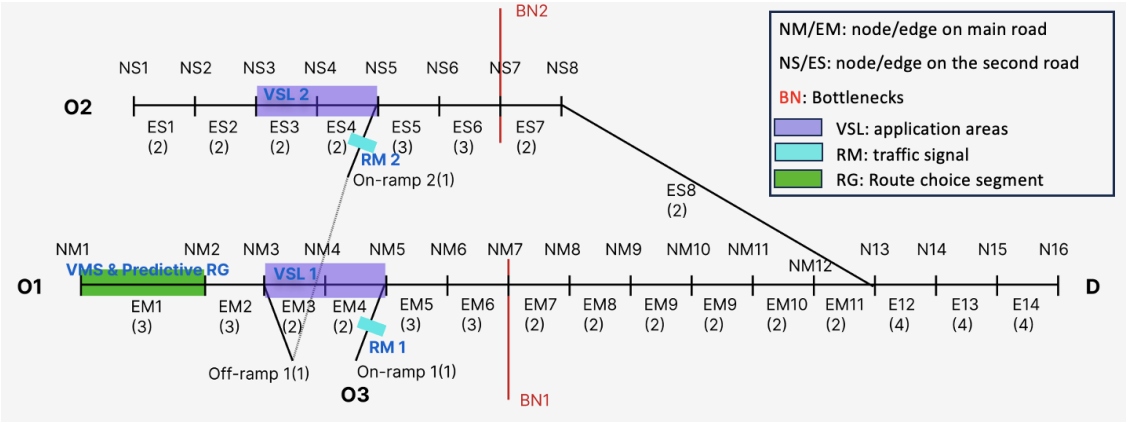

Figure 5.21: Simulation network with DTM locations

ple times based on the updated travel time information. Once a vehicle reaches EM2 (300m from the split point), no route choice can be made.

In this case, the queue before off-ramp can still happen. To alleviate this phenomenon, the travel time of lane instead of edge is used on EM2. This ensures that the queue before the off-ramp can be considered in the travel time of Route 2 and prevents more vehicles from joining the queue.

With the DTM measures shown in the network, there are too many possible scenarios. Instead of selecting some of them to create a scenario, the approach of this research is to use "available DTM sets" to create scenarios. This means that once a certain type of DTM is available in this scenario, it has the possibility of being active during the traffic state evolution. The activation of RM and VSL could be triggered by a certain traffic state. Since the simulation time is set to 1 hour with customised demand, RG is assumed to be always on or always off during the simulation.

Table 5.9 shows an overview of the simulation scenarios. Inclusion of DTMs varies in dif-

ferent scenarios. The check mark means that the DTM measure is available in the scenario and a cross means that the DTM measure is not. A special case is VSL 1 and VSL2 in the first coordination scenario, in which both VSL measures are off during the entire simulation duration. VMS RG is applied in all scenarios to ensure route changing of vehicles. To limit the number of scenarios, there are no cases where RM or VSL is only available on one of the roads.

Table 5.9: Overview of simulation scenarios

Scenario	**VMS RG**	**RM1**	**RM2**	**VSL1**	**VSL2**	**Predictive RG**
Base	✓	×	×	×	×	×
RM only	✓	✓	✓	×	×	×
VSL only	✓	×	×	✓	✓	×
RG only	✓	×	×	×	×	✓
RM+VSL	✓	✓	✓	✓	✓	×
RM+RG	✓	✓	✓	×	×	✓
VSL+RG	✓	×	×	✓	✓	✓
RM+VSL+RG	✓	✓	✓	✓	✓	✓
Coordination	✓	✓	✓	(✓)	(✓)	✓
Coordination (with VSL rule)	✓	✓	✓	✓	✓	✓

The difference between the first and the second coordinated cases is the inclusion of VSL. As introduced in Section 5.2.4, the coordinated MPC control seems to turn VSL on quite rarely. This is why VSL cannot be seen as included in the first coordination scenario. In the second coordinated scenario, there is a special rule for VSL which is isolated from the MPC controller. That is, the VSL will be on when RM is off for discharging the queue on the ramps.

5.6 Performance indicator calculation

The average travel time for each vehicle and the total delay are used to compare the performance of the network. To understand the effect of DTMs on different routes, the travel times are collected for different routes in the network. As shown in Figure 5.22, there are in total 4 routes for three OD pairs O1D, O2D and O3D. Routes OD1-1 and O1D-2 are referred to as Routes 1 and 2 discussed in the RG algorithm part.

To calculate the delay and the travel time, entry and exit points are set for each route. The entry points for routes are the first edge of each route, and all the vehicles exit the

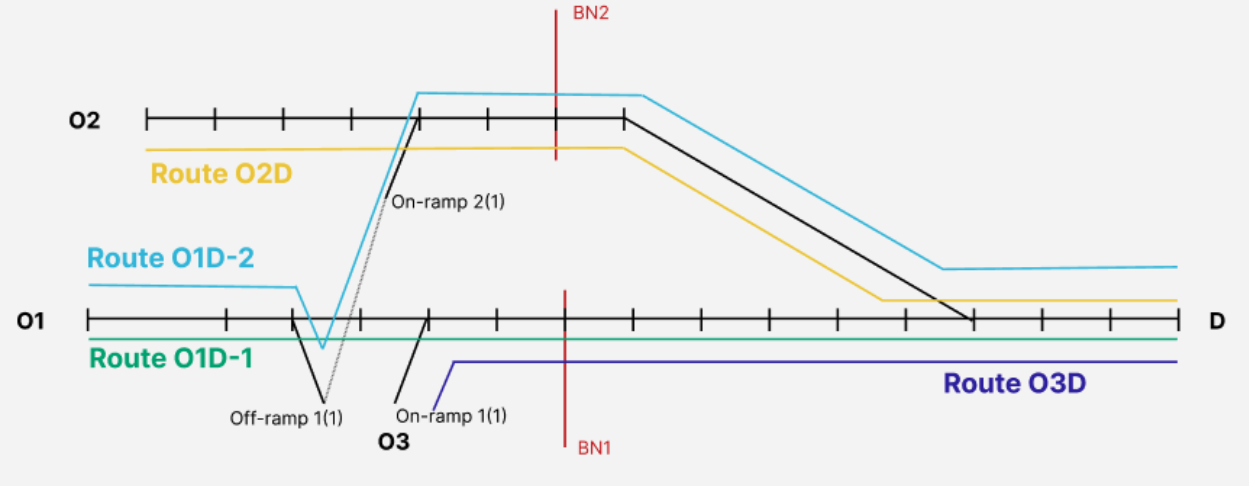

Figure 5.22: Routes in the network

network via the last edge after the merge. When a vehicle is detected for the first time on the entry edge, the time step will be recorded. When it is detected for the first time on the exit point, the exit time step will also be recorded. The total travel time for this vehicle will be the subtraction of the two recorded time steps.

To calculate the delay, a reference travel time is required for different routes. This is usually calculated by the free flow speed and the length of the route. As mentioned in Table 5.2, 30m/s and 15m/s are used as the speed limit for main road edges and ramp edges. According to SUMO User Documentation (n.d.), there is a speed factor distribution, which makes vehicles to have a desired travel speed higher or lower than the speed limit. The default distribution is normc(1,0.1,0.2,2), which means a normal distribution with a mean of 1, standard deviation of 0.1, a lower bound of 0.2 and an upper bound of 2. However, the speed is also restricted by the maximum speed of the vehicle type. In this simulation, the maximum speed of vehicles is also 30m/s. This makes the overall desired speed lower than 30, since there are vehicles that have a desired speed lower than 30 but there is no vehicle that has a desired speed higher than 30. The actual average free-flow speed v^{max} is then:

$$v^{max} = v^{limit} * \bar{x} \tag{5.2}$$

Where v^{limit} is the speed limit of the edges and $\bar{x}$ is the mean of speed factor. Assuming that the probability density function of the speed factor x is $f(x)$, then $\bar{x}$ is:

$$\bar{x} = \frac{\int_{0.2}^{1} x * f(x)dx}{\int_{0.2}^{1} f(x)dx} + \frac{\int_{1}^{2} x * f(x)dx}{\int_{1}^{2} f(x)dx} \tag{5.3}$$

With the restriction of vehicles' maximum speed, the second term in Eq. 5.3 is equal to 1. The calculated value of the first term is 0.92, which makes the average free-flow speed for main road $0.96 * 30 = 28.8m/s$. This problem does not exist for ramp vehicles, since their desired speed can exceed 15m/s. Therefore, the average free-flow speed for ramp vehicles

equal to the mean of the speed distribution (15m/s).

The length and travel time reference can be seen in Table 5.10. It can be seen that the travel times of the alternative routes O1D-1 and O1D-2 are close (208 and 221 s, respectively). This ensures the route-changing behaviour when the congestion occurs on Route O1D-1.

The delay is then calculated by $TT_j - TT_j^{ref}$ for each vehicle j. Where TT_j is the travel time collected from the vehicle and TT_j^{ref} is the reference travel time for the route of the vehicle j. The delay calculated this way depends totally on the travel time. Therefore, the delay and travel time are obtained from the same performance measure. For this reason, some other ways to measure performance indicators should be included as a new indicator.

Table 5.10: Length and travel time reference of 4 routes

Route	O1D-1	O1D-2	O2D	O3D
Length [m]	6016	5931	4685	4284
Travel time reference TT^{ref}[s]	208	221	162	171

In TraCI, there is also a function to collect the delay for vehicles (traci.vehicles.getTimeLoss). According to Reddy (2020), the time loss of a vehicle j is calculated as:

$$TimeLoss_j = \sum_{t=t_j^{enter}}^{t_j^{exit}} dt * (1 - \frac{v_j(t)}{v^{max}}) \tag{5.4}$$

Where t is the index of the simulation step, and dt is the step length. $v_j(t)$ is the speed of the vehicle in this time step, and v^{max} is the speed limit of the route on which the vehicle j is travelling. t_j^{enter} and t_j^{exit} are the entry and exit time of vehicle j.

Table 5.11: Time loss and calculated delay comparison

Simulation	1	2	3	4	5
Time loss [s]	282084	287056	286792	285399	307715
Calculated delay [s]	290963	296151	295686	294543	316587

To verify the calculation of the TimeLoss function, the delay calculated by TimeLoss is compared with the delay calculation method using experienced travel time. Table 5.11 shows the comparison between the results of the embedded time loss function and the delay calculation. It could be seen that the calculated delay is about 9000s higher than the time loss (3%). This error could be due to the shape of the road structure. That is, the speed limit may be lower for road segments with an angle. This is neglected in the reference travel time calculation.

Chapter 6

Result analysis

This chapter presents the analysis of the simulation results. In Section 6.1, the simulation results are analysed for different routes of the network. To test the sensitivity of the simulation results to several parameters, a sensitivity analysis is presented in Section 6.2.

6.1 Simulation results

The simulations are run on a 1.4 GHz Quad-Core Intel Core i5 MacBook with 8GB RAM. TraCI codes are written in PyCharm, using SUMO version 1.17.0. The Genetic Algorithm library is PyGAD 3.1.0. For the 1-hour research duration, it takes around 300s to run a non-coordinated scenario and 500s to run a coordinated scenario (6-10s for each control step). Since there is randomness in the microsimulation, each scenario is run at least 20 times to get the mean value and the distribution of the performance indicators.

6.1.1 Travel time on each route

In order to evaluate the control scenarios more detailed, the mean of the average travel time is organised for each route (routes are shown in Figure 5.22). The results are shown in Table 6.1. In this table, the darker green indicates lower indicator values and the darker red indicates higher indicator values. The comparison (reference for coloring) is made within each column, which aims to find the difference in indicators in different control scenarios. The values shown in Table 6.1 are all the mean of the 20-time simulation run. To test whether the indicators in controlled cases are different from them in the base case, t-test is performed. With a confidence level of 95%, several indicator values are not significantly different from indicator values. These values are marked with "($\times$)". The p-value results of the t-tests can be found in Table D.1.

In Table 6.2, the percentages of improvement are listed. It can be seen that the reduction in total delay is much higher than the reduction in average travel time for the same scenario. This is because the segments where congestion may occur are only part of the network. After the only two bottlenecks, vehicles will always travel at free-flow speed. This will dilute the magnitude of the reduction in average travel time.

Single controlled cases

For single DTM control scenarios, it can be seen that RG has the best performance compared to RM and VSL. Since the flow from Route 1 to Route 2 is distributed more evenly with predictive RG, the travel time on Route O1D-2 is considerably reduced. With the predictive control strategy, congestion on Route 2 is also alleviated. This can be seen in the reduction in travel time on Route O2D. It can be seen that there is an increase in travel time on Route O1D-1. This could be because there is more route-changing behaviour included when both VMS RG and predictive RG are on, and all the necessary lane change for route change happens on edge 1 on Route O1D-1.

RM and VSL have slightly longer average travel times. This is because the capacity drop cannot be captured well in the current simulation setting. In other words, the congestion in the no-control case is not severe enough so that applying RM and VSL can have obvious benefits. RM case has three indicators that are not significantly different from the base case and VSL case has 5 out of six. However, RM still has the effect of changing the location of congestion. RM has the best improvement on Route O2D. This is because regulated ramp flow can alleviate congestion before bottleneck 2. Travel time on routes with on-ramps increases considerably (O1D-2 and O3D). There is also a slight increase in travel time on Route O1D-1. In the base case, the congestion on Route 1 is less severe compared to Route 2, as vehicles will switch to Route 2 when the travel time on Route 1 is longer. This explains why there is no considerable reduction in travel time on Route O1D-1. The reason why there is even an increase in travel time on Route O1D-1 is the existence of the queue discharge rule (as mentioned in Section 5.2.1). When the queue is released, the flow merging to the main road will increase suddenly, which may lead to severe congestion for a short period.

The overall effect of VSL is not significant, since the speed limit is only reduced for a short period of time. It can be seen that the travel time on Route O1D-2 and O3D is reduced, whereas the travel time on Route O1D-1 and O2D increases. This is because Route O1D-2 and O3D are not in the VSL application area, while Route O1D-1 and O2D are. The overall increase in network average travel time means that the reduced travel time by alleviating congestion cannot exceed the additional travel time caused by the reduced speed limit. It can be noticed that the total delay in the VSL-only case is lower than it in the base case. This is because the method for the calculation of the total delay (Eq. 5.4) takes the current speed limit on the road segments as the reference.

Combined cases

In the combined control cases, the inclusion of RG ensures the overall reduction in travel time. In addition, no combined case shows better network average travel time than the RG-only case. This means that the redistribution of flow in this network is the strongest measure. The combination of RM and VSL has quite close performance indicators as in the RM-only case. However, the travel time on Route O1D-2 (not in the VSL application) is even higher. With the VSL available on Route O1D-1, the instantaneous travel time may

Table 6.1: Performance indicator mean value comparison for all control scenarios (values noted in (×) represent the mean is not statistically different from it in the base case)

Scenarios	Travel time [s]					Total Delay [veh*h]
	Network average	Route O1D-1 average	Route O1D-2 average	Route O2D average	Route O3D average	
Base	229.8	257.0	286.6	200.4	217.2	82.6
RM only	230.5(×)	257.6(×)	313.7	194.4	242.1	84.3(×)
VSL only	230.1(×)	257.1(×)	286.2(×)	201.1(×)	216.9	81.8(×)
RG only	228.2	257.6(×)	277.1	197.5	217.3(×)	79.5
RM+VSL	230.6(×)	257.7(×)	315.0	194.5	240.5	83.0(×)
RM+RG	228.3	258.2	297.1	191.3	236.9	79.9
VSL+RG	228.3	257.5(×)	276.9	197.9	216.7	78.6
RM+VSL+RG	228.5	258.4	297.7	191.4	237.3	79.5
Coordination	228.2	257.1(×)	299.6	193.1	233.0	79.8
Coordination (with VSL rule)	227.6	256.6	297.3	192.9	230.1	78.1

exceed the travel time on Route O1D-2 earlier than the base case. Therefore, the total number of vehicles travelling through on-ramp 2 (following VMS RG) increases. These vehicles will be regulated by RM on ramp 2 and have a longer travel time. This makes the average travel time on Route O1D-2 longer.

The most important improvement in the RM+RG case compared to the RG-only case is the travel time on Route O2D. Compared to the RM-only case, the travel time on each route is shorter in the RM + RG case, except for it on Route O1D-1. There are two reasons for this increase in travel time. First, there will be more lane change behaviour when predictive RG is on, which may lead to more hindrance between vehicles. In addition, vehicles can queue before the off-ramp on Route 1 due to their already-made route choice. When RM on ramp 2 is on, this queue may occur more often. These two reasons cause the increase in travel time in both the RM-only (257.6s) and RG-only (257.6s) cases compared to the base case (257.0s). In the combined RM+RG case, the increase in travel time on Route O1D-1 is even greater.

The VSL+RG case has almost no difference compared to the RG-only case. This is because there is less congestion due to the effect of RG, and the VSL is triggered less often.

The difference between the RM+RG+VSL case and the RM+RG case is the inclusion of

Table 6.2: Performance indicator improvement comparison for all control scenarios (values noted in (×) represent the mean is not statistically different from it in the base case)

Scenarios	Travel time change [%]					Total delay change[%]
	Network average	Route O1D-1	Route O1D-2	Route O2D	Route O3D	
Base	229.8	257.0	286.6	200.4	217.2	82.6
RM	0.3%(×)	0.2%(×)	9.5%	-3.0%	11.5%	2.1%(×)
VSL	0.1%(×)	0.0%(×)	-0.2%(×)	0.3%(×)	-0.2%	-0.9%(×)
RG	-0.7%	0.2%(×)	-3.3%	-1.5%	0.0%(×)	-3.7%
RM+VSL	0.4%(×)	0.3%(×)	9.9%	-2.9%	10.7%	0.5%(×)
RM+RG	-0.6%	0.5%	3.6%	-4.6%	9.1%	-3.3%
VSL+RG	-0.6%	0.2%(×)	-3.4%	-1.2%	-0.2%	-4.9%
RM+VSL+RG	-0.5%	0.5%	3.8%	-4.5%	9.2%	-3.7%
Coordination	-0.7%	0.0%(×)	4.5%	-3.7%	7.3%	-3.3%
Coordination (with VSL rule)	-0.9%	-0.1%	3.7%	-3.7%	5.9%	-5.5%

VSL, while VSL has a limited effect when RG is also available. The expected phenomenon would be that the travel time is longer on routes with VSL application area (O1D-1 and O2D), while the travel time should be slightly better for routes without VSL application area(O1D-2 and O3D). The result in the RM+RG+VSL case is partially in line with the expectation. The difference is that the performance on Routes O1D-2 and O3D is also slightly worse than in the RM+RG case. An interpretation of this is that there exists a delay in response between RM and VSL. The queue discharge on RM is activated regardless of the state of the main road traffic. When RM is off, it can cause severe congestion. In this case, VSL can only respond to this congestion after the congestion occurs.

In Figure 6.1, it can be seen that the VSL has overlapped duration with the queue discharging on the ramp, while the queue discharge usually occurs before the speed limit reduction. The part when ramp flow exceeds 720veh/h means that RM is off. This figure shows that VSL is sometimes on because of the congestion caused by the queue discharge on the ramp.

Coordinated control

With the coordination algorithm, the speed limit will not be reduced since it has a negative effect on the control objective (i.e. the total outflow). In the first coordination case, only RM and RG are available. Compared to the RM + RG case without coordination, there

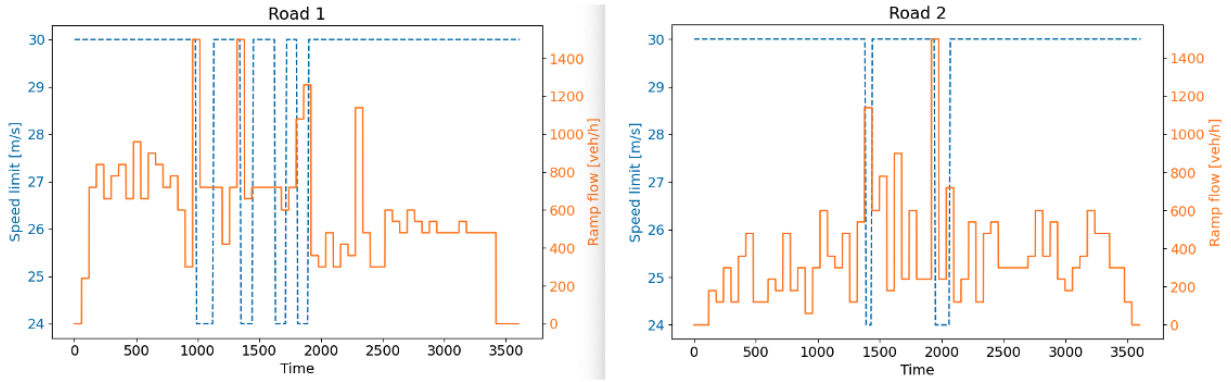

Figure 6.1: RM+RG+VSL case: Speed limit and ramp flow

is a reduction in travel time on Routes O1D-1 and O3D. This means that the coordination algorithm improves travel time more on Road 1, while the predictive RG strategy has slightly more improvement on Road 2.

In the second coordination case, VSL and RM will act alternatively to reduce total flow before the bottleneck. That is, VSL is on when RM is off for queue discharging on ramp. The travel time is reduced on all routes compared to the first coordination case, especially on the routes with ramps (Route O1D-2 and O3D). The network average travel time and the total delay in this scenario are the lowest among all scenarios. This shows the value of coordination.

Figure 6.2 shows the speed limit curve and the ramp flow curve in the coordinated scenario with the VSL rule. Compared to Figure 6.1, the VSL is on simultaneously with the discharge of the queue on the ramp. That is, in coordinated control, the VSL can prevent congestion caused by high ramp flow, instead of solving the already existing congestion caused by ramp queue discharge.

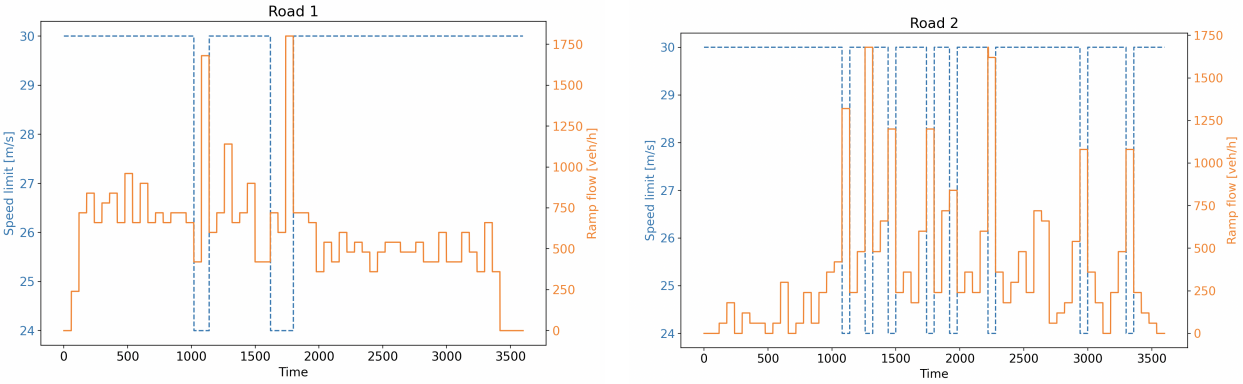

Figure 6.2: Coordinated case: Speed limit and ramp flow

6.1.2 Travel time variation in different scenarios on each route

Besides the average travel time, the variation in travel time can also indicate the performance of a controlled scenario. In Table 6.3, the standard deviation of the travel time between simulation runs in each scenario is summarised.

In Table 6.3, the general trend is that the travel time with higher mean values usually has a larger standard deviation. When looking at the standard deviation of network average travel time and the total delay, it could be seen that the application of DTMs makes the network performance more stable. RM-only case has a higher network average travel time than the VSL-only case in Table 6.1. However, it has a better effect on stabilising network performance. RM-only case has the effect of redistributing the congestion, while the VSL-only case is very similar to the performance in the base case.

Table 6.3: Performance indicator standard deviation comparison for all control scenarios

Scenarios	Standard deviation of travel time [s]					Standard deviation of total delay[s]
	Network average	Route O1D-1	Route O1D-2	Route O2D	Route O3D	
Base	1.80	0.89	2.86	3.17	0.48	12274
RM only	1.27	1.27	4.30	1.40	3.32	8617
VSL only	1.79	0.75	3.01	3.25	0.53	12157
RG only	1.39	1.15	1.35	2.21	0.54	9595
RM+VSL	0.89	0.89	4.33	1.24	2.21	6186
RM+RG	0.92	1.18	2.76	1.25	3.20	6246
VSL+RG	1.20	0.97	1.26	2.40	0.72	8025
RM+VSL+RG	0.70	1.18	2.78	0.73	2.00	4739
Coordination	1.00	1.31	2.97	1.15	3.87	6827
Coordination (with VSL rule)	0.68	0.80	2.01	0.66	3.86	4385

Among these three DTMs, RM has the strongest effect in stabilising travel time. This is because that RM can change the total demand in a more certain control strategy. RM controls ramp vehicles based on aggregated main road demand and ramp demand. This makes the result more stable. However, in the VSL and RG cases, more randomness is included. For VSL, the speed before the bottleneck may not always reduce to a lower threshold at the same time period. For predictive RG, the states in each control step may also vary since some of the vehicles will not obey the guidance.

In cases including RM, the variance in travel time on Route O1D-2 and O3D is greater.

In the two coordinated cases, the standard deviation on Route O3D is the highest among all scenarios. This is because the metering rate on Route O1D-1 varies more in the coordinated case.

The coordinated scenario with the VSL rule has the best stability among all control scenarios. Compared to the base case, it has considerable improvement on the travel time on two main roads. The standard deviation of travel time for is 0.80 (0.89 in the base case) on Route O1D-1 and 0.66 (3.17 in the base case)Route O2D.

Table 6.4: Coefficient of variation comparison for all control scenarios

Scenarios	Coefficient of variation of travel time					Total delay coefficient of variation
	Network average	Route O1D-1	Route O1D-2	Route O2D	Route O3D	
Base	7.8E-03	3.5E-03	1.0E-02	1.6E-02	2.2E-03	4.1E-02
RM only	5.5E-03	4.9E-03	1.4E-02	7.2E-03	1.4E-02	2.8E-02
VSL only	7.8E-03	2.9E-03	1.1E-02	1.6E-02	2.4E-03	4.1E-02
RG only	6.1E-03	4.4E-03	4.9E-03	1.1E-02	2.5E-03	3.4E-02
RM+VSL	3.9E-03	3.5E-03	1.4E-02	6.4E-03	9.2E-03	2.1E-02
RM+RG	4.0E-03	4.6E-03	9.3E-03	6.5E-03	1.4E-02	2.2E-02
VSL+RG	5.3E-03	3.8E-03	4.6E-03	1.2E-02	3.3E-03	2.8E-02
RM+VSL+RG	3.0E-03	4.6E-03	9.3E-03	3.8E-03	8.4E-03	1.7E-02
Coordination	4.4E-03	5.1E-03	9.9E-03	6.0E-03	1.7E-02	2.4E-02
Coordination (with VSL rule)	3.0E-03	3.1E-03	6.8E-03	3.4E-03	1.7E-02	1.6E-02

The vertical comparison of standard deviations in Table 6.3 shows which control scenarios lead to more stable network or route performance. However, the variation of each indicator cannot be compared without normalisation. Therefore, the coefficient of variation (standard deviation divided by mean) is used to explore the different levels of variation between indicators in different scenarios. The results are shown in Table 6.4. In this table, the green colour still means lower values, and the red colour means higher values. The difference is that it compares all values in the table instead of the values in each column (as in Table 6.1 and 6.3).

In general, the level of variation is quite low for all indicators in all cases. The variation level of the total delay is much higher than that of the average network travel time. This is because the travel time includes delay, while delay is the major change in different cases. For the four routes, the variation levels of Route O1D-2 and O2D are in general higher than those of other routes. This indicates that congestion is more severe before bottleneck 2 than before bottleneck 1. Route O1D-1 has the lowest level of variation. This is because the existence of VMS RG makes the congestion before bottleneck 1 more stable. Vehicles will

switch to Route O1D-2 once the congestion reaches a certain location.

6.1.3 Travel time equity among routes

In Table 6.1, it can be seen that the travel time for routes that include ramps increases significantly in cases with RM. Although overall performance has some improvement in some of these scenarios, it may worsen the travel time equity between routes. To explore the effect of different control scenarios on the travel time equity, a comparable indicator is required first. Due to the different length and speed limits on different routes, the travel times are not comparable. A suitable indicator is the travel time index (TTI), which is the ratio between the average experienced travel time and the free-flow reference travel time (Federal Highway Administration, n.d.). When the TTIs on different routes are closer, it can be interpreted as the traffic situation being more equal for all routes. Therefore, the standard deviation of TTIs on different routes can be used as an indicator for equity.

As shown in Table 6.5, the application of RM increases the imbalance between routes, while adding the predictive RG can reduce the inequity. The inequity issue does not improve much in the coordination scenario. Therefore, the RG only scenario may be the best choice considering the equity issue among routes.

Table 6.5: Travel time index and variation on different routes for all control scenarios

Scenario	**Travel time index**				**Standard deviation of TTIs on four routes**
	Route O1D-1	**Route O1D-2**	**Route O2D**	**Route O3D**	
Base	1.28	1.34	1.28	1.31	0.03
RM only	1.29	1.47	1.25	1.46	0.11
VSL only	1.29	1.35	1.30	1.31	0.03
RG only	1.27	1.30	1.29	1.31	0.01
RM+VSL	1.30	1.48	1.26	1.45	0.11
RM+RG	1.28	1.40	1.25	1.42	0.09
VSL+RG	1.28	1.32	1.30	1.30	0.01
RM+VSL+RG	1.29	1.42	1.25	1.43	0.09
Coordination	1.28	1.40	1.24	1.40	0.08
Coordination (with VSL rule)	1.28	1.40	1.25	1.41	0.08

6.2 Sensitivity analysis

To test the influence of different parameter values, a sensitivity analysis is performed for several parameters in the simulation. From the analysis in Section 6.1, RG and queue discharging of RM are two most effective factors for total travel time. Therefore, a sensitivity analysis is more important for parameters that can influence RG control and queue discharging behaviour. In the following part of this section, sensitivity analyses are performed for four parameters. They are the compliance rate for both VMS RG and predictive RG, the maximum queue length, and the length of queue detectors for RM. For each parameter value, 20 simulation runs are performed. In Table 6.6 to Table 6.9, the average travel time means the mean of the average travel time per vehicle for the 20 simulation runs. The standard deviation also represent the variation among simulation runs.

Compliance rate for VMS RG and predictive RG

The compliance rates to both VMS RG and predictive RG are crucial parameters for simulation. The former determines how many vehicles will change route when the travel time on the longer route is shorter, and the latter decides how many vehicles will follow the optimal split rate. Table 6.6 shows the simulation results under different compliance rate values to VMS RG. It can be seen that the average travel time decreases when the compliance rate changes from 1 to 0.4. This is because the flow on the main road of Road 2 keeps at a high value. When the compliance rate is higher, there are more vehicles merging to the main road on Road 2. This increases total flow before the bottleneck on Route 2, making it more possible for severe congestion to occur there. The average travel time increases again from 0.4 to 0.2. There may exist a route changing proportion between 0.4 to 0.2, which can lead to the least congestion for the whole network. Considering the given demand profile, the total demand during congestion before bottleneck 1 is 4600veh/h (3800 on main road and 800 on the ramp), while the demand for road 2 is 3400veh/h. Assuming that the total travel time is the lowest when the two routes have the same demand before bottlenecks, there should be a flow of 600veh/h switching to route 2. This means a compliance rate of $600/(0.5 * 3800) = 0.32$ in the base case. This is also in line with the finding from the sensitivity analysis. When the compliance rate is 0, it is equivalent to when there is no route change behaviour. Simulation runs show an average travel time of around 245s for the no-route-change case. This shows the importance of RG for the considered network structure.

As shown in Table 6.7, the simulation result is much less sensitive to the compliance rate of the predictive RG. According to the statistical test (p-values listed in Table D.2), all other scenarios have the same mean as when the compliance rate is 0.8. This is because in the RG only case both RG are available. Even when there are fewer vehicles obeying predictive RG, VMS RG can still guide other vehicles to route 2. When there is only predictive RG, the average travel time increases from 231s to 238s when the compliance rate decreases from 0.8 to 0.2. When the compliance rate for predictive RG is 0, it is equivalent to the base case when the compliance rate for VMS RG is 0.8, and hence the mean of the average travel time is 230.1s. This means that the combination of these two types of RG forms a more stable RG control. Although the optimal split rate may not be reached all the time, the predictive RG

in this scenario can still balance the flow between routes to improve network performance.

Table 6.6: Base case: travel time under different compliance rate settings (values noted in (×) represent the mean is not statistically different from it when the compliance rate is 0.8)

VMS RG		
Compliance rate	Average teavel time [s]	Standard deviation
1	232.1	2.6
0.9	231.1(×)	2.4
0.8	230.1	1.9
0.7	229.3(×)	1.8
0.6	228.3	1.1
0.4	227.9	1.3
0.2	228.5	1.2

Table 6.7: RG only case: travel time under different compliance rate settings (values noted in (×) represent the mean is not statistically different from it when the compliance rate is 0.8)

Predictive RG (VMS RG has a compliance rate of 0.8)		
Compliance rate	Average teavel time [s]	Standard deviation
1	228.0(×)	1.4
0.9	228.6(×)	1.8
0.8	228.2	1.4
0.7	228.1(×)	1.1
0.6	228.7(×)	1.8
0.4	227.8(×)	1.3
0.2	228.1(×)	1.2

Maximum queue length and queue detector length

The discharging of the queue on the ramps also affects the performance of the network. When the maximum queue length is set too long, the high outflow from the ramp will retain for a longer duration and may lead to more severe congestion before the bottleneck. It should also not be too close to the stop line, since then the ramp cannot store vehicles and the RM will be turned off more frequently. As mentioned in Section 5.2.1, the queue detection is performed by lane area detectors. Figure 6.3 shows the tuning of the location and length of

these detectors. The detector location change is only applied on Ramp 1. This is because RM 2 is located on Route 2. When the maximum queue length is changed on ramp 2, the route changing behaviour will also change. In that case, it will be difficult to evaluate the effect of maximum queue length. Scenarios are created by three different maximum queue length values under a certain detector length and three different detector lengths when the maximum queue length is fixed.

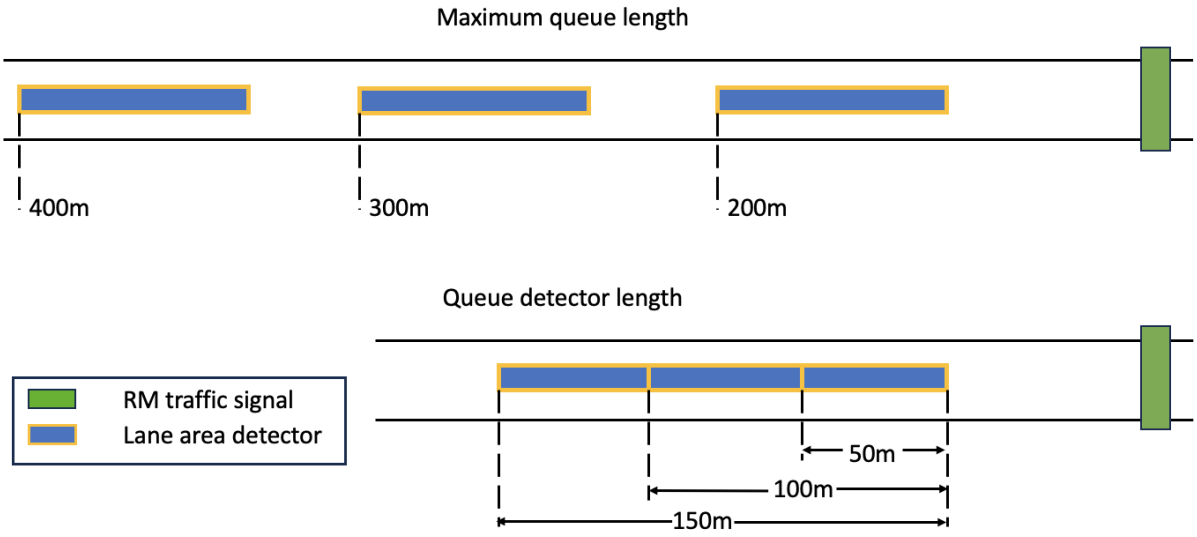

Figure 6.3: Illustration for the tuning of parameters of lane area detectors

Table 6.8 shows the simulation results when the maximum queue length value is set to 200, 300 and 400m. It could be seen that the simulation output is sensitive to the maximum queue length value, considering that the parameter is only changed for RM1. From the results, 300m and 400m are both too long for the ramp to store vehicles. The maximum queue length of 200m has the shortest travel time. This means that queue discharge in this case causes the least congestion.

Table 6.8: RM only case: travel time under different Maximum queue length settings

Detector length = 150m		
Maximum queue length [m]	Average travel time [s]	Standard deviation
200	230.5	1.3
300	232.0	0.9
400	233.7	1.3

Compared to the maximum queue length value, the length of the lane area detector has less influence on the simulation results. In Table 6.9, it can be seen that there is no

significant difference between scenarios with detector length of 150m and 100m. However, the difference seems to be larger when the detector length is even shorter. This is because the average travel time on a shorter detector can change more often, which causes more frequent switch-on and-off of RM.

Table 6.9: RM only case: travel time under different queue detector length settings

Maximum queue length = 200m		
Detector length [m]	Average travel time [s]	Standard deviation
150	230.5	1.3
100	230.8	1.1
50	231.4	1.1

Chapter 7

Conclusion

The subquestions presented in Section 3.2 are solved during the process of the research. After solving all of them, the main research question can be answered. The answers to the subquestions are listed below:

1. **In what kind of road structure will RM, VSL, and RG have potential conflicting effect?**
   The research network (shown in Figure 3.2) is designed based on real-life road structure. In this network, RM and VSL on each route are conflicting when congestion occurs before the bottleneck on road 1, given that there exists RG. The potential conflict between DTM measures is the reason why the coordination of DTMs is required in this network.
2. **What are appropriate control algorithms for each DTM?**
   To better explore the effect of DTM coordination, the control parameters used in individual DTM measures and in coordinated control should be the same. That is, the control parameters are determined by local control objectives in the non-coordinated cases and by the objective of the coordination in the coordinated case. For this purpose, RM with demand-capacity algorithm, road side VSL and a predictive in-vehicle RG are selected. Road side RG using VMS is also added to the simulation to create realistic route changing behaviour in the base case.
3. **What kind of coordination method can be used to tackle the conflict and improve network performance?**
   Model predictive control is a suitable method to include all control variables. The objective of the designed coordinated MPC is to maximise the total outflow passing through bottlenecks on two routes. The conflict is eliminated since all controllers now serve the same control objective.
4. **How should the simulation be set?**
   To include more detailed vehicle behaviour such as lane changing of vehicles, microsimulation software SUMO is selected to configure the simulation and implement DTM measures. Scenarios are created by combining different types of DTMs. VMS RG is included in all scenarios since it is part of the no-control case.
5. **What are suitable indicators to measure network performance?**
   The average travel time of vehicles and the total delay are used to compare whether

a scenario performs better than another. The average travel time on each route is also collected to see what the effects of DTMs are on different parts of the network. Besides, travel time equity is measured as the standard deviation of the travel time index on each route. It can be used to determine whether a scenario sacrifices vehicles on one route too much to create a better overall network performance.

The answer to the main research question **What is the impact of coordinating RM, VSL and RG on a road structure where they have potential counter-effects on each other when following local objectives?** is: The coordinated control has positive effect on network performance. The performance indicator is better than when DTM measures work together but with their local control objectives. However, its effect is not as strong as the effect of predictive RG. The latter also has a better performance in travel time equity among routes. Therefore, the conclusion is that a suitable RG is more decisive for this research network structure than a coordinated RM, RG and VSL control. This conclusion is limited to the simulation setting in this research, since RM and VSL are not performing well due to the absence of capacity drop.

From the simulation results, more detailed conclusions can be drawn from the perspective of the road structure, the effect of DTMs and the counter effect between them, and the value of coordination.

Road structure

In the simulation, the network has two roads that end at the same destination. The ramp connecting two roads provides an additional route option for vehicles from O1 to D (O1D-1 and O1D-2 in Figure 5.22). When a suitable RG is included, a more stable two-bottleneck system is formed. Even when only VMS RG is included, the mechanism can also dynamically balance the flow on each route. This feature of this road structure also makes it more difficult to improve compared to a one-bottleneck corridor. The average travel time is much longer when no route change is included (245.8s) than in the base case (229.8s). This shows the importance of RG in such a road structure. The best case (RG only case) also proves the benefit of applying RG with system optimal objective.

Effect of individual DTMs and non-coordinated DTM combination

Among the three DTMs, RG is the most effective. The absence of capacity drop is the reason for the worse performance in the RM and VSL scenarios. RM has a considerable effect on reducing congestion on Road 2, which leads to travel time reduction of 6 seconds for each vehicle on Route O2D. However, vehicles on ramp 1 and ramp 2 experience a longer travel time due to signal control (27s in average for vehicles passing ramp 1 and 25s for vehicles passing ramp 2), and the overall average travel time does not improve. As for VSL, the reduction in travel time by preventing congestion can not compensate for the additional travel time caused by the reduction in speed limits.

The counter effects between DTMs are not as significant as expected. However, it can

be seen in Table 6.1 that none of the combined control cases has further improvement compared to the best case among the single control scenarios. As mentioned above, the effect of predictive RG is to balance the flow on two main roads, while the benefit of using RM is to reduce congestion on Road 2. It can be seen that in the RM+RG case, the combination of these two effects has a further improvement in travel time on Route O2D (191.3s, 194.4s in the RM only case). This means that adding RM to this road structure when RG exist (or vice versa) can have additional benefits, even when they are not coordinated.

Value of coordination

The two coordination cases have some slight improvement compared to the combined control cases. When the VSL rule is not included, the indicator values are quite similar to them in the RM+RG case. Coordinated MPC control leads to a longer travel time on Road 2 (Routes O1D-2 and O2D) while a shorter travel time on Road 1 (O1D-1 and O3D). This may be due to the difference in the formulation of predictive models in predictive RG and coordinated MPC control. That is, minimising average travel time and maximising total outflow may lead to different desired demands before bottlenecks on each route.

The second coordination case uses VSL to prevent congestion caused by the queue discharging of ramps. Compared to the RM+VSL+RG case, it has around 1 second reduction in the network average travel time and a 4-hour reduction in the total delay. This is because it solves the problem of the late response of VSL to the ramp queue discharging. In the combined case, VSL is on after congestion is caused by the sudden increase in ramp flow. In the coordinated case with VSL rule, the VSL is activated simultaneously when RM is required to be turned off. When there is capacity drop phenomenon, the ramp queue discharge may also cause the decrease in capacity. In this case, using VSL to compensate for ramp queue discharge is expected to have more benefit.

In conclusion, network performance can improve more when coordinated control is used. However, the magnitude of the improvement is not significant enough compared to RG only case. Besides, the RG only case also has a better travel time equity (as shown in Table 6.5). This means that route guidance is more important for this two-road system. In real-life traffic management, it may also be more beneficial to improve the route guidance system than to implement a coordination controller.

Chapter 8

Discussion

The main contribution of this research is the analysis of DTM measures and the combination of DTM for the road structure where two freeways merge to a same destination. In addition, a predictive RG algorithm and an MPC coordination control strategy are designed for parallel road bottlenecks. Network performance is improved with predictive RG and coordinated control. Another contribution is that the simulation is performed in a microsimulation environment. That is, the traffic flow model used to predict traffic states is not the same as the model used for the simulation. Then the optimisation cannot directly affect the simulation output, but via the implemented controllers in the microsimulation, where more uncertainty and randomness are included. This is not common in other DTM coordination research, unless lane-changing control is discussed. One of the reasons may be that microsimulation increases the complexity of implementing DTM control algorithms and analysing the simulation results. For example, the effect split rate will only be a number in macrosimulation, which also leads to determined simulation results. However, in microsimulation this needs to be a process of random vehicle drawing for route change. The advantage of microsimulation is that it is more realistic and that it can better test the effect of DTMs. However, with the research network in this research, tuning and adjustment of DTMs are quite time-consuming. This feature also restricts the space to apply more complex predictive models or DTM algorithms. Thus, more assumptions are made, and they lead to limitations of the research.

In Section 8.1, the limitations of this research are discussed. In Section 8.2, discussion is made about future research directions.

8.1 Limitations of the research

The limitations are divided into five aspects. The first aspect is about the conceptual network. Compared to the structure of the roads in real life, the research network is simplified. With fewer entries (origins) and exits (destinations) in the network, the vehicle demands is also simplified. In the simulation, only vehicles from O1 to D use the ramp between Road 1 and 2. When the travel time on Route 1 is shorter than on Route 2, no vehicle will pass through the ramp in the base case. This is not the case in the real-life situation, as there are also vehicles that are travelling to a different destination via Road 2.

The second aspect is about DTM algorithms and predictive models. The two predictive models in predictive RG and coordinated MPC control are only for a certain part of the network. This simplifies the formation and implementation. Meanwhile, it also limits the performance of the model. A typical example is that the queue model cannot be included accurately in this case. With a traffic flow model for the entire research network, the number of vehicles waiting outside of the network can be calculated. However, in the predictive model for predictive RG and coordinated control, the model boundary is not the simulation network boundary. Therefore, it is difficult to get the queue length, especially on the main road. The result of this is that the total travel time cannot be used as the control objective, since the waiting time caused by RM and the additional travel time caused by VSL cannot be properly included in the current predictive model. Additionally, the effect of turning off RM also cannot be captured in the predictive model for coordinated control. This is why separate rules are used for the ramp queue discharge.

The third aspect is about the simulation environment and the setting. The most important limitation is that the capacity drop phenomenon is not captured in SUMO with the current simulation setting. For this reason, there is no benefit for applying RM and VSL. This shows the drawbacks of using SUMO for DTM coordination research, especially when the source of congestion is the road bottleneck. This has also affected the conclusion of this research. Since RM and VSL have no overall improvement, the effect of RG is more significant among all control cases.

For other studies using microsimulation, Roncoli et al. (2016) captures the capacity drop in AimSun using the intelligent driver model (IDM) as the car-following model. A comparison between European microsimulation tools is presented by Boukhellouf et al. (2023), in which it is also found that capacity drop is not identified in SUMO, but captured in Aimsun and SymuVia. That is, the embedded car-following and lane-changing models are quite complex and difficult to adjust. The capacity drop is more convenient to be captured in macroscopic traffic flow model. It can be added by using a fundamental relation which captures capacity drop (e.g., inverse lambda Fundamental Diagram (Koshi et al., 1981)).

In an environment where capacity drop is captured, all three DTM measures are expected to have more significant improvements. However, the performance when combining them without coordination may not be good enough even compared to the single control cases. With this coordination method, the improvement is expected to be the largest among all control scenarios. Hence, the value of coordination is larger, and the coordination control then becomes the most recommended control strategy. The larger improvement of coordinated control is expected not only in travel time but also in travel time equity. With capacity drop, the travel time on main roads where congestion occurs is expected to be much longer than on other routes. Therefore, solving congestion with RM and coordinated control may also improve travel time equity.

The fourth limitation is that all the parameters used in the simulation are not calibrated with traffic data. There may still be a huge difference between the simulation data and the

data on real-life roads. Although the relative improvement of different control scenarios can also be compared. They may not accurately reflect the travel time reduction that can be reached in real world.

The fifth limitation is that the sensitivity analysis is only performed for several parameters. For example, there is only one demand profile, and the RM control parameters are not systematically tuned. The effect of the proportion of users of VMS RG and predictive RG is not explored. Besides, different car-following model and lane changing model are not tested, which can also change the simulation results.

8.2 Further research

With the development of communication technology, there might be more DTM measures available on a freeway network. Therefore, it is necessary to explore more possibilities of coordination under more different road structures. In this way, different DTM combinations and the corresponding ways of coordinating can be tested and implemented to act in different traffic situations.

Regarding to the network structure, RG is more effective for a larger spatial scope with more origins and destinations included. With a longer considered freeway segment, there will also be more RM or VSL DTM measures. The coordination for a larger network may have more significant effects. For example, RG can be coordinated with coordinated RM. The travel time for a corridor that includes several on-ramps is affected by the CRM strategy, and the travel time can affect the on-ramp demand, given that some of the ramps are connected to other freeways where RG is active.

As for innovative technology, this coordination research can also be extended by including automated and cooperative vehicles. However, the first step is to prove the effectiveness of such a coordination method without involving automated vehicles, preferably in a field test. After that, the coordination strategy can adapt to automated or cooperative vehicles. Further simulations can be performed to explore whether the coordination method is more effective given different penetration rates of automated or cooperative vehicles.

For further research, the prediction models can be extended from both the perspectives of range and complexity. For example, the flow model could be METANET (Messmer and Papageorgiou, 1990) for the entire road network. In that case, more control objectives for coordinated control can be explored. The control strategy can also be improved, especially for VSL. There are more delicate algorithms for both roadside VSL (e.g., SPECIALIST (Hegyi & Hoogendoorn, 2010)) and cooperative VSL (e.g., COSCAL (Mahajan et al., 2015), COBRA (Overvoorde, 2020)). Another direction could be including more DTM measures in the coordination, such as lane changing control. Although it can be implemented in microsimulation, the predictive model used in coordination needs to adapt to the heterogeneity between lanes. This could be a microscopic model or a macroscopic model that includes lateral flow (Tajdari et al., 2019).

To improve the quality of the simulation, parameter calibration for simulation settings should be performed. This ensures that the attributes of the real-life roads can be captured in the simulation. This can be done for both no-control cases and some of the controlled cases. If the real-life network is already equipped with DTM measures, the effect of DTMs can also be calibrated. The data used for the calibrations can be collected from similar road structures in real life (such as the one shown in Figure 3.3). The simulation should also capture the capacity drop phenomenon. According to Y. Zhang and Ioannou (2017), the capacity drop can be captured in VISSIM (also a microsimulation tool). It would be better for similar simulation research to be performed in a different simulation tool.

One of the problems in multi-DTM coordination research is that there are too many possibilities and combinations. In this research, the scenarios where RM and VSL is only active on one of the roads are not explored. Meanwhile, there might be more DTM measures in such a road structure in real life, such as more on-ramps. To have a case study based on a real-life road network, the possible number of scenarios also increases. In that case, there will be more control variables. One way to tackle this issue is to use learning techniques, where the control inputs of DTMs are actions, and the prediction model will be the rules of state changing in the learning environment. This has already been applied to improve VSL in research (Han et al., 2022; Cheng et al., 2022). To use the learning process to optimise the coordination, a macroscopic flow model is more feasible, as there are a lot of simulation runs for learning.

Bibliography

Ahn, K. ., & Rakha, H. A. (2013). Network-wide impacts of eco-routing strategies: A large-scale case study. *Transportation Research Part D: Transport and Environment*, *25*, 119–130. https://doi.org/10.1016/j.trd.2013.09.006

Amini, M., Hatwagner, M. F., & Koczy, L. T. (2022). Fuzzy system-based solutions for traffic control in freeway networks toward sustainable improvement. *Communications in Computer and Information Science*, *1602 CCIS*, 288–305. https://doi.org/10.1007/978-3-031-08974-9_23

Boukhellouf, M., Buisson, C., & Chiabaut, N. (2023). Merging and diverging operations: Benchmark of three european microscopic simulation tools and comparison with analytical formulations. *European Transport Research Review*, *15*(1). https://doi.org/10.1186/s12544-023-00586-1

Carlson, R., Papamichail, I., Papageorgiou, M., & Messmer, A. (2010). Optimal mainstream traffic flow control of large-scale motorway networks. *Transportation Research Part C: Emerging Technologies*, *18*, 193–212. https://doi.org/10.1016/j.trc.2009.05.014

Carlson, R., Papamichail, I., & Papageorgiou, M. (2014). Integrated feedback ramp metering and mainstream traffic flow control on motorways using variable speed limits. *Transportation Research Part C: Emerging Technologies*, *46*, 209–221. https://doi.org/10.1016/j.trc.2014.05.017

Carlson, R., Ragias, A., Papamichail, I., & Papageorgiou, M. (2011). Mainstream traffic flow control of merging motorways using variable speed limits. *2011 19th Mediterranean Conference on Control Automation (MED)*, 674–681. https://doi.org/10.1109/MED.2011.5983115

Cassidy, M. J., & Windover, J. R. (1995). Methodology for assessing dynamics of freeway traffic flow. *Transportation Research Record*, (1484), 73–79. https://trid.trb.org/view/451861

Cheng, M., Zhang, C., Jin, H., Wang, Z., & Yang, X. (2022). Adaptive coordinated variable speed limit between highway mainline and on-ramp with deep reinforcement learning. *Journal of Advanced Transportation*, *2022*, 1–16. https://doi.org/10.1155/2022/2435643

Daganzo, C. F. (1994). The cell transmission model: A dynamic representation of highway traffic consistent with the hydrodynamic theory. *Transportation Research Part B: Methodological*, *28*(4), 269–287. https://doi.org/https://doi.org/10.1016/0191-2615(94)90002-7

Daganzo, C. F., Laval, J. A., & Muñoz, J. C. (2002). SOME IDEAS FOR FREEWAY CONGESTION MITIGATION WITH ADVANCED TECHNOLOGIES. *Traffic engineer-*

ing and control, *43*(10), 397–403. https://www.researchgate.net/profile/Jorge_Laval/publication/237296939_SOME_IDEAS_FOR_FREEWAY_CONGESTION_MITIGATION_WITH_ADVANCED_TECHNOLOGIES/links/0a85e52e876b277d28000000.pdf

Definition of vehicles, vehicle types, and routes - sumo documentation. (n.d.). https://sumo.dlr.de/docs/Definition_of_Vehicles%2C_Vehicle_Types%2C_and_Routes.html#available_vehicle_attributes

Duanmu, Z. (2023). *Impacts of autonomous vehicle heterogeneity on traffic flow*. https://repository.tudelft.nl/islandora/object/uuid%3A88211712-296c-429f-9ba8-2e0bbb0cb145?collection=education

Extended intelligent driver model - sumo documentation. (n.d.). https://sumo.dlr.de/docs/Car-Following-Models/EIDM.html

Federal Highway Administration. (n.d.). *Travel time reliability measures - operations performance measurement - fhwa operations*. https://ops.fhwa.dot.gov/perf_measurement/reliability_measures/index.htm

Geistefeldt, J. (2012). Operational experience with temporary hard shoulder running in germany. *Transportation Research Record: Journal of the Transportation Research Board*, *2278*, 67–73. https://doi.org/10.3141/2278-08

Goatin, P., Göttlich, S., & Kolb, O. (2016). Speed limit and ramp meter control for traffic flow networks. *Engineering Optimization*, *48*, 1121–1144. https://doi.org/10.1080/0305215X.2015.1097099

Gong, S., & Du, L. (2016). Optimal location of advance warning for mandatory lane change near a two-lane highway off-ramp. *Transportation Research Part B: Methodological*, *84*, 1–30. https://doi.org/10.1016/j.trb.2015.12.001

Greguric, M., Ivanjko, E., & Mandzuka, S. (2015). A neuro-fuzzy based approach to cooperative ramp metering. *2015 IEEE 18th International Conference on Intelligent Transportation Systems*, 54–59. https://doi.org/10.1109/ITSC.2015.17

Günther, G. ., Coeymans, J. E., Muñoz, J. C., & Herrera, J. C. (2012). Mitigating freeway off-ramp congestion: A surface streets coordinated approach. *Transportation Research Part C: Emerging Technologies*, *20*(1), 112–125. https://doi.org/10.1016/j.trc.2011.05.004

Guo, Y., Xu, H., Zhang, Y., & Yao, D. (2020). Integrated variable speed limits and lane-changing control for freeway lane-drop bottlenecks. *IEEE Access*, *8*, 54710–54721. https://doi.org/10.1109/ACCESS.2020.2981658

Hadj-Salem, H., Blosseville, J.-M., & Papageorgiou, M. (1990). Alinea: A local feedback control law for on-ramp metering; a real-life study. *International Conference on Road Traffic Control, 3rd, 1990, London, United Kingdom*, (320), 194–198. https://ieeexplore.ieee.org/document/114406/

Han, Y., Hegyi, A., Zhang, L., He, Z., Chung, E., & Liu, P. (2022). A new reinforcement learning-based variable speed limit control approach to improve traffic efficiency against freeway jam waves. *Transportation Research Part C: Emerging Technologies*, *144*, 103900. https://doi.org/10.1016/j.trc.2022.103900

Hegyi, A., Bellemans, T., & Schutter, B. D. (2009). Freeway traffic management and control. In R. Meyers (Ed.), *Encyclopedia of complexity and systems science* (pp. 3943–3964). Springer. https://doi.org/10.1007/978-0-387-30440-3_232

Hegyi, A., & Hoogendoorn, S. P. (2010). Dynamic speed limit control to resolve shock waves on freeways - field test results of the specialist algorithm. *13th International IEEE Conference on Intelligent Transportation Systems*, 519–524. https://doi.org/10.1109/ITSC.2010.5624974

Hegyi, A., Hoogendoorn, S., Schreuder, M., Stoelhorst, H., & Viti, F. (2008). Specialist: A dynamic speed limit control algorithm based on shock wave theory. *2008 11th International IEEE Conference on Intelligent Transportation Systems*, 827–832. https://doi.org/10.1109/ITSC.2008.4732611

Hegyi, A., Schutter, B. D., & Hellendoorn, H. (2005). *Transportation Research Part C: Emerging Technologies*, *13*. https://doi.org/10.1016/j.trc.2004.08.001

Holland, J. H. (1992). *Adaptation in Natural and Artificial Systems: An Introductory Analysis with Applications to Biology, Control, and Artificial Intelligence*. The MIT Press. https://doi.org/10.7551/mitpress/1090.001.0001

International Energy Agency, I. (2020). Global CO2 emissions in transport by mode in the Sustainable Development Scenario, 2000-2070 – Charts – Data Statistics. https://www.iea.org/data-and-statistics/charts/global-co2-emissions-in-transport-by-mode-in-the-sustainable-development-scenario-2000-2070

Kan, Y., Wang, Y., Papageorgiou, M., & Papamichail, I. (2016). Local ramp metering with distant downstream bottlenecks: A comparative study. *Transportation Research Part C: Emerging Technologies*, *62*, 149–170. https://doi.org/10.1016/j.trc.2015.08.016

Khanjary, M., & Hashemi, S. M. (2012). Route guidance systems. *Proceedings of the 6th Euro American Conference on Telematics and Information Systems*, 269–275. https://doi.org/10.1145/2261605.2261646

Knoop, Hegyi, Salomons, van Lint, Yuan, & Landman. (2020, November 2). *Traffic flow modelling control-cie4825 and cie5821 lecture notes*. https://brightspace.tudelft.nl/d2l/le/content/399379/viewContent/2518928/View

Koshi, Iwasaki, & Ohkura. (1981). Some findings and an overview on vehicular flow characteristics. *In Proceedings of the 8th International Symposium on Transportation and Traffic Theory*, 403–426.

Kurzhanskiy. (2023). *Ctmsim - an interactive freeway traffic macrosimulator*. Retrieved March 5, 2023, from https://www.mathworks.com/matlabcentral/fileexchange/21977-ctmsim-an-interactive-freeway-traffic-macrosimulator

Lu, X.-Y., & Shladover, S. E. (2014). Review of variable speed limits and advisories. *Transportation Research Record: Journal of the Transportation Research Board*, *2423*, 15–23. https://doi.org/10.3141/2423-03

Lu, X.-Y., Varaiya, P., Horowitz, R., Su, D., & Shladover, S. E. (2010). A new approach for combined freeway variable speed limits and coordinated ramp metering. *13th International IEEE Conference on Intelligent Transportation Systems*, 491–498. https://doi.org/10.1109/ITSC.2010.5625107

Mahajan, N., Hegyi, A., Van De Weg, G. S., & Hoogendoorn, S. P. (2015). Integrated variable speed limit and ramp metering control against jam waves – a coscal v2 based approach. *2015 IEEE 18th International Conference on Intelligent Transportation Systems*, 1156–1162. https://doi.org/10.1109/ITSC.2015.191

Martínez, I., & Jin, W. L. (2020). Optimal location problem for variable speed limit application areas. *Transportation Research Part B: Methodological*, *138*, 221–246. https://doi.org/10.1016/J.TRB.2020.05.003

Masher, D. P. (1975). *Guidelines for design and operation of ramp control systems*. https://trid.trb.org/view.aspx?id=33060

Messmer, A., & Papageorgiou, M. (1990). Metanet: A macroscopic simulation program for motorway networks. *Traffic Engineering Control*, *31*(8-9), 466–470. https://www.scopus.com/inward/record.uri?eid=2-s2.0-0025572909&%20partnerID=40%20&%20md5=00203776dc7e610b5b9e28b5b8037495

Middelham, F., & Taale, H. (2006). Ramp metering in the netherlands: An overview. *IFAC Proceedings Volumes*, *39*(12), 267–272. https://doi.org/10.3182/20060829-3-nl-2908.00047

Ministerie van Infrastructuur en Waterstaat. (2022, April 6). *Mobiliteitsbeeld 2021*. https://www.kimnet.nl/publicaties/publicaties/2021/11/18/mobiliteitsbeeld-2021

Mizuta, A., Roberts, K., Jacobsen, L., Thompson, N., & Colyar, J. (2014). *Ramp metering: A proven, cost-effective operational strategy: A primer* (tech. rep.). United States. Federal Highway Administration.

Müller, E. R., Carlson, R. C., & Kraus, W. (2016). Cooperative mainstream traffic flow control on freeways. *IFAC-PapersOnLine*, *49*, 89–94. https://doi.org/10.1016/J.IFACOL.2016.12.195

Newell, G. F. (2002). A simplified car-following theory: A lower order model. *Transportation Research Part B: Methodological*, *36*(3), 195–205. https://doi.org/10.1016/s0191-2615(00)00044-8

Nissan, A., & Koutsopoulosb, H. N. (2011). Evaluation of the impact of advisory variable speed limits on motorway capacity and level of service. *Procedia - Social and Behavioral Sciences*, *16*, 100–109. https://doi.org/10.1016/J.SBSPRO.2011.04.433

Overvoorde, R. (2020). *Cobra: A cooperative breakdown prevention algorithm*. http://resolver.tudelft.nl/uuid:b565395c-aa55-4db4-81dd-a6917fdaefb8

Papageorgiou, M., & Kotsialos, A. (2002). Freeway ramp metering: An overview. *IEEE Transactions on Intelligent Transportation Systems*, *3*(4), 271–281. https://doi.org/10.1109/tits.2002.806803

Papamichail, I. ., & Papageorgiou, M. . (2008). Traffic-responsive linked ramp-metering control. *IEEE Transactions on Intelligent Transportation Systems*, *9*(1), 111–121. https://doi.org/10.1109/tits.2007.908724

Papamichail, I., Papageorgiou, M., Vong, V., & Gaffney, J. (2010). Heuristic ramp-metering coordination strategy implemented at monash freeway, australia. *Transportation Research Record*, 10–20. https://doi.org/10.3141/2178-02

Park, H., & Smith, B. L. (2012). Investigating benefits of intellidrive in freeway operations: Lane changing advisory case study. *Journal of Transportation Engineering*, *138*, 1113–1122. https://doi.org/10.1061/(ASCE)TE.1943-5436.0000407

Pasquale, C. ., Sacone, S. ., Siri, S. ., & De Schutter, B. . (2017). A multi-class model-based control scheme for reducing congestion and emissions in freeway networks by combining ramp metering and route guidance. *Transportation Research Part C: Emerging Technologies*, *80*, 384–408. https://doi.org/10.1016/j.trc.2017.04.007

PyGAD 3.2.0 documentation. (n.d.). *Pygad - python genetic algorithm! — pygad 3.2.0 documentation*. https://pygad.readthedocs.io/en/latest/index.html

Reddy, R. (2020, August 6). *Re: [sumo-user] the definition of time loss in tripinfo output*. https://www.eclipse.org/lists/sumo-user/msg07554.html

Rijkswaterstaat. (n.d.). *Spitsstroken*. Retrieved January 20, 2023, from https://www.rijkswaterstaat.nl/wegen/wegbeheer/spitsstroken

Roncoli, C., Papamichail, I., & Papageorgiou, M. (2016). Hierarchical model predictive control for multi-lane motorways in presence of vehicle automation and communication systems. *Transportation Research Part C: Emerging Technologies*, *62*, 117–132. https://doi.org/10.1016/J.TRC.2015.11.008

Schelling, I., Hegyi, A., & Hoogendoorn, S. P. (2011). Specialist-rm x2014; integrated variable speed limit control and ramp metering based on shock wave theory. *2011 14th International IEEE Conference on Intelligent Transportation Systems (ITSC)*, 2154–2159. https://doi.org/10.1109/ITSC.2011.6083116

SUMO User Documentation. (n.d.). *Definition of vehicles, vehicle types, and routes - sumo documentation*. https://sumo.dlr.de/docs/Definition_of_Vehicles%2C_Vehicle_Types%2C_and_Routes.html#individual_speed_factor

Syswerda, G. (1989). Uniform crossover in genetic algorithms. *international conference on Genetic algorithms*, 2–9. http://dblp.uni-trier.de/db/conf/icga/icga1989.html#Syswerda89

Taale, H. (2022). Effecten van benutting in nederland: Een overzicht van 270 praktijk evaluaties.

Taale, H. (2023). *Description of the rws algorithm for ramp-metering*. report, Rijkswaterstaat, January 2023.

Tajdari, F., Roncoli, C., Bekiaris-Liberis, N., & Papageorgiou, M. (2019). Integrated ramp metering and lane-changing feedback control at motorway bottlenecks. *2019 18th European Control Conference, ECC 2019*, 3179–3184. https://doi.org/10.23919/ECC.2019.8795763

Texas A&M Transportation Institute: Mobility Division. (2021, June 29). *2021 urban mobility report and appendices - mobility division*. https://mobility.tamu.edu/umr/report/

Traci - sumo documentation. (n.d.). https://sumo.dlr.de/docs/TraCI.html

Treiber, M., Hennecke, A., & Helbing, D. (2000). Congested traffic states in empirical observations and microscopic simulations. *Physical review*, *62*(2), 1805–1824. https://doi.org/10.1103/physreve.62.1805

Wang, Z., Luo, D., & Huang, Z. (2009). Integration control for traffic corridors considering guidance information. *Journal of Control Theory and Applications*, *7*, 445–453. https://doi.org/10.1007/s11768-009-8026-1

Wardrop, J. G. (1952). Road paper. some theoretical aspects of road traffic research. *Proceedings of the Institution of Civil Engineers*, *1*(3), 325–362. https://doi.org/10.1680/ipeds.1952.11259

Winyoopadit, S. . (2007). Development and comparative evaluation of ramp metering algorithms using microscopic traffic simulation. *Journal of Transportation Systems Engineering and Information Technology*, *7*(5), 51–62. https://doi.org/10.1016/s1570-6672(07)60039-7

Yang, X.-S. (2021). Chapter 6 - genetic algorithms. In X.-S. Yang (Ed.), *Nature-inspired optimization algorithms (second edition)* (Second Edition, pp. 91–100). Academic Press. https://doi.org/https://doi.org/10.1016/B978-0-12-821986-7.00013-5

Yuan, K., Knoop, V. L., & Hoogendoorn, S. P. (2015). Capacity drop: Relationship between speed in congestion and the queue discharge rate. *Transportation Research Record*, *2491*(1), 72–80. https://doi.org/10.3141/2491-08

Zhang, C., Sabar, N. R., Chung, E., Bhaskar, A., & Guo, X. (2019). Optimisation of lane-changing advisory at the motorway lane drop bottleneck. *Transportation Research Part C: Emerging Technologies*, *106*, 303–316. https://doi.org/10.1016/j.trc.2019.07.016

Zhang, Y., & Ioannou, P. A. (2017). Combined variable speed limit and lane change control for highway traffic. *IEEE Transactions on Intelligent Transportation Systems*, *18*, 1812–1823. https://doi.org/10.1109/TITS.2016.2616493

Zhao, Z., Wu, G., & Barth, M. (2021). Corridor-wise eco-friendly cooperative ramp management system for connected and automated vehicles. *Sustainability*, *13*(15), 8557. https://doi.org/10.3390/su13158557

Appendix A

Network layouts in literature

The figures listed below are network layouts in some existing DTM coordination studies. They are discussed in Section 3.4.

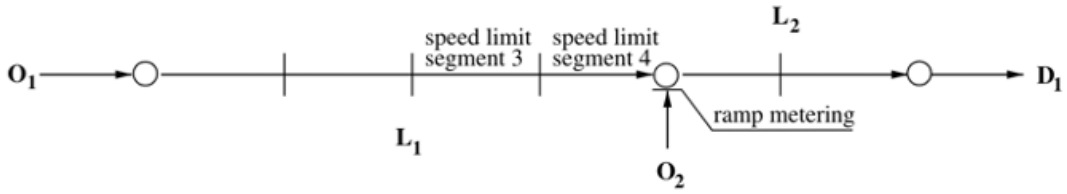

Fig. 6. The benchmark network includes two sections with speed limits, and a metered on-ramp.

Figure A.1: Network for RM+VSL coordination research(Hegyi et al., 2005)

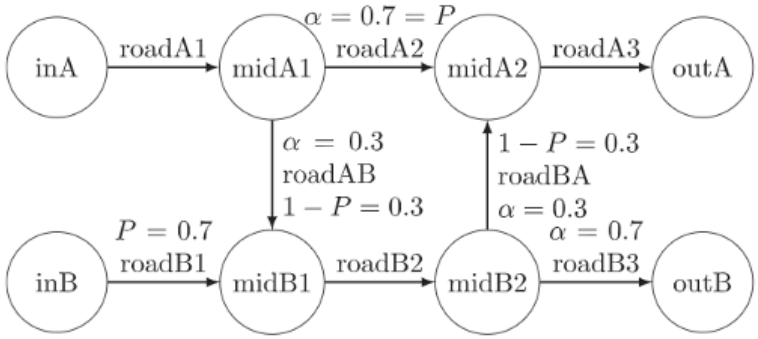

Figure 5. Road network with two main roads.

Figure A.2: Network for VSL research (Goatin et al., 2016)

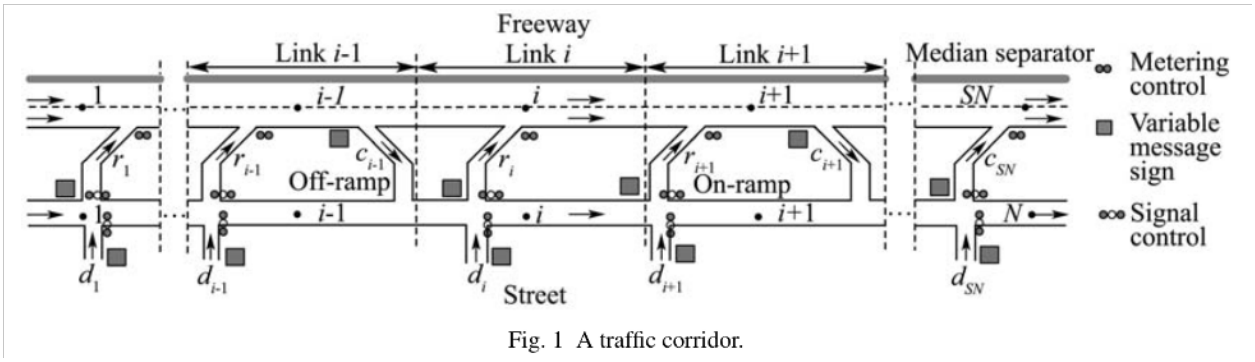

Fig. 1 A traffic corridor.

Figure A.3: Network for RM+VSL+RG research (Wang et al., 2009)

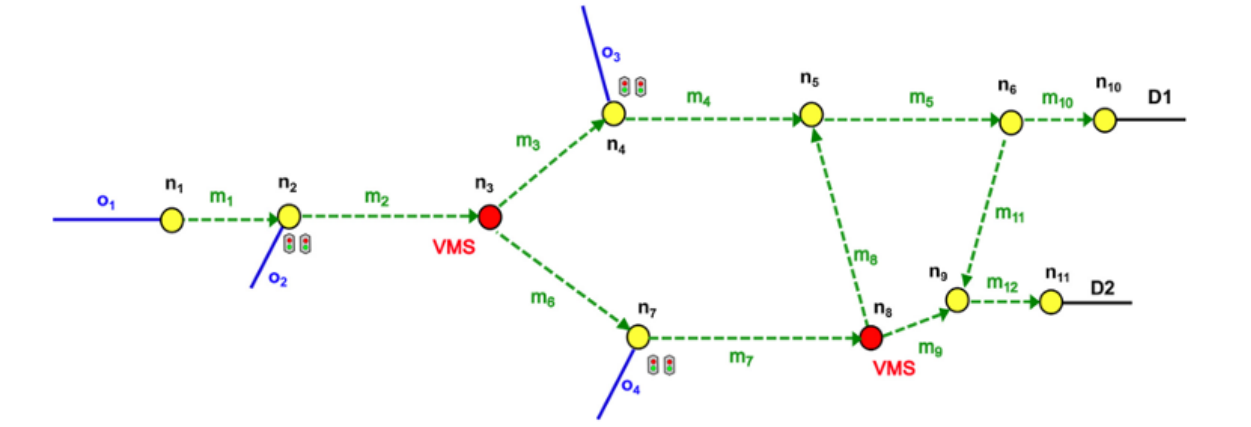

Fig. 5. Layout of the case study freeway network.

Figure A.4: Network for RM+RG research (Pasquale et al., 2017)

Appendix B

Capacity estimation based on FD fitting

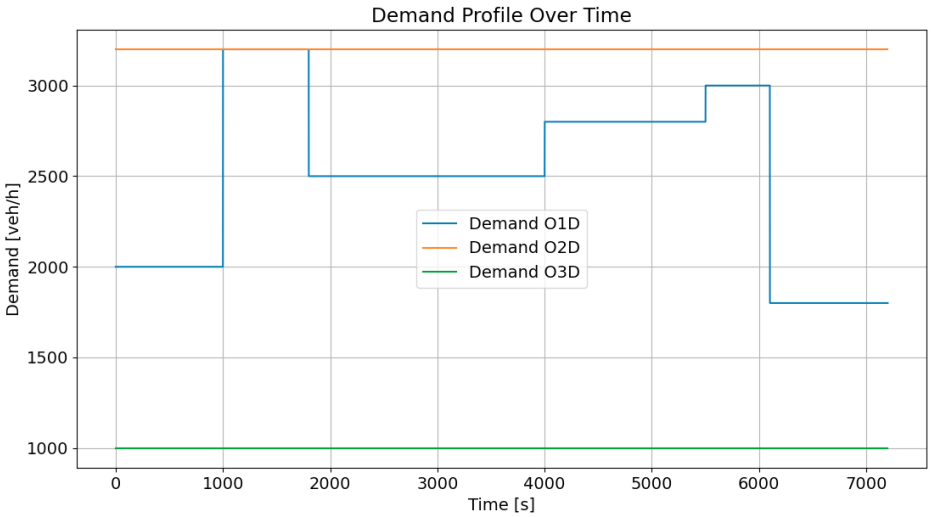

Figure B.1: Demand profile for FD estimation

Figure B.1 is the demand profile for the capacity estimation. It considers a longer simulation period (7200s) with a large variation in the demand value of O1D. During the simulation, speed and density data were collected on Edges EM5, EM6 ans ES5, ES6. The selection of edges considers that both congested and uncongested states can occur on the selected segments because there are downstream bottlenecks. With the speed-density scatter plot, the FD of the selected segments can be estimated; hence, the capacity is determined.

Appendix C

Vehicle behaviour tuning

The most significant limitation of the research is that the capacity drop is not captured in the simulation. However, a process of tuning vehicle parameters has been used to try to capture this phenomenon. The adjustment is made in parameters related to the lane-changing behaviour of vehicles.

Table C.1: Simulation scenarios for tuning vehicle parameters

Parameters	lcSublane	lcPushy	lcAssertive	lcSpeedGain	Note
Range	0-inf	0-1	0-1	0-inf	
Default	1	0	0	1	No Capacity Drop
Scenario 1	0	0	0	1	Vehicles brakes urgently all the time, collision happens
Scenario 2	1	1	0	1	Vehicles brakes urgently all the time, collision happens
Scenario 3	1	0	1	1	No Capacity Drop
Scenario 4	1	0	0	10	Vehicles brakes urgently all the time, collision happens
Scenario 5	0	1	-	10	Slight Capacity Drop
Scenario 6	0	1	-	100	Capacity Drop exists; Travel time is too long
Scenario 7	0	0	-	10	No Capacity Drop
Scenario 8	1	0	-	1	No Capacity Drop
Scenario 9	0	0	-	1	No Capacity Drop; slightly more delay than 8
Scenario 10	1	0	-	100	No Capacity Drop

According to SUMO documentation ("Definition of vehicles, vehicle types, and routes - SUMO Documentation", n.d.), there are several vehicle parameters that affect the lane

changing and merging behaviour of vehicles. lcSublane is the willingness to sacrifice speed for lateral alignment. A higher value means a more strict sublane model. lcPushy is the willingness to encroach laterally on other vehicles. With an lcPushy higher than 0, vehicles will start to change lanes even when the target sublane is still occupied. lcAssertive is the willingness to accept lower front and rear gaps in the target lane. A higher value of lcAssertive encourages more lane changes. lcSpeedGain is the eagerness to change lanes for higher speed. A higher value also means more lane change.

To explore the effect of each parameter on the simulation, several scenarios are tested as shown in Table C.1. Slanted cumulative curves are shown in Figures C.1 to C.7. In Scenarios 1 to 4, only one of the parameters is changed. However, vehicles collide very often in Scenarios 1, 2, and 4. Although it is stated in the documentation that the default value of lcAssertive is 0, setting it specifically to 0 leads to strange vehicle behaviour. Therefore, lcAssertive is not defined in the rest of the scenarios, so its value is the actual (while unknown) default. There is no significant difference between scenarios 8 and 9. That is, the sublane model is already not strict and changing lcSublane to a lower value does not have much effect. Scenario 5 and 6 show the capacity drop phenomenon (as shown in Figures C.2 and C.3). However, in Scenario 6 the travel time is almost four times compared to other scenarios. When lcPushy is 0, capacity drop is not obvious with the same lcSpeedGain setting (comparing Scenarios 7 and 5, 10 and 6). This means that lcPushy is the most crucial parameter for including capacity drop, and an extremely high lcSpeedGain will enhance the effect of lcPushy.

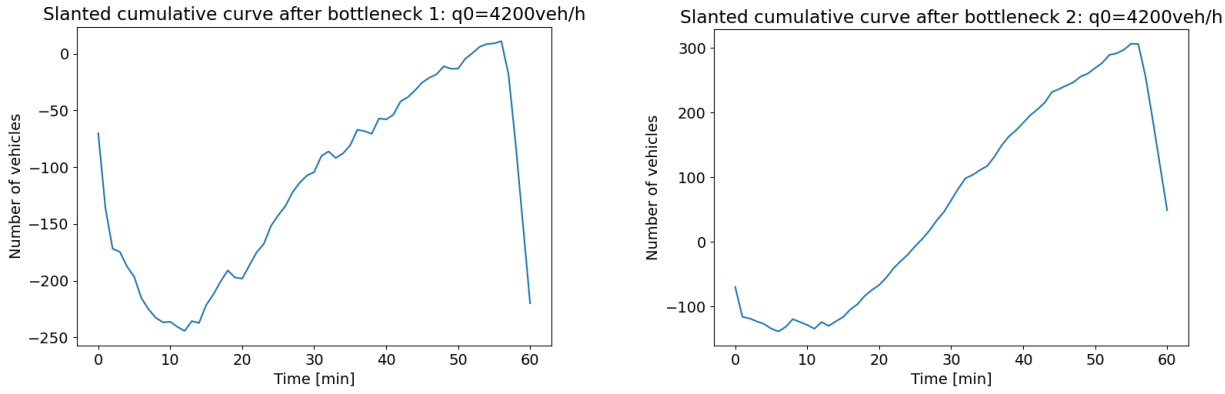

(a) Road 1

(b) Road 2

Figure C.1: Slanted cumulative curves after the bottlenecks: Scenario 3

However, the observed flow decrease in the cumulative curves in Scenarios 5 and 6 is not due to capacity drop, but to the queue before the off-ramp (as the phenomenon shown in Figure 5.20a). Figure C.8 shows the cumulative curve and the speed contour on Road 1. It could be seen that the hollows on the cumulative curve are not due to congestion before the lane drop bottleneck, but to the segments before the off-ramp.

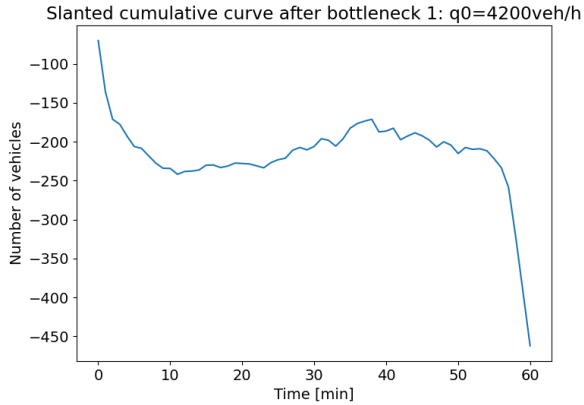

(a) Road 1

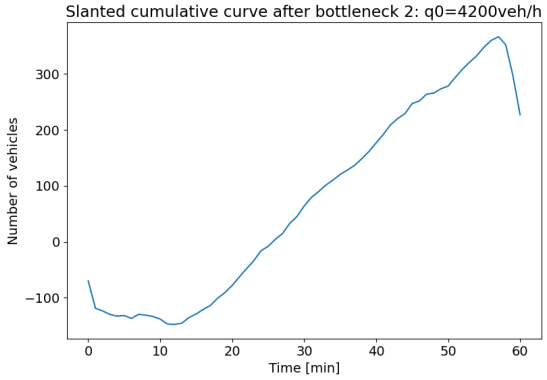

(b) Road 2

Figure C.2: Slanted cumulative curves after the bottlenecks: Scenario 5

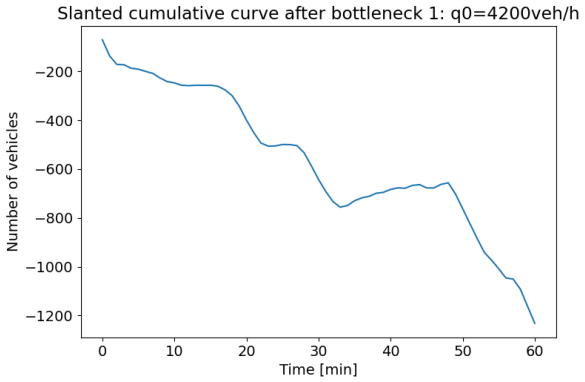

(a) Road 1

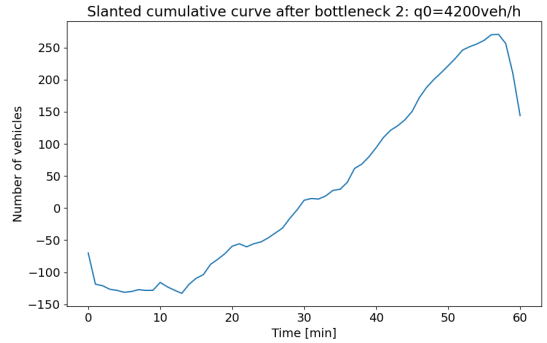

(b) Road 2

Figure C.3: Slanted cumulative curves after the bottlenecks: Scenario 6

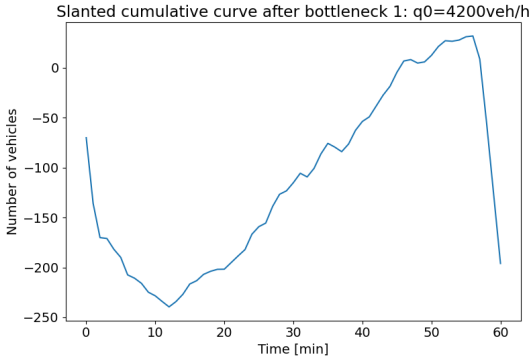

(a) Road 1

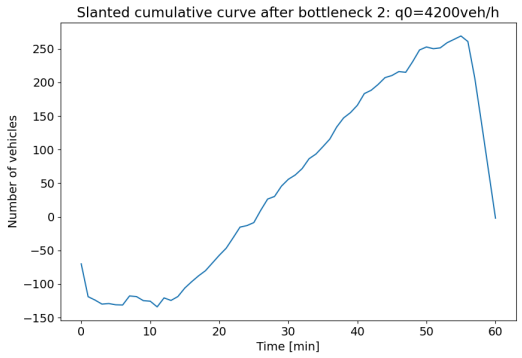

(b) Road 2

Figure C.4: Slanted cumulative curves after the bottlenecks: Scenario 7

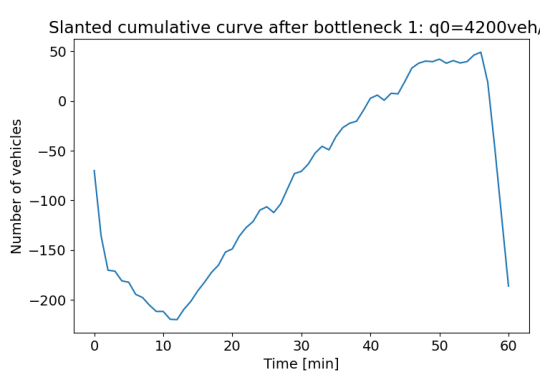

(a) Road 1

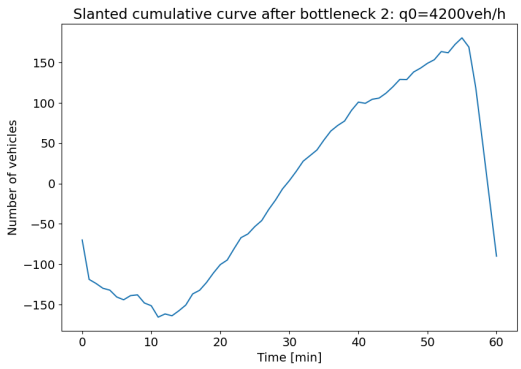

(b) Road 2

Figure C.5: Slanted cumulative curves after the bottlenecks: Scenario 8

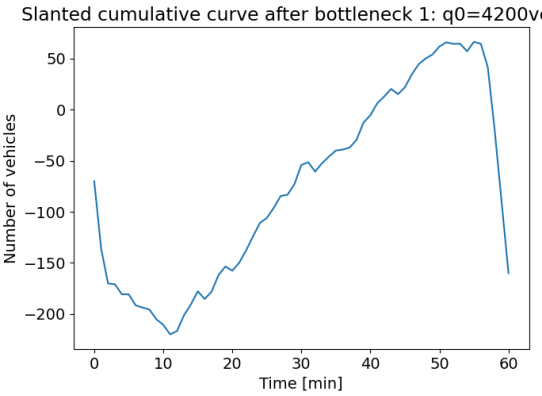

(a) Road 1

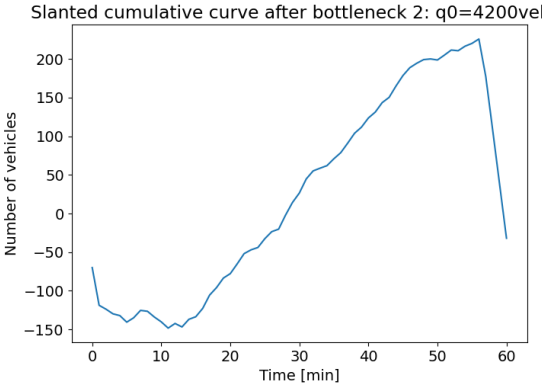

(b) Road 2

Figure C.6: Slanted cumulative curves after the bottlenecks: Scenario 9

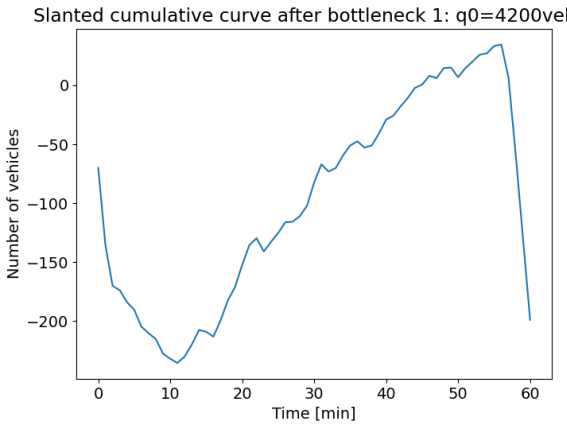

(a) Road 1

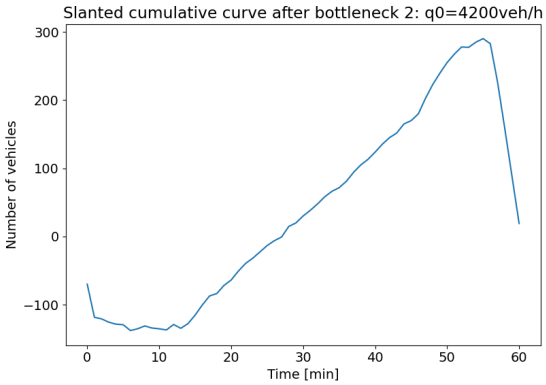

(b) Road 2

Figure C.7: Slanted cumulative curves after the bottlenecks: Scenario 10

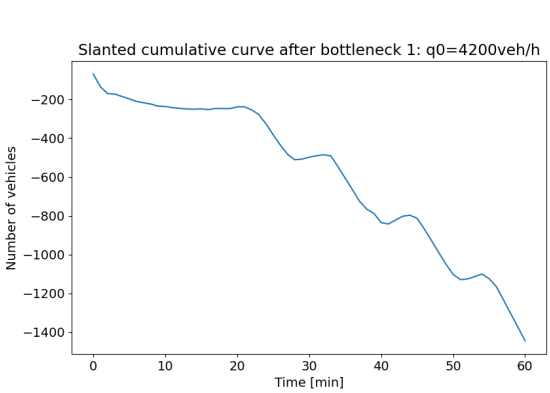

(a) Slanted cumulative curve

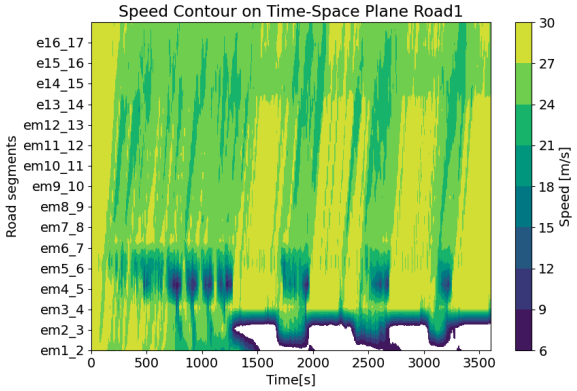

(b) Speed contour

Figure C.8: Slanted cumulative curves after the bottleneck 1 and speed contour on Road 1

Appendix D

Statistical test

Table D.1: T-test: p-values of different indicators compared to the base case

Scenarios	P-values compared to the base case					Total delay
	Network average	Route O1D-1	Route O1D-2	Route O2D	Route O3D	
RM	4.75E-01	1.61E-01	4.99E-25	2.71E-09	9.02E-29	3.20E-01
VSL	9.19E-01	6.60E-01	5.26E-01	9.72E-01	2.72E-02	2.27E-01
RG	1.43E-03	1.37E-01	2.19E-15	4.04E-04	7.13E-01	8.73E-04
RM+VSL	3.21E-01	9.57E-02	3.18E-24	2.36E-09	1.50E-34	7.58E-01
RM+RG	8.67E-04	3.17E-03	1.84E-13	5.04E-14	4.44E-26	9.25E-04
VSL+RG	1.78E-03	3.04E-01	5.13E-16	2.52E-03	9.39E-03	3.43E-05
RM+VSL+RG	2.14E-03	1.25E-03	3.92E-14	2.76E-14	1.08E-33	2.32E-04
Coordination	5.41E-04	6.25E-01	1.94E-15	1.93E-11	3.74E-19	1.15E-03
Coordination (with VSL rule)	7.24E-06	3.35E-02	7.23E-15	2.75E-12	9.44E-18	1.32E-06

Table D.2: T-test: p-values of network average travel time compared to the when compliance rate is 0.8

Compliance rate	VMS RG	Predictive RG
1	1.81E-02	7.82E-01
0.9	1.73E-01	1.15E-01
0.7	2.08E-01	8.73E-01
0.6	1.80E-03	1.50E-01
0.4	7.44E-04	2.87E-01
0.2	6.50E-03	8.15E-01

Appendix E

Codes for simulation

The codes used in the simulation and the raw simulation result data can be found in the following repository: https://github.com/Jiayiguo11/Master_thesis. The function of different files are listed in Table E.1.

Table E.1: Simulation codes and corresponding functions

Module	File name	Function
Network setting	Network_new_no _dsbnk_new.net.xml	Determines the network structure
	Network3.rou.xml	Determines the demand and vehicle parameters
	Network1.sumocfg	Configuration file
Main simulation codes	Main.py	Main simulation codes including calling DTM functions and traffic state collection
	Main_Coordination.py	Main simulation codes for coordination scenarios including calling DTM functions and traffic state collection
Coordinated MPC control	CTM.py	MPC algorithm, including the CTM model and the GA optimisation process
	test_ctm.py	A test of MPC control algorithm including several visualisation
Predictive RG	RGswitch.py	Apply route change on vehicles (both VMS and predictive RG)
	MPC_RG.py	Predictive algorithm to determine the optimal split rate
RM	RM.py	Change traffic signal according to Demand-capacity algorithm
	RM_for_coordination.py	Change traffic signal according to desired cycle time for coordinated control
	RMswitch.py	Turn RM on/off based on the traffic states
VSL	VSL.py	Change the speed limit on VSL application area
Visualisation	Plot.py	Includes functions for generating required plots